# Spatial and temporal variability of hydrological behaviour and leachate composition in a landfill stabilized by in-situ aeration

An experimental and numerical study on the cause and mitigation of reduced aeration efficiency

**Ties de Jong**

TU Delft

CURE

AFVALZORG

[Cover picture taken by Julia Gebert on the 9th of December 2020]

# Spatial and temporal variability of hydrological behaviour and leachate composition in a landfill stabilized by in-situ aeration

An experimental and numerical study on the cause and mitigation of reduced aeration efficiency

by

**Ties de Jong**

**4594576**

in fulfilment of the requirements for the degree of

**Master of Science**
in
Applied Earth Sciences

at the Delft University of Technology,
to be defended publicly on Thursday August 26, 2021 at 9.00 AM

Thesis committee:

| | |
|---|---|
| Dr. J. Gebert (Chair) | TU Delft Geo-Engineering |
| Prof.dr.ir. T.J. Heimovaara | TU Delft Geo-Engineering |
| Dr. T.A. Bogaard | TU Delft Water Management |
| Drs. H. Lammen | Afvalzorg |

Department of Geoscience & Engineering
Delft University of Technology


# Summary

Landfills form the final stage in waste processing and are sources of multiple environmentally harmful emissions. Due to the biodegradation of organic material, methane, a strong greenhouse gas, is released into the air and soluble pollutants, like ammonium or heavy metals, are flushed out of the landfill waste. In modern landfills, the waste body is isolated from the environment by an impermeable liner and both the gas and the leachate fluxes are collected and treated. However, sealing the landfill reduces the emissions on the short term but gives no sustainable solution as eternal active aftercare is needed and the emission potential is not reduced. The goal of the CURE project is to develop methods to enable the sustainable management of Dutch landfills. One of these methods is piloted at the Braambergen landfill, which is the in-situ aeration of the waste body with the goal of speeding up the biological degradation of organic matter to reduce the emission potential relatively quickly below the values in the Dutch regulations, such that the eternal active aftercare is not required anymore. The issue that the landfill operator, Afvalzorg, is facing is that in compartment 11Z of the landfill the aeration efficiency is poor due to ponding leachate.

The objective of this thesis is to quantify the relation between the water level in the landfill and the efficiency of aeration, and to research the spatial and temporal variability of the water levels, leachate composition and hydraulic conductivity of the waste body to investigate the nature of the water and to find a suitable solution to mitigate the reduced aeration efficiency. To reach this goal, multiple types of field and lab measurements have been performed and the results of a water balance model have been used for a numerical evaluation.

In the field, water tables have been measured as well the magnitude and composition of landfill gas extracted by the aeration wells. Pumping tests have been performed on the wells to assess the hydrological behaviour of the leachate surrounding the wells and to determine the horizontal hydraulic conductivity of the waste. Leachate samples from all the wells have been collected and analysed in the lab on pH, redox potential, electrical conductivity, DOC and ammonium concentration. Also were CTD-divers installed in some of the wells to monitor the response to rainfall and the medium long term behaviour of the water level and the electrical conductivity.

From these measurements was found that even for neighbouring aeration wells there are large differences in measured water level, indicating that there is limited horizontal flow. The temporal variability of the water level is in some aeration wells very large, while for others there does not seem to be any temporal variability at all. There is a linear relation between the water column inside the aeration well and the aeration efficiency. The average magnitude of the extracted gas per well is for compartment 11Z at least a factor ten lower than for compartment 11N and this will most likely still be the case if maximum efficiency per well is reached in compartment 11Z by lowering the water column, because of the poor flow conditions of the waste in compartment 11Z compared to the waste in compartment 11N. The response to the pumping test as well as the large spatial variability of the leachate composition lead to the conclusion that it is likely that the water that is present in the landfill does not form an interconnected water body, but instead separate ‘buckets’ of leachate are present with different sizes.

As the amount of measurements of the water levels is not numerously spread over the last years, it is not clear what the influence of the seasons is on the distribution of water levels and whether in general the amount of water in the compartment is decreasing over the years. To assess this, the results of a water balance model were combined with the van Genuchten equation to determine the average water level over the last years. There was a clear mismatch between the predicted and measured average water level, but based on the model it seems that the total amount of water in compartment

11Z is decreasing over the years and that there is a strong response to the seasonal variation of the weather.

Because of the lack of connectivity of the present water in compartment 11Z, lowering the water column in the aeration wells by installing a gravel column or a pump will not be effective on the scale of the entire compartment. Instead the water column must be actively lowered in each single well for which is water column is too high to allow for gas extraction. For this the best option seems to be to lift the filter screen of the aeration wells above the water level. This would increase the extraction rates for the aeration wells in compartment 11Z, but the extraction rates will still be low compared to the current rates observed for compartment 11N.

# Preface

*With this master thesis I present the final product of my master studies at the Geo-Engineering section of the TU Delft. For the past nine months I have had the pleasure to work on a subject which both reflects my interest in the environmental area of my studies and gave me the opportunity to work outside in the field and set up my own fieldwork campaigns. I am very happy that even while during most of the time of the project there were a lot of restrictions due to the current COVID-19 pandemic, I have still been able to conduct the research as intended. I can only be proud on the result and I hope that this small contribution will help to reach the broader goals of the CURE project.*

*I want to thank my supervisors, Julia, Timo and Thom, for their time and effort put into the research and their guidance. I want to especially thank Julia for introducing me to the CURE project and for her enthusiasm. I worked with and also for her for the past two years and I have always enjoyed the collaboration.*

*I also want to thank the academic staff further involved in the CURE project that has helped me with my research, both for physically helping on fieldwork days and helping with directing my research, for this I want to thank Susan Buisma-Yi, Nathali Meza Ramos, André van Turnhout and Liang Wang in particular, as he provided the modelling effort that ties this thesis together. I also want to thank Tristan Rees-White and Richard Beaven from the University of Southampton, who are involved in the CURE project and possess a lot of knowledge on on-site measurements of landfill characteristics. I want to express my gratitude to the technical staff of the TU Delft: Roland Klasen, Marc Friebel, Jens van den Berg and Jolanda van Haagen, as without them the project could never have gone so smoothly.*

*Lastly, I want to thank my roommates Jan, Dennis and Kevin, as they provided a lot of unconditional support.*

*Ties de Jong*

*Delft, 30 July 2021*

# Nomenclature

## Abbreviations

| | |
|---|---|
| CTD | Conductivity, temperature and depth |
| DF | Dilution factor |
| DOC | Dissolved organic carbon |
| EC | Electrical conductivity |
| HDPE | High-density polyethylene |
| LFG | Landfill gas |
| MSW | Municipal solid waste |
| NAP | Amsterdam Ordnance Datum |
| pEV | Potential evapotranspiration |
| TDS | Total dissolved solids |
| TW | Total water |
| UV | Ultraviolet |
| WC | Water column |
| WL | Water level |

## Chemical formulas

| | |
|---|---|
| $CH_4$ | Methane |
| $CO_2$ | Carbon dioxide |
| $H_2O$ | Water |
| $H_3O^+$ | Hydronium |
| $NH_4^+$ | Ammonium |
| $O_2$ | Oxygen |

## Greek symbols

| | | |
|---|---|---|
| $\alpha$ | Van Genuchten parameter | $[LM^{-1}T^2]$ |
| $\alpha, \beta$ | Scaling parameters | $[L^{-3}M]$ |
| $\varepsilon$ | Molar attenuation coefficient | $[L^2]$ |
| $\eta$ | Efficiency | [-] |
| $\theta$ | Temperature coefficient | $[\Theta^{-1}]$ |
| $\theta$ | Water content | [-] |
| $\nu$ | Kinematic viscosity | $[L^2T^{-1}]$ |

| | | |
|---|---|---|
| $\rho$ | Mass density | [$L^{-3}M$] |
| $\sigma'$ | Effective stress | [$L^{-1}MT^{-2}$] |
| $\varphi$ | Porosity | [-] |

## Latin symbols

| | | |
|---|---|---|
| $a$ | Scaling parameter | [X] |
| $A$ | Absorbance | [-] |
| $b$ | Scaling parameter | [-] |
| $c$ | Concentration | [$L^{-3}N$] |
| $d$ | Dip meter constant | [L] |
| $d$ | Distance | [L] |
| $D$ | Tube diameter | [L] |
| $E_h$ | Redox potential | [$L^2MT^{-3}I^{-1}$] |
| $g$ | Gravitational constant | [$LT^{-2}$] |
| $h$ | Hydraulic head | [L] |
| $k$ | Intrinsic permeability | [$L^2$] |
| $K$ | Hydraulic conductivity | [$LT^{-1}$] |
| $K$ | Electrical conductivity | [$L^{-3}M^{-1}T^3I^2$] |
| $l$ | Pathlength | [L] |
| $L$ | Length or depth | [L] |
| $n$ | Van Genuchten parameter | [-] |
| $p$ or $P$ | Pressure | [$L^{-1}MT^{-2}$] |
| $q$ | Specific discharge | [$LT^{-1}$] |
| $Q$ | Discharge | [$L^3T^{-1}$] |
| $r$ | Radius | [L] |
| $Re$ | Reynolds number | [-] |
| $S$ | Storativity | [-] |
| $S$ | Storage | [L] |
| $t$ | Time | [T] |
| $T$ | Transmittance | [-] |
| $T$ | Transmittivity | [$L^2T^{-1}$] |
| $T$ | Temperature | [Θ] |
| $v$ | Velocity | [$LT^{-1}$] |
| $V$ | Volume | [$L^3$] |
| $z$ | Elevation | [L] |

# List of figures

# List of tables

# Contents

# 1. Introduction

This chapter gives a general overview of the studied problem and discusses the added value of this research in the broader goal of going to a more sustainable way of maintaining landfills. Also the setup of this report is mentioned and discussed.

## 1.1 Landfills

Landfills can be seen as the final stage of waste processing. Waste mass can be reduced by the recycling of waste, or by the transformation of waste, in which case the waste is converted to another product, for example compost, or to energy through combustion. All the waste that still remains after this reduction must be disposed in a landfill (Garrod & Willis, 1998).

The emission potential of the waste remains large when it is landfilled compared to when it is recycled of transformed. The emission potential of a landfill is the total amount emissions that can potentially still be released from the waste. Landfilling is therefore not preferred, but in 2012, 64.5% of the municipal solid waste (MSW) generated in the US was still landfilled and this is a worldwide trend (Omar & Rohani, 2015). Luckily does the EU takes a leading role in the reduction of emission potential by slowly banning the disposal of biodegradable waste in landfills (Directive 1999/31/EC). There are two types of environmentally harmful emissions that come from landfills: the landfill gas (LFG) that is released from the surface of a landfill and the landfill leachate that flows out of the bottom of the waste body. Figure 1.1 shows a schematic of a modern landfill and its emissions. LFG is formed by the biodegradation of organic material within the waste, and consists roughly out of 40% carbon dioxide ($CO_2$) and 60% methane ($CH_4$) (Scheutz et al., 2009). Both $CO_2$ and $CH_4$ are greenhouse gases that contribute to global warming, especially methane is an issue as it has a global warming potential of 28 (IPPC, 2014). About 18% of the global anthropogenic methane emissions comes from waste degradation (IEA, 2021), meaning the landfills play a substantial role in global warming. Besides that can LFG be explosive and therefor a threat to human health and can the odour of the LFG be problematic for the surroundings.

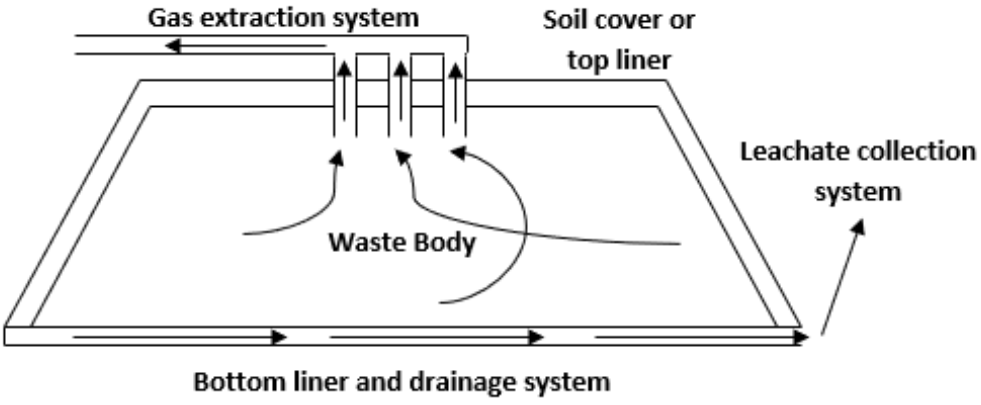


*Figure 1.1: Schematic landfill representation*

The landfill leachate is water which flows through the landfill and collects contaminants from the waste. The leachate often contains among others dissolved organic matter, ammonia-nitrogen, and heavy metals (Renou et al., 2008), the concentrations of which vary in relation to the waste inventory. The leachate must be collected and treated, as the leachate should never be able to contaminate the groundwater. One method of reducing the emissions that has been used in the past is to completely seal the landfill, using impermeable bottom liners and drainage systems to capture the leachate, and a surface sealing cover to limit the infiltration of rainwater. The major drawback of this sealing is that

the emission potential is not reduced, and the contaminated lifespan of the landfill is extended up to centuries (Heimovaara et al., 2010).

In the Netherlands, the regulations even describe that landfills have a surface and a bottom sealing and that the surface sealing system should be regularly replaced. This is not at all a sustainable situation, also because the emission potential does not reduce and the landfill has to be monitored for centuries. Therefore one topic regularly studied is how to sustainably manage these landfills. One approach is the so called in-situ stabilization (Leikam et al., 1999), during which the biodegradation and the related (im)mobilization of contaminants are stimulated by the addition of water and air into the waste body (Brand et al., 2014). This aim of in-situ stabilization is to stimulate biological waste degradation under controlled conditions and actively treat the LFG and leachate fluxes until the emissions are reduced to acceptable values. After the active treatment, top liners should no longer be necessary and the costs and time spent on aftercare could be reduced. To make sustainable landfilling possible in the future, the Dutch regulations need to be changed. In order to make this possible three pilot landfills have been chosen by among others the Stichting Duurzaam Storten (SDS) and national and local governments, for the research program of introductie Duurzaam Stortbeheer (iDS, more information can be found on https://duurzaamstortbeheer.nl/) which has the goal of monitoring the long term effects of active treatment on these three pilot landfills, of which one, the Braambergen landfill, is studied in this thesis.

## 1.2 Landfill aeration

The degradation of organic matter is a complex chemical process, which can be represented in a very simplified form by reaction 1 and 2. In reality there are many types of chemical structures representing organic material, but the decomposition always follows a similar reaction. Reaction 1 shows the fully anaerobic decomposition and reaction 2 the fully aerobic decomposition. The true reaction occurring in the landfill will be a combination of these two, because in some parts of the landfill anaerobic conditions are present and in other parts aerobic conditions. The exact pathway of degradation depends on the nature of the organic matter and on external factors, such as moisture content and temperature, but also the bacteria present and the amount of available oxygen (Renou, 2008).

$$(C_6H_{12}O_6)_n \rightarrow n3CO_2 + n3CH_4 \quad (1)$$

$$(C_6H_{12}O_6)_n + n6O_2 \rightarrow n6CO_2 + n6H_2O \quad (2)$$

The goal of active treatment through aerobic stabilisation is to stimulated this reaction by supplying air, and thus oxygen, to the waste body. There are two types of in-situ aeration systems currently piloted in the Netherlands, overextraction and injection-extraction, which both are shown in figure 1.2.

The overextraction aeration system has as the goal to draw air into the landfill through the unsealed cover layer and extract the LFG generated in the waste body. The LFG generation is enhanced due to supply of oxygen. The extraction-injection system also extracts LFG from the landfill, but injects air in the waste body as well instead of letting the air infiltrate solely through the top of the landfill. This has the advantage that the air is more equally divided over the waste body. The extracted LFG can then be treated, for example by supplying the LFG a biofilter that contains methanotrophs, a group of bacteria that converts methane to carbon dioxide (Huber-Humer et al., 2008), or by a flare which burns the LFG, also converting the methane to carbon dioxide. With the aeration the time it takes to reduce the landfill emission potential can be decreased drastically.

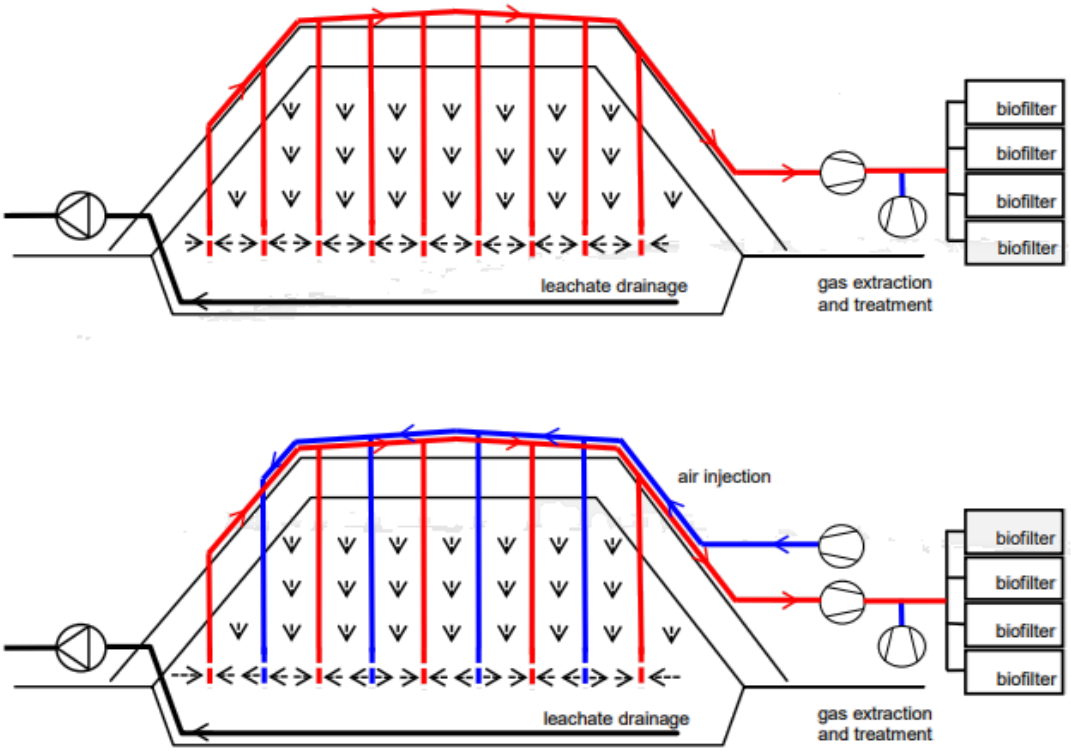


*Figure 1.2: In-situ aeration: overextraction (top) and injection-extraction (bottom) (Scharff, 2020)*

With the degradation of organic material dissolved organic carbon (DOC) is generated. The DOC can mobilize heavy metals and organic contaminants (Sherene, 2009) which then end up in the leachate, which has to be treated such that these harmful contaminants do not enter the groundwater with concentrations higher than is in the regulations. Aerating the waste body reduces the emission potential of both the emission of LFG and the emission of contaminants through the leachate.

To assure that the in-situ aeration is successful, the design of the system must be adequate for the landfill. This concerns well design and the well spacing in relation to the spatial outreach and also selecting the appropriate volumes and pressures of injection and extraction (Ritzkowski & Stegmann, 2012). For example, the well spacing should depend on the waste permeability such that area of influence of each well is sufficient to aerate the full waste body.

## 1.3 Problem description

In this subsection the problem that is analysed in this thesis is introduced and described. The research questions that are answered in this report are discussed as well as the approach to the investigation.

### 1.3.1 Problem statement

Ideally, the aeration system on a landfill works as described in section 1.2. However, in one of the compartments of the Braambergen landfill that are currently being aerated the efficiency of the aeration system is drastically lower than expected. In the aeration wells in this part of the landfill elevated water levels have been measured that were not expected. Ponded water in the waste body indicates reduced, insufficient, waste permeability and it is hypothesized that there is a relation between the elevated water levels and the reduced aeration efficiency. Reduced aeration efficiency due to high water levels has also been reported for other in-situ aerated landfills (Hrad et al., 2013).

One of the reasons that it is difficult to predict the hydrological behaviour in landfills is because of the large heterogeneity of waste properties. Often in models that capture flow through landfills it is

wrongfully assumed that the hydrological properties are horizontally homogenous (Slimani et al., 2017 and Khanbilvardi et al., 1995). Also there is often a lack of in-situ measurement to characterize the hydrological properties, even though it is known that the behaviour in the lab is often poorly representing the behaviour in the field (Hrad et al., 2013). Thus, more insight is needed on how the heterogeneity of a landfill can be quantified.

### 1.3.2 Objective

This research aims to determine the relationship between the high water levels and the reduced efficiency of aeration in the Braambergen landfill. To obtain more insight into the dynamics of the ponded water, it is also the goal to quantify the spatial and temporal variability of the leachate levels and their chemical characteristics.

Furthermore, for the purpose of mitigating the reduced aeration efficiency, it is the objective to determine a viable approach to increase the efficiency of the aeration system. This thesis objective falls within the broader objective of the CURE (Coupled multi-process research for reducing landfill emissions) project, which aims to find methods that enable sustainable management of contaminated sites.

### 1.3.3 Research questions

The following main research question has been formulated to accomplish the objective:

How do the elevated water levels in compartment 11Z of the Braambergen landfill influence the efficiency of the waste aeration, and how can the reduced efficiency be mitigated effectively?

To answer this question, the following sub questions need to be resolved:

1. What are the water levels in the Braambergen landfill and how does this influence the magnitude of LFG fluxes in the aeration system?

2. How does the water level in the Braambergen landfill vary spatially and temporally, and why is this variability present?

3. What is the spatial variability of the horizontal hydraulic conductivity in compartment 11Z of the Braambergen landfill?

4. What is the spatial variability of the leachate composition and properties in compartment 11Z of the Braambergen landfill?

5. What is a realistic representation of the water distribution in the Braambergen landfill?

6. Can the observed temporal variability of water levels in compartment 11Z be explained with a water balance model?

### 1.3.4 Hypothesis

The hypothesis is that the reduction of aeration efficiency is caused by the presence of water in the landfill, which does not flow away through the basal drains due to zones of very low vertical permeability, which is often encountered in landfills, as is schematized in figure 1.3. These zones could be present due to plastic sheets and zones of high compaction (Fellner & Brunner, 2010), but for example also because of trapped LFG that reduces the pores available for water flow or because of pores which became clogged due to precipitation of poorly soluble salts (Islam & Singhal, 2004). This occurs often in landfills, but when this occurs, normally there is still some pathway towards the

drainage system if the leachate is able to flow horizontally, which is also shown in figure 1.3. The presence of ponded water indicates that in this case either the extent of the zones of low vertical permeability is almost the full compartment and there is no flow path around the low permeability zone, or there are also zones of low horizontal permeability present, limiting the horizontal flow as well.

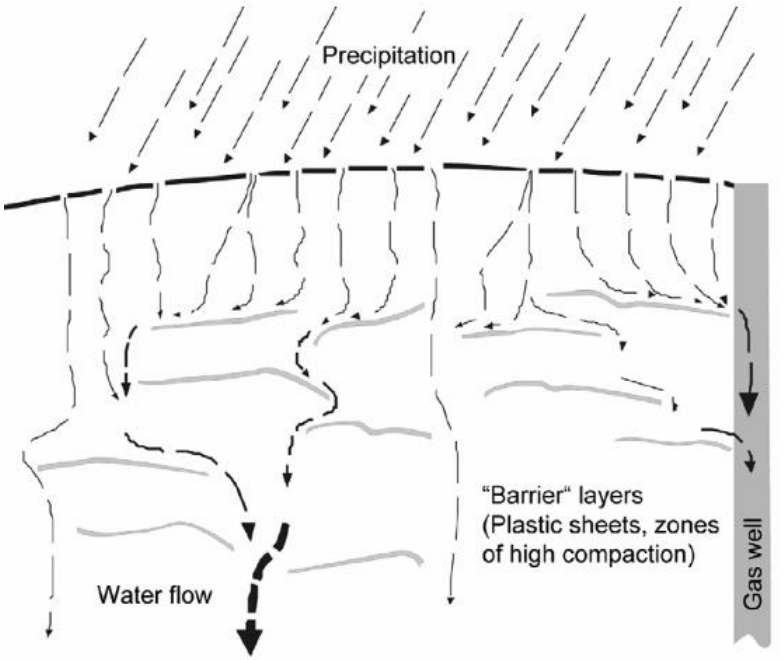


*Figure 1.3: Schematization zones of low vertical permeability (Fellner & Brunner, 2010)*

### 1.3.5 Approach

The first three sub-questions will be answered based on the results from field measurements. The answer to the fourth sub-question is based on laboratory work performed, while the fifth sub-question is answered the aid of both the field and laboratory measurement. To answer the sixth sub-question a water balance model developed in the CURE project is used. The field, laboratory and numerical study are all based upon the findings from literature study.

## 1.4 Thesis structure

The thesis is divided into five parts, consisting of multiple chapters. Part I gives the background information that is necessary to follow the steps taken during the research. Chapter 2 contains general information about the landfill and the waste body. The theoretical background that contains the concepts needed to understand the methods used in this thesis is presented in chapter 3.

Part II is about the physical measurements performed. This comprises of both measurements that where taken on site as well as the measurements done in the lab. Chapter 4 contains a small introduction to the lab and field measurements and chapter 5 shows the materials and methods used for these measurements. Chapter 6 provides the results and the discussion of the results, while the conclusion on the measurements are given in chapter 7.

Part III contains information on the numerical investigation. Chapter 8 introduces the numerical work, and chapter 9 explains the used method. Chapter 10 provides the results and discussion and chapter 11 give the conclusion that can be drawn based on the numerical part of this thesis.

Part IV concludes the thesis with the conclusions and recommendations for further research. With chapter 12 conclusion on all the work performed are presented and in chapter 13 the recommendations for further research are given.

Part V contains the appendices.

# Part I - Background

# 2. The Braambergen landfill

The goal of this chapter is to give a full description of the studied landfill, the Braambergen landfill, which is located near Almere in the Dutch province of Flevoland. Knowing the characteristics of the landfill is vital in the interpretation of the experimental results, as each landfill containing MSW or different types of waste, has different properties, even though often in literature all landfills are assumed to be comparable in hydrological behaviour. First a general overview is given of the studied landfill, then a more detailed description of the aeration system is given.

## 2.1 General overview

Figure 2.1 shows the full extent of the Braambergen landfill. There are three hills which each are divided into multiple compartments. The studied part of the landfill, where the aeration pilot takes place, is the north-eastern hill, shown on the right of figure 2.1. This hill consists of compartments 11N, 11Z, 12O and 12W, which can be seen in the blueprint of the hill given in figure 2.2.


*Figure 2.1: Aerial view of the Braambergen landfill (Afvalzorg, 2021)*

The combined surface area of compartments 11 and 12 is approximately 9.7 hectares and the total amount of waste present is roughly 1.2 million tons, all deposited between 1999 and 2008. The landfill is in its methanogenic phase (Bröcker & Kaiser, 2011). The hill has a height of 15 meters and on top of waste body is a soil cover of minimally one meter thick. The bottom sealing consists out of a 50 centimetre sand-bentonite mixture and a HDPE foil. Leachate is formed by the infiltration of rain and the leaching of substances from the waste body into the water. There are three separate leachate collection systems, one for compartment 12 and two for compartment 11, which is therefore divided in 11Z (the southern part) and 11N (the northern part) (van Turnhout et al., 2020). The subdivision is based on the order in which the waste was disposed in the landfill. The compartments have different leachate collection points, which are in the map given in figure 2.2 indicated as PP. The compartments are separated by two meter high bunds, also shown on the map. The drainage system operates such that if the water level in the drainage system exceeds a certain limit, the leachate is pumped out of the drainage system, such that the water level will never be so high that it submerges the waste body or overflows the bunds.

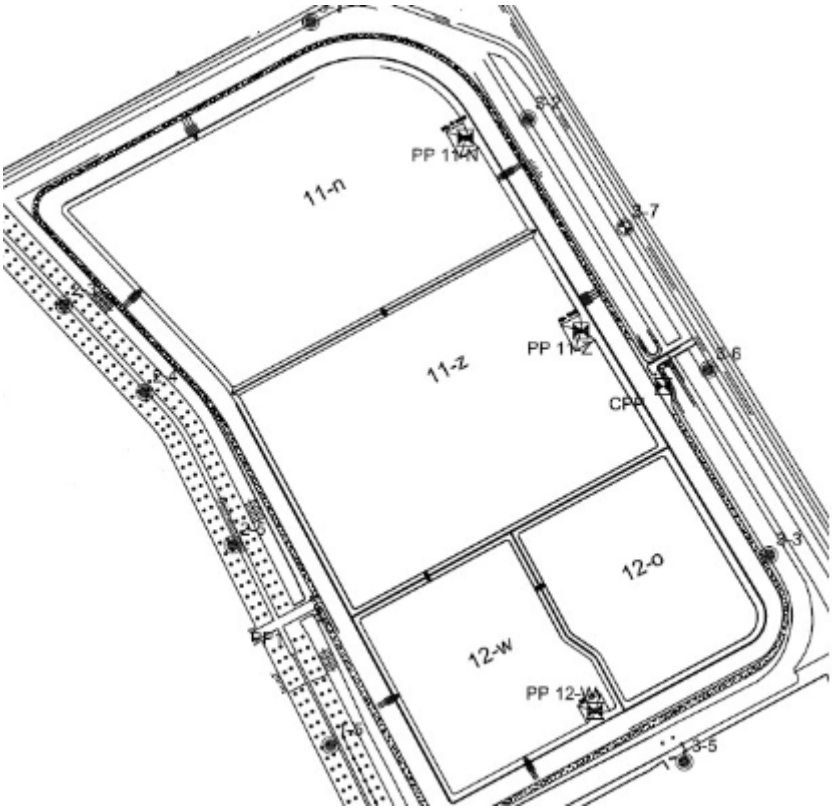


*Figure 2.2: Map of the subdivision of compartments 11 and 12 (Vereniging Afvalbedrijven, 2014)*

## 2.2 Waste characteristics

The type of waste present determines the characteristics of the landfill, such as the hydrological properties but also the amount of organic material that can be degraded. Table 2.1 shows a list of how many tons of waste are present in compartments 11 and 12, subdivided by origin. Figure 2.3 shows a pie chart with the same information making the relative amounts more apparent. Appendix A gives a more detailed overview of the waste types. Over 80% of the waste consists of soil or soil decontamination residues. The residues come from the extractive decontamination of soils, from which the fine soil particles (< 63 µm) are extracted, and these form the residue that ends up in the landfill. This type of waste has therefore similar hydrological properties as a clay, and is thus very poorly permeable to water. Some waste types such as asbestos are landfilled in big bags, which have therefore different hydrological properties. The diversity of soils and other waste types that are landfilled is so large that the landfill is very heterogenous in hydrological behaviour, contrary to natural soils.

*Table 2.1: Amount and origin of waste in compartments 11 and 12 (Vereniging Afvalbedrijven, 2014)*

| Waste origin | Landfilled waste in tons |
|---|---|
| **Soil and soil decontamination residues** | 981,019 |
| **Construction and demolition waste** | 53,855 |
| **Commercial waste** | 123,098 |
| **Shredder waste** | 11,737 |
| **Street cleansing waste** | 1,397 |
| **Coarse domestic waste** | 4,438 |
| **Sludge and composting waste** | 5,406 |
| **Household waste** | 35,773 |
| **Total** | 1,216,723 |

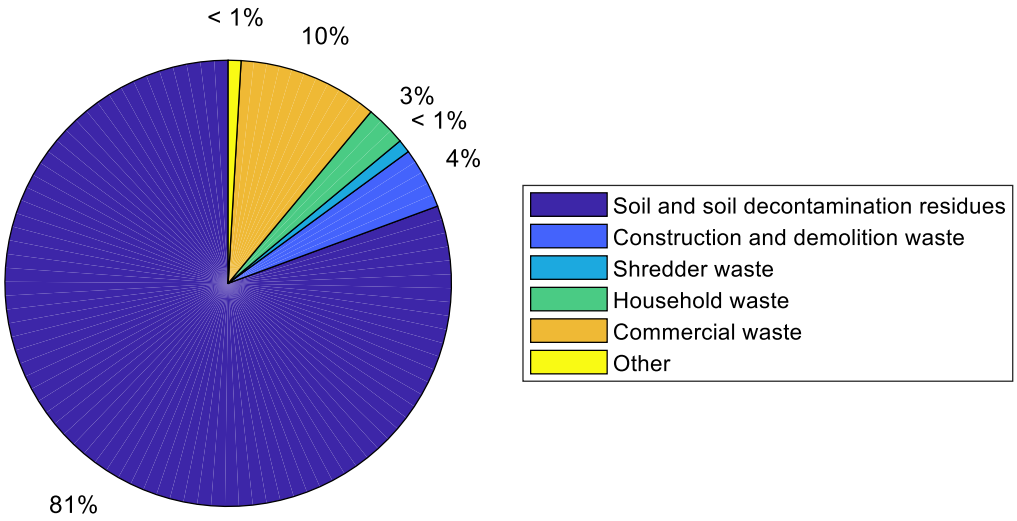


*Figure 2.3: Pie chart of waste types in mass percentage for compartments 11 and 12*

## 2.3 Organic material

The goal of the active treatment through aerobic stabilisation is to enhance the decomposition of organic material. Organic material in a landfill can be distinguished in four types based on the degradability. Inert organic material can never be degraded (an)aerobically, permanently unfavourable organic material would be degradable but is not because of the unfavourable conditions in the landfill. Then there is degradable and potentially degradable waste, of which the last one is only degradable if the conditions in the landfill change, for example due to extra oxygen supply by aeration.

For compartments 11 and 12, it is thought that the maximum amount of organic carbon that has been present originally in the landfill was 20.000 tons, after the last waste was landfilled 2008, of which 7.000 tons belongs to the two non-reactive types (Vereniging Afvalbedrijven, 2014).

## 2.4 The aeration system

The aeration system present on compartments 11 and 12 is an injection-extraction system, which can also be operated as an only extraction system, and consists out of 230 aeration wells, 64 in 11N, 110 in 11Z and 56 in 12. Figure 2.4 shows a picture of one of these aeration wells.

*Figure 2.4: Opened aeration well and piping system leading to the divider*

The black piping is connected to a system that applies alternately an over or under pressure to either extract LFG of inject air. In the picture the well is opened and therefore the white pipe that extends into the waste is visible, which has a diameter of 2.4 centimetre. The wells extend until roughly two meters below NAP, and have therefore a length between 10 and 12 meters. The bottom 1.8 meter of the well is perforated, so only in this 1.8 meter gases can be exchanged with the waste. The wells are in direct contact with the waste and are installed by pushing them into the landfill, without removing any of the waste. Figure 2.5 shows a map with the locations of the aeration wells. The wells are all labelled by a letter and number, for example A1, according to their position in the grid, where the letters increase with alphabetical order from north to south, and the numbers increase from west to east. The system is designed such that the four closest neighbouring wells of an injection well are extracting wells and vice versa. The distance between the wells is 20 or 15 meters. As can be seen in figure 2.5, for rows G to R, the distance between the wells is smaller than for the other rows, which is because in 11Z the conditions for gas transport through the waste are less favourable.

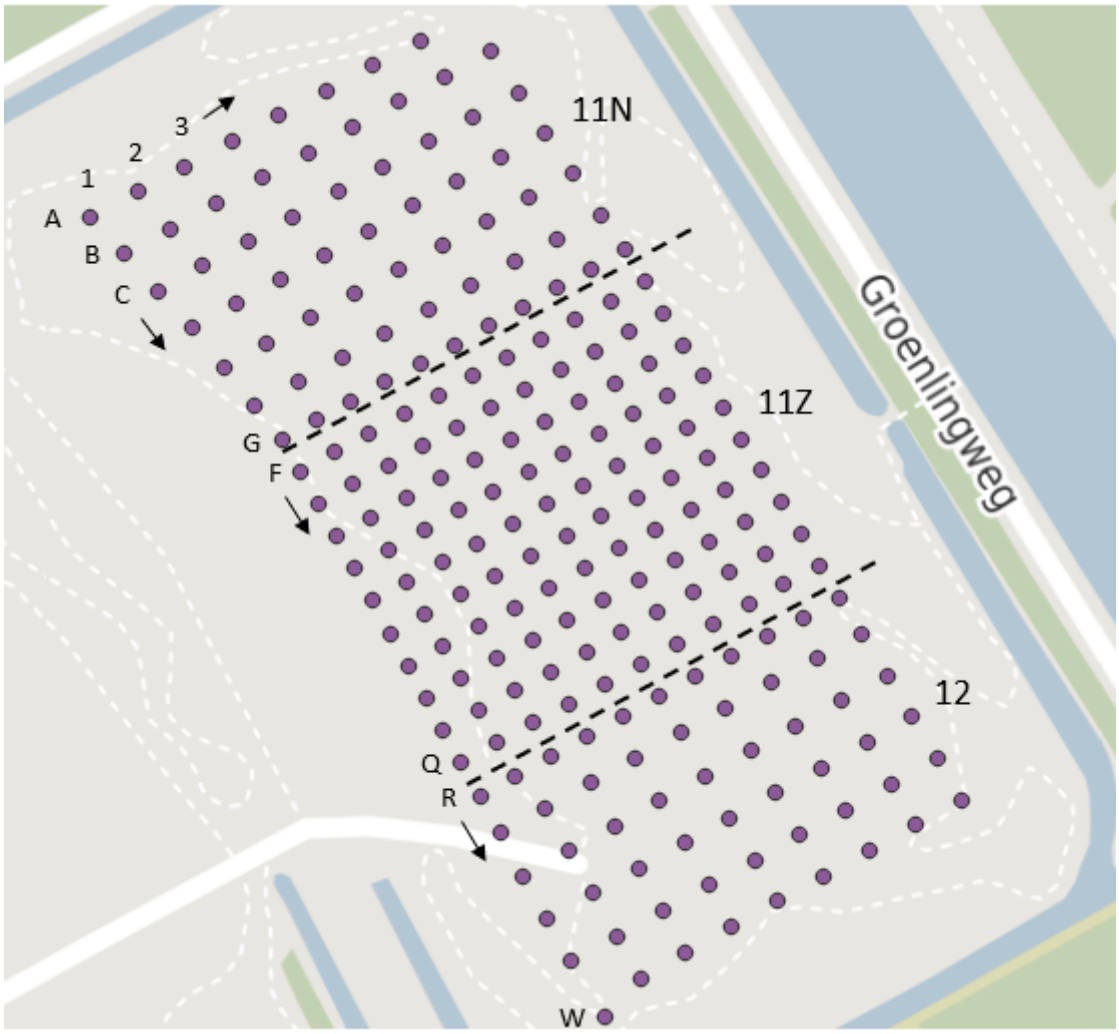


*Figure 2.5: Aeration well locations and naming system*

Figure 2.6 gives a simplified schematic of the full aeration system. The gas station contains the central blower that injects or extracts by putting a pressure onto the system of dividers. The purpose of the dividers is to equally divide the pressure over the aeration wells. The gas that is extracted is then transported to the treating facility, which currently consists out of four container sized biofilters.

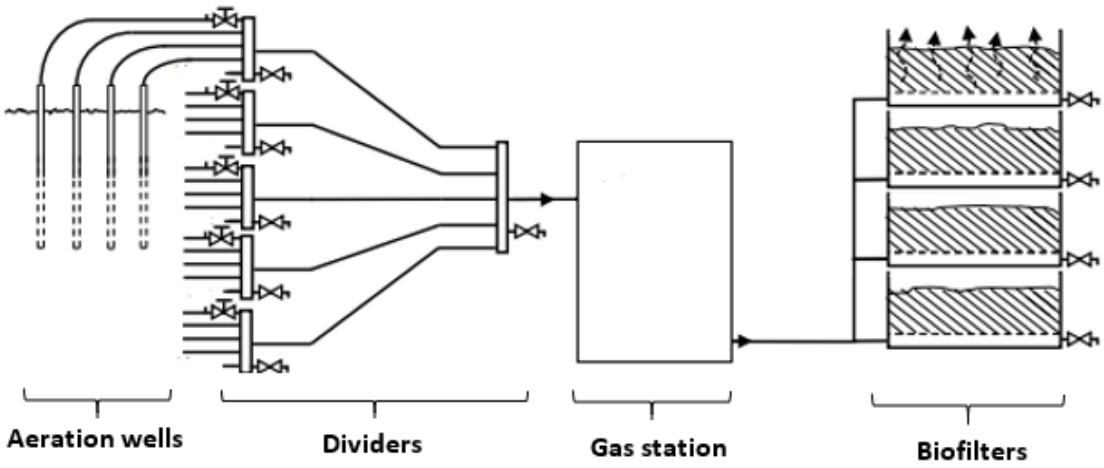


*Figure 2.6: Schematic of the full aeration system*

## 2.5 Old gas wells

Before the current aeration system was installed, there was already a gas collection system consisting of 36 larger gas wells. The positions and names are given in appendix B. These wells are no longer in use, but they are still present. Figure 2.7 shows one of these old gas wells. Their presence is relevant because of the way they were constructed. In contrast to the aeration wells, there is a layer of gravel surrounding the old gas wells, which is connected to the leachate drainage layer, so that there is no direct contact with the waste. The old gas wells extend all the way to the drainage layer. These two facts cause water near the old gas wells to drain relatively easily from the waste towards the basal drain through the gravel layer.


*Figure 2.7: Old gas well GB51*

# 3. Theoretical background

In this chapter the theoretical background needed to understand the concepts that have been used as a basis for the interpretation of the performed measurements and the set-up for the numerical evaluation are explained. First the principles of fluid flow through a landfill are discussed, followed by a description of the different chemical properties of landfill leachate that have been used as a measure of variability. After this the fundamentals of a landfill water balance model are explained.

## 3.1 Fluid flow in landfills

To understand the hydrological issues that are present on the Braambergen landfill it is important to understand what influences the flow of fluids in the first place. The term fluid includes both the liquid and gas phase.

### 3.1.1 Darcy's law

Darcy's law is an empirical equation that relates a hydraulic head gradient to a magnitude and direction of fluid flow through a porous medium, such as soil or waste. The original law as found by Darcy was for one dimension, but this can be easily extended to a three dimensional form, which is given in equation 3.1.

$$\mathbf{q} = -K(x,y,z)\nabla h \tag{3.1}$$

Where $\mathbf{q}$ is the specific discharge [$LT^{-1}$], $K$ is the hydraulic conductivity [$LT^{-1}$] and $\nabla h$ is the hydraulic head gradient [-]. From Darcy's law it follows that that fluid flows towards a decreasing hydraulic head, and that the magnitude of the flow is also related to the hydraulic conductivity, which is a property of both the fluid and the porous medium. The hydraulic head consists out of three components, specifically the elevation head, the pressure head and kinetic energy head, as is shown in equation 3.2, and be derived from Bernoulli's principle.

$$h = z + \frac{p}{\rho g} + \frac{v^2}{2g} \approx z + \frac{p}{\rho g} \tag{3.2}$$

Where $h$ is the hydraulic head [L], $z$ is the elevation from a fixed datum [L], $p$ is the fluid's pressure [$L^{-1}MT^{-2}$], $\rho$ is the fluid's mass density [$L^{-3}M$], $g$ is the gravitational constant [$LT^{-2}$] and $v$ is the fluid's velocity [$LT^{-1}$]. The kinetic energy head is often ignored, as velocities are small in porous media and therefore the value of the kinetic energy head is negligible compared to the elevation head and the pressure head (Fitts, 2002). The hydraulic head can be measured in a well as its value is the height of the water table above a fixed datum.

The hydraulic conductivity is a function of the properties of both the soil and the fluid. Equation 3.3 gives the definition of the hydraulic conductivity. Unlike what its name might suggest, the hydraulic conductivity is a fluid property that exists for all fluids and not only for water.

$$K = \frac{kg}{\nu} \tag{3.3}$$

Where $K$ is the hydraulic conductivity [$LT^{-1}$], $k$ is the soil's intrinsic permeability [$L^2$], $g$ is the gravitational constant [$LT^{-2}$] and $\nu$ is the fluid's kinematic viscosity [$L^2T^{-1}$].

### 3.1.2 Permeability

The intrinsic permeability of a porous medium is a measure of how easily the medium allows flow of any fluid. There are many empirical equation established to approximate the intrinsic permeability of soils. These equation often include the following two soil properties: porosity and a measure of the

grain size distribution. The porosity is the relative volume of soil that is occupied by voids and its definition is given in equation 3.4. That an increase in porosity results in an increase in permeability feels intuitive as more space available for flow would result in more flow for the same pressure gradient. The grain size distribution is important as the grainsize distribution together with the compaction level of the soil determines the pore size distribution. Smaller pores give a lower flow rate than larger pores even if the area of flow is the same. This follows from the Hagen-Poiseuille law, an equation that is used to determine flow rates through pipes, which when used to calculate the mean velocity through a pipe gives the relationship shown in equation 3.5 (Bird et al., 2006). A pore in a porous medium can be roughly approximated as an circular pipe.

$$\varphi = \frac{V_v}{V_b} = \frac{V_v}{V_v + V_s} \tag{3.4}$$

Where $\varphi$ is the porosity [-], $V_v$ is the volume of the voids of the soil [$L^3$], $V_b$ is the bulk volume of the soil [$L^3$] and $V_s$ is the volume of solids of the soil [$L^3$].

$$v_m \propto r^2 \tag{3.5}$$

Where $v_m$ is the mean velocity in the pipe or pore [$LT^{-1}$], and $r$ is radius of the pipe or pore [L].

The waste in a landfill is not the same as a soil, but waste is a porous medium and when looking at water flow through a landfill, waste is often assumed to behave similarly as a soil. There are however differences between the hydraulic properties of regular soils and waste. One example of this is that in waste bodies large sheets of plastics could be present, because this was used to store the waste, which forms an impermeable boundary. Also is the permeability in landfills highly variable. Vertically the permeability is decreasing with depth, because the increasing effective stress from the weight of the overlying waste. Powrie & Beaven (1999) suggest the empirical relationship shown in equation 3.6 between hydraulic conductivity and effective stress. Because of the higher compressibility of waste, this relationship between effective stress and hydraulic conductivity is much stronger for waste than for soils. Xu et al. (2020) found vertical permeabilities in MSW landfills between $10^{-10}$ and $10^{-17}$ $m^2$. Also the horizontal permeability can be highly variable, because the waste deposited is often very heterogenous in origin and therefore in pore size distribution.

$$K = 2.1 \cdot \sigma'^{\,-2.71} \tag{3.6}$$

Where $K$ is the hydraulic conductivity [$LT^{-1}$], which in this empirical relationship has the units of m/s and $\sigma'$ is the effective stress [$L^{-1}MT^{-2}$], which in this empirical relationship has the units of kPa.

The waste is reducing in permeability over time, because when organic material in the waste body is degrading, the grain size reduces leading to a smaller average pore size and therefore a reduction of permeability (Hossain et al., 2009). Also is any porous medium through which leachate flows susceptible to clogging by microbial organisms and deposited inorganic salts, reducing the permeability (Rees-White et al., 2013).

The formation of LFG that occupies the pore space in competition with leachate also reduces the effective permeability for the flow of liquids. Equation 3.7 gives the relationship between the effective and intrinsic permeability. The relative permeability is a number between 0 and 1 and decreases exponentially with decreasing saturation, meaning that if gas is present in the pore system the effective permeability for liquid transport decreases (Scanlon et al., 2002).

$$k_{eff} = k_r k \tag{3.7}$$

Where $k_{eff}$ is the effective permeability [$L^2$], $k_r$ is the relative permeability [-] and $k$ is the soil's intrinsic permeability [$L^2$],.

### 3.1.3 Theis solution

The Theis solution is used to analyse problems involving radial flow towards a well. The exact geometry for which the Theis solution commonly used is shown in figure 3.1. The Theis solution in terms of drawdown caused by the pumping well is given in equation 3.8. For the Theis solution the superposition principle holds, meaning that the response of the system to two actions can be found by simply adding the functions.

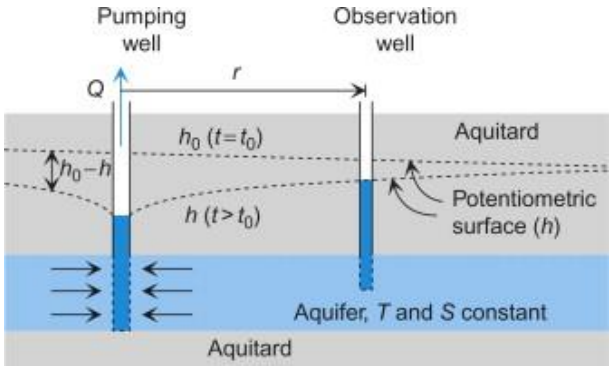


*Figure 3.1: Geometry of the Theis solution (Fitts, 2002)*

$$h_0 - h = \frac{Q}{4\pi T} W(u) \tag{3.8}$$

Where $h$ is the hydraulic head [L], $h_0$ is the steady-state head [L], $Q$ is the well discharge [$L^3T^{-1}$], $T$ is the transmittivity of the aquifer [$L^2T^{-1}$] and $W(u)$ is the well function [-], in which $u$ is a dimensionless parameter defined in equation 3.9. Equation 3.10 gives the definition and a useful approximation of the well function (Fitts, 2002). The transmittivity is a measure of how much water the aquifer can transmit horizontally, and is therefore the product of the thickness and hydraulic conductivity of the aquifer.

$$u = \frac{r^2 S}{4T(t - t_0)} \quad (t > t_0) \tag{3.9}$$

Where $r$ is the radius measured from the middle of the pumping well [L], $S$ is the storativity of the aquifer [-], $t$ is the current time [T] and $t_0$ is the time at which pumping started [T]. From the last two definitions follows that $t - t_0$ is the time since the start of pumping. The storativity can be seen as the volume of water that is released from storage per decline in hydraulic head, per area of the aquifer.

$$W(u) = \int_u^\infty \frac{e^{-m} dm}{m} = -\gamma - \ln(u) + u - \frac{u^2}{2(2!)} + \frac{u^3}{3(3!)} - \cdots (u < \pi) \tag{3.10}$$

Where $\gamma$ is the Euler–Mascheroni constant, which is roughly 0.577 [-].

The Theis solution can thus be used to determine the reduction in hydraulic head a certain distance away from the pumping well if the relevant properties of the aquifer are known (transmittivity and storativity) and a constant pumping rate is applied. Or if the head is monitored, the Theis solution can be used to determine the aquifer properties. If the superposition principle is used, also the properties can be deduced from the recovery of head after the ceasing of pumping. A well that starts pumping with pumping rate $Q$ at time $t_0$ and ceases at time $t_1$ can mathematically be seen as two wells at the

same location, one pumps with rate $Q$ starting at time $t_0$ and one with rate $-Q$ starting at time $t_1$. Equation 3.11 shows the resulting expression for the residual drawdown following from applying the superposition principle in this situation (Kruseman et al., 2000).

$$h_0 - h = \frac{Q}{4\pi T}\{W(u) - W(u')\} \tag{3.11}$$

Where $u'$ is has the same definition as $u$ but for the recovery phase. If $u$ and $u'$ are sufficiently small, and therefore all the terms in equation 3.10 after $\ln(u)$ can be ignored and is assumed that the storativity of the aquifer is the same during the pumping and the recovery phase, equation 3.11 can be simplified to the final expression given in equation 3.12 (Kruseman et al., 2000), which can be used to determine the hydraulic conductivity of an aquifer when measuring the hydraulic head on any location in the aquifer, as the radius drops out of the equation.

$$h_0 - h = \frac{\ln(10)\,Q}{4\pi T}\log\left(\frac{t - t_0}{t - t_1}\right)(t > t_1) \tag{3.12}$$

Where $h$ is the hydraulic head [L], $h_0$ is the steady-state head [L], $Q$ is the well discharge [$L^3T^{-1}$], $T$ is the transmittivity of the aquifer [$L^2T^{-1}$], $t$ is the current time [T], $t_0$ is the time at which pumping started [T] and $t_1$ is the time at which pumping ceased [T].

## 3.2 Chemical properties leachate

In this section the five different leachate properties that have been analysed during this thesis are explained. To interpret the results it is essential to know how the different properties are related to each other and what they can tell about the interplay between the waste, the water and the degradation process.

### 3.2.1 pH

The pH is a dimensionless measure of the acidity or basicity of an aqueous solution. Equation 3.13 gives the definition of the pH. A pH value below 7 indicates an acidic solution and a pH value above 7 indicates a basic solution. Landfill leachate pH values are generally between 4.5 and 9 (Christensen et al., 2001). When the landfill gets older, and moves from the acetic to the methanogenic phase, the average measured pH of the landfill leachate increases from 6.1 to 8.0 (Ehrig, 1983).

$$pH = -\log\left(\frac{[H_3O^+]}{c_0}\right) \tag{3.13}$$

Where $[H_3O^+]$ is the concentration of hydronium ions [$L^{-3}N$] and $c_0$ the standard state concentration [$L^{-3}N$], which is needed in the equation as it is only possible to take the logarithm of an dimensionless quantity.

### 3.2.2 Electrical conductivity

The electrical conductivity (EC) of a solution is a measure of its ability to conduct electricity. This ability comes from the presence of electrically charged ions that can move through the solution. Therefore the electrical conductivity can be seen as a rough measure of the total dissolved solids (TDS). Equation 3.14 gives an empirical relation between the EC and TDS of an aqueous solution (Fitts, 2002). Rainwater has an EC that is generally lower than 10 µS/cm (Zdeb et al., 2018), while landfill leachate EC values are often between 2500 and 35000 µS/cm (Christensen et al., 2001). The specific electrical conductivity is the EC measured at 25 °C.

$$EC \approx A \cdot TDS \quad 3.14$$

Where $EC$ is the electrical conductivity [$L^{-3}M^{-1}T^{3}I^{2}$], $A$ is a constant in the range of 0.55 to 0.75 (µS/cm)/(mg/L) [$M^{-2}T^{3}I^{2}$] and $TDS$ is the total dissolved solids [$L^{-3}M$].

### 3.2.3 Redox potential

The redox potential is in aqueous solutions a measure of the tendency of the solution to gain or lose electrons. If the reducing species dominate in the solution, the environment is reducing and can easily donate electrons to other substances, which corresponds to a lower redox potential, and the other way around for dominating oxidizing species. The redox potential relative to the standard hydrogen electrode is the $E_h$ value [$ML^{2}T^{-3}I^{-1}$].

In soils the redox potential can drop rapidly if the soil pore space is saturated, due to the fact that oxygen diffuses ten thousand times slower trough water than trough air and because the oxygen that is present is consumed by microorganisms (Blume et al., 2010). Under very anoxic conditions corresponding to $E_h$ values below -120 mV, carbon dioxide is reduced to methane. Also under reducing conditions poorly soluble salts can form which tend to precipitate.

### 3.2.4 DOC

DOC is one of the major groups of pollutants in landfill leachate. DOC consists of a collection of biological degradation products. DOC is a pollutant itself, but it also influences the behaviour of other contaminants by its contribution to redox processes and the ability to form complexes making heavy metals more mobile (Christensen et al., 1998). The DOC content in leachate is a combination of the organic content in the waste and how far the degradation process has progressed. The DOC concentration in landfill leachate can be up to thousands of milligrams per litre and this decreases over time as the landfill matures (Ehrig, 1983).

### 3.2.5 Ammonium

Ammonium ($NH_4^+$) is apart from organics the principle pollutant in landfill leachate. Ammonium is present in the leachate due to the deamination of amino acids during microbial degradation of organic material and because of nitrate ammonification, the reduction of nitrate to ammonia (Blume et al., 2010), of which the last process can only occur under aerobic landfill conditions. The ammonium concentrations in landfill leachate are initially increasing with time and generally reach a stable mean value between 500 and 1500 mg $N_{NH4}$/l (Kulikowska & Klimiuk, 2008).

## 3.3 UV absorbance

The absorbance of an aqueous solution is a measure for how much energy from electromagnetic waves is absorbed by the solution. The absorbance is defined as shown in equation 3.15. The Lambert-Beer law is given in equation 3.16, which relates the absorbance to the concentration of a certain species. This relation can be used to measure the absorbance of a specific wavelength with a spectrophotometer and then relate that to a concentration of a certain species, if is assumed that the species in question is the only one that absorbs energy from that specific wavelength. For example the absorbance at a wavelength of 254 nanometre is often used as a proxy for the DOC concentration (Hansen et al., 2016). If the absorbance is too high the linear relationship shown in equation 3.16 no longer holds.

$$A = -\log(T) = -\log\left(\frac{I_0}{I_1}\right) \quad 3.15$$

Where $A$ is the absorbance [-], $T$ is the transmittance [-], $I_0$ is the light intensity received [$MT^{-3}$] and $I_1$ is the light intensity transmitted [$MT^{-3}$].

$$A = \varepsilon c l \tag{3.16}$$

Where $\varepsilon$ is the species' molar attenuation coefficient [$L^2$], $c$ is the species' concentration [$L^{-3}N$] and $l$ is the pathlength [L].

## 3.4 Water retention

Solid porous material has the potential to retain water. Water will retain because of the molecular forces between the solids and the water, which causes a thin layer of adsorbed water to be present around the solids, and because of capillarity. Capillarity in soils or waste occurs if the solid particles form a pore and the force needed to overcome the intermolecular forces between the water and solid (adhesive force) and force of the surface tension of the water present in the pore (cohesive force) is larger than the gravity force, meaning the water will not be able to percolate and will retain in the pore. Smaller pores will hold on to the water stronger than larger pores, as both the adhesive and cohesive forces are larger for smaller pores. Figure 3.2 gives three typical water retention curves for soils, in this figure the effects of pore size are clearly visible. For waste the curves are different because the pore size distribution will be different, but the typical features are similar.

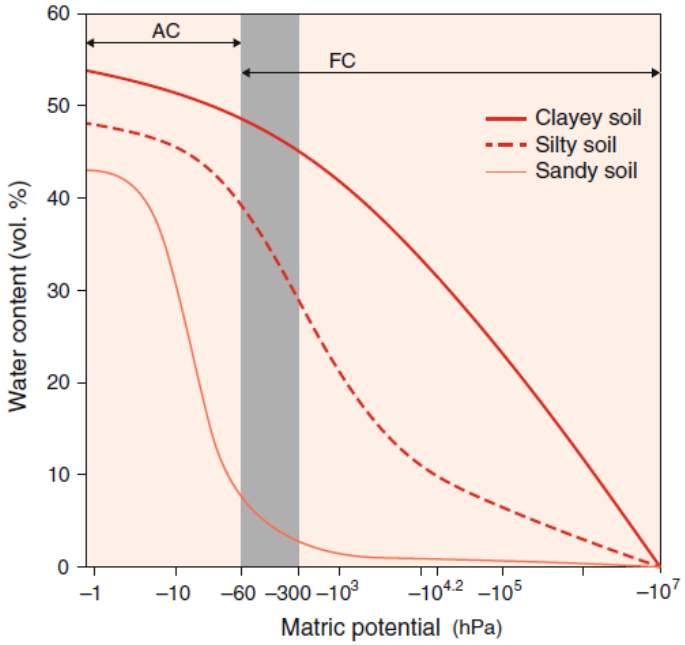


*Figure 3.2: Water retention curves (adapted from Blume et al., 2010)*

The most common formulation of a water retention model is the van Genuchten equation shown in equation 3.17, which gives the water content for negative pressure heads. If the pressure head is positive the pores are fully filled and then the water content is equal to the saturated water content.

$$\theta = \theta_r + \frac{\theta_s - \theta_r}{[1 + (\alpha|h|)^n]^{1-\frac{1}{n}}} \quad h \leq 0 \tag{3.17}$$

Where $\theta$ is the water content [-], $\theta_r$ is the residual water content [-], $\theta_s$ is the saturated water content [-], $\alpha$ is a curve fitting parameter related to the air entry value [$L^{-1}$] or [$LM^{-1}T^2$], $h$ is the pressure head [L] or [$LM^{-1}T^2$] and $n$ is a curve fitting parameter related to the pore size distribution [-].

## 3.5 Landfill water balance

A water balance is a method to calculate the change in water storage in a given system. Modelling the water balance is a useful tool in a landfill as often it is not feasible to model the physical flow of water through the different landfill components, especially because of the large heterogeneity present in a landfill. Using a water balance allows to learn something about the long term and large scale hydraulic behaviour. Water balances can become very complex, but in the end always represent equation 3.18.

$$water\ in\ -water\ out = \ change\ in\ storage \tag{3.18}$$

Figure 3.3 gives a schematic of the most important components for a water balance for an unsealed landfill. This particular example is a landfill which has no bottom sealing, however with a bottom sealing the only difference would be that the leachate flow is pumped out of the drainage system instead of leaking into the environment. The simplest landfill water balance that is possible, while still keeping the most important terms, is given in equation 3.19.

$$P - AEP - Q - RO\ = \Delta S \tag{3.19}$$

Where $P$ is the inflow of precipitation [L$^3$], $AEP$ is the actual evapotranspiration [L$^3$], $Q$ is the outflow of leachate [L$^3$], $RO$ is the surface runoff [L$^3$] and $\Delta S$ is the change in storage [L$^3$].

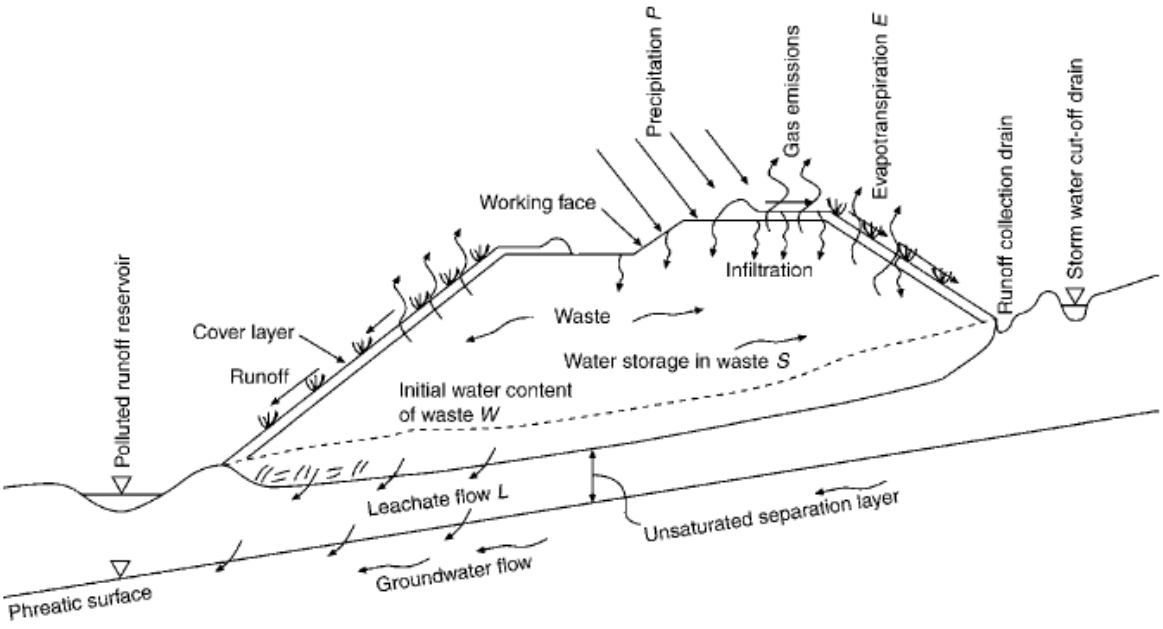


*Figure 3.3: Schematic of a landfill water balance (Blight & Fourie, 1999)*

# Part II - Lab and Field Measurements

# 4. Introduction to the lab and field experiments

The overall goal of this thesis is to quantify the causes of the low aeration efficiency and to find an effective solution for mitigating the reduced aeration efficiency. The presence of the aeration system allows for measurements to be performed that are unique to the Braambergen landfill. Often in literature is mentioned that due to the large heterogeneity of landfills, parameters derived at small scale are not appropriate to characterize entire landfills (Fellner et al., 2009), but with small scales measurements from the 132 relevant aeration wells, this heterogeneity can be quantified and used to characterize the whole compartment.

In order to describe the hydrology of the waste body and, in particular, the spatial variability of the hydrological properties of the waste and the leachate composition (see sub-questions formulated in section 1.3.3) the following five types of measurements have been carried out:

1. Water levels in the aeration wells, using dip meters.
2. Velocity and composition of the LFG extracted by the individual wells.
3. Response of the leachate to pumping leachate out of the wells.
4. Chemical properties of leachate in aeration wells.
5. Long-term monitoring of water head, temperature and electrical conductivity in a selection of fifteen aeration wells.

A detailed explanation of the measurements can be found in chapter 6. Chapter 7 contains the results of the measurements and the discussion of these results. The conclusions that drawn from the measurement results are presented in chapter 8.

# 5. Materials and Methods

This chapter presents the materials and methods used for the field and lab measurements. The subsections correspond to the different types of measurements mentioned in chapter 4.

## 5.1 Water table measurements

The water table measurements were performed in the aeration wells. The water levels were measured with a dip meter that is shown in figure 5.1. The dip meter is a measuring tape that makes a sound once the electrical circuit is completed, which happens once the part of the dip meter that lowered into a well makes contact with water.

*Figure 5.1: Dip meter*

To take the measurement, first the aeration wells was opened and therefore disconnected from the aeration system, then the dip meter was lowered into the well. Once the dip meter starts making a sound, the distance from the top of the well to the water level can be seen on the measuring tape. Then the dip meter was further lowered until the apparent bottom of the well is reached, which is the case when the dip meter cannot be lowered any further. This is the apparent bottom because there could also be another reason why the dip meter cannot be lowered more, for example when the well is broken or crushed by the waste. As the coordinates of the top of the wells are known, the water level, well depth and water column can be calculated with equations 5.1, 5.2 and 5.3.

$$WL = Z_{ToW} - L_W \quad 5.1$$

$$WD = Z_{ToW} - L_B + d \quad 5.2$$

$$WC = WD - WL = L_W - L_B + d \quad 5.3$$

Where $WL$ is the water level in the well relative to NAP [L], $Z_{ToW}$ is the height of the top of the well relative to NAP [L], $L_W$ is the length of the measuring tape when water is found [L], $WD$ is the well depth relative to NAP [L], $L_B$ is the length of the measurement tape when the apparent bottom is reached [L], $d$ is a dip meter constant [L], which is the distance between the electrode and the actual end of the dip meter and $WC$ is the water column [L].

## 5.2 Landfill gas velocity and composition measurements

The LFG flux measurements were performed on the metal pipes that connect the aeration wells to the blower. Figure 5.2 shows the divider, that guides the gas to or from the wells, and shows the access point to the inside of the pipes. Once the black cap is removed and the valve opened, the measuring devices can be inserted in or around the protrusion. Two devices were used, a gas velocity meter (Hoentzsch, TA10) and a gas composition analyser (Geotech, Biogas 5000). The gas velocity meter measures the velocity of the gas in the middle of in the pipe by determining the heat transfer between the device and the gas, which increases with increasing flow velocity. The gas composition analyser determines the volumetric fraction of carbon dioxide, methane (both by infrared sensors) and oxygen (by an electrochemical sensor), and is attached around the protrusion for the gas extraction.

*Figure 5.2: Divider system (left) and access point to the tubing (right)*

The gas composition was only analysed for the tubes extracting gas from the wells, as the injected gas is regular air. The velocity is measured is the maximum velocity in the pipe. The flux is always proportional to the maximum velocity in the pipe, but for turbulent flow the scaling parameter is larger than for laminar flow. For measured velocities below 15 meters per second, which is derived in equation 5.4, laminar flow holds and all measured velocities scale the same to volumetric flux.

$$v_{max,lam} = \frac{Re_{max,lam} \cdot \nu}{D} \approx 15.5\ m/s \qquad 5.4$$

Where $v_{max,lam}$ is the maximum velocity for which laminar flow occurs [$LT^{-1}$], $Re_{max,lam}$ is the maximum Reynolds number for which laminar flow occurs [-], which is 2100 (Bird et al., 2006), $\nu$ is the kinematic viscosity [$L^2T^{-1}$] and $D$ is the tube diameter [$L^2$].

The gas composition analysis reveals the share of landfill gas, additional carbon dioxide from aerobic degradation of waste and/or oxidation of methane, and of air in the total gas mixture. As the interest lies in the total amount of methane and carbon dioxide extracted, and not in their origin, the corrected LFG velocity is defined as in equation 5.5, although the origin of the measured gas concentrations does not have to LFG.

$$v_{LFG} = v \cdot (\varphi_{CH_4} + \varphi_{CO_2}) \quad 5.5$$

Where $v_{LFG}$ is the corrected LFG velocity [LT$^{-1}$], $v$ is the measured velocity [LT$^{-1}$], $\varphi_{CO_2}$ is the volumetric fraction of carbon dioxide [-] and $\varphi_{CH_4}$ is the volumetric fraction of methane [-].

To quantify the efficiency of the waste aeration, the definition presented in equation 5.6 is used. One possible way of describing efficiency would be to compare every well to the well with the highest LFG flow velocity/flux, however not alls well have the same potential of LFG that can be produced by the waste that surrounds the well, so in that case this would underestimate the efficiency of some wells. Therefore it was decided that the efficiency is evaluated based on only data from that particular well and is defined as the ratio between the measured LFG flow velocity and the theoretical maximum LFG velocity, which is the same as the ratio between the LFG flux and theoretical maximum LFG flux.

$$\eta = \frac{v_{LFG}}{v_{LFG,max}} \quad 5.6$$

Where $\eta$ is the efficiency [-], $v_{LFG}$ is the measured LFG flow velocity [LT$^{-1}$] and $v_{LFG,max}$ is the maximum LFG flow velocity [LT$^{-1}$], which is different for each well.

## 5.3 Pumping test

The pumping test was designed to determine the hydrological behaviour of the wells and the waste around the well. The goal of the pumping test was to determine the hydraulic conductivity of the waste. For this test a datalogger and a pumping device were needed. Figure 5.3 shows the used dataloggers, a CTD-diver (Model DI271, van Essen instruments) and a Baro-diver (Model DI500, van Essen Instruments), and the used pumping device, which is a jiggle pump. The jiggle pump is a long tube, with on the bottom a small opening that is blocked by a metal ball. When inserting the pump in a well and applying a continuous up and down motion water moves up in the pump. When the pump is pushed down, leachate can flow in around the metal ball, and when the pump is pulled up, the opening is blocked by the ball such that no percolate can flow out. The jiggle pump can be manually operated or with a mechanical driver, which is shown in figure 5.4.


*Figure 5.3: Divers (left) and jiggle pump (right)*

*Figure 5.4: Jiggle pump installed in aeration well with mechanical driver*

The mechanical driver was used in the wells where the water flowed back from the surrounding well so quickly with manual pumping that the recovery of the water level could not be determined. The mechanical driver allows for a more steady outflow of water for a longer duration.

The following procedure was used for the pumping test:

1. First the datalogger with the Baro- and CTD-diver was started with a measurement interval that is sufficient to capture the behaviour during and after the pumping. The chosen measurement interval was two seconds.
2. The well was opened and the CTD-diver, attached to a wire, was lowered into the well until the bottom was reached. The Baro-diver remained in the open air to measure the ambient pressure.
3. The jiggle pump was inserted into the well and lowered until the CTD- diver was felt. Then the jiggle pump was slightly raised such that during pumping the CTD-diver was not hit. The pumping starts by applying an up and down motion to the jiggle pump or by turning on the mechanical driver. The pumping stopped once the well was dry, or a sufficient amount of water was removed such that could be concluded that during pumping already the leachate in the well was supplemented with leachate from the waste body, which is about four litres.
4. The jiggle pump was removed from the well, while the CTD-diver stayed on the bottom of the well and keeps logging to measure the restoring of the water level.
5. Lastly after the water level had time to restore also the CTD-diver was removed from the well and the well was closed again.

The pumping test gave two types of valuable information: the variation of the electrical conductivity during/after pumping and the recovery of the water level in the well after the ceasing of pumping. The variation of the electrical conductivity can be used to determine whether the leachate further away from the aeration well has different chemical properties compared to the leachate within or close to

the well. The CTD-diver measures pressure, temperature and electrical conductivity. The Baro-diver only measures pressure. The water column in the well can then be calculated with equation 5.7. Equation 5.8 shows the equation that is used by the CTD-Diver to calculate the specific electrical conductivity.

$$WC = \frac{P_{CTD} - P_{Baro}}{\rho g} \quad 5.7$$

Where $P_{CTD}$ is the pressure measured by the CTD-Diver [$L^{-1}MT^{-2}$], $P_{Baro}$ is the pressure measured by the Baro-Diver [$L^{-1}MT^{-2}$] and $\rho$ the density of the leachate [$L^{-3}M$].

$$K_{T_{ref}} = \frac{K}{1 + \theta(T - T_{ref})} \quad 5.8$$

Where $K_{T_{ref}}$ is the specific electrical conductivity [$L^{-3}M^{-1}T^{3}I^{2}$], $K$ is the measured electrical conductivity [$L^{-3}M^{-1}T^{3}I^{2}$], $\theta$ is the temperature coefficient [$\Theta^{-1}$], which is 0.0191 $^{o}C^{-1}$, $T$ is the temperature [$\Theta$] and $T_{ref}$ is the reference temperature [$\Theta$], which is 25 $^{o}C$.

Figure 5.5 shows the expected curve of the measured water column during the pumping test. Five phases can be distinguished. Phase I is the pre-pumping phase when the diver is logging but is not yet inserted into the well, giving a water column of zero meters. Then in phase II, the diver is inserted into the well and measures the full water column. Phase III is the onset of pumping, where is water level is either almost fully lowered or only a small amount depending on how fast the percolate flows back into the well compared to the pumping rate. The water level is never fully lowered to zero as the diver is still at the bottom of the well. Phase IV is the ceasing of pumping and therefore the recovery of the water level, which exact shape is depending on the storativity and the transmittivity of the waste body. Lastly in phase V the water column is restored and no longer changing. The water level does not restore fully, because the water body in not infinite and some water is removed. With equation 5.9 can be calculated roughly what the volume of water is that is influenced by one well.

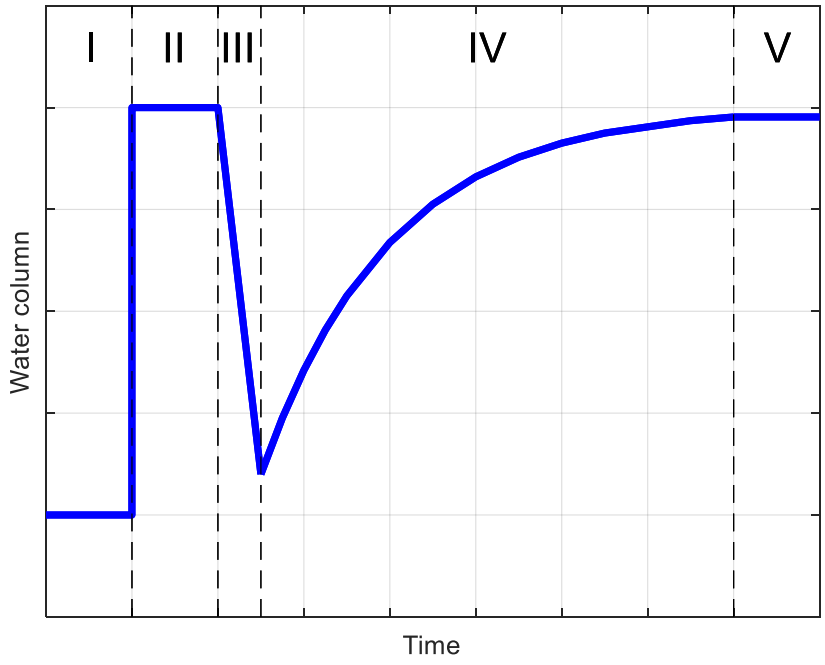


*Figure 5.5: Expected water column during the pumping test*

$$V = \frac{Q \cdot t_{III}}{WC_V - WC_{II}} \cdot (WC_{II} + d) \quad 5.9$$

Where $V$ is the total volume of the water body [$L^3$], $Q$ is the pumping rate [$L^3T^{-1}$], $t_{III}$ is the duration of phase III [T], $WC_{II}$ is the water column during phase II [L], $WC_V$ is the water column in phase V [L] and $d$ the distance between the bottom of the well and the bottom of the water body [L].

The distance $d$ is not a known factor, it could be anything between zero and the distance between the bottom of the well and the basal drain. Therefore it can be useful not to use the volume as a description of the water body that surrounds the well, but the radius of the water body. If is assumed that the water body has a cylindrical shape, then the radius of the water body is given by equation 5.10.

$$r = \sqrt{\frac{Q \cdot t_{III}}{(WC_V - WC_{II}) \cdot \pi}} \cdot \frac{1}{\varphi} \quad 5.10$$

Where $r$ is the radius of the cylindrical water body [L], $Q$ is the pumping rate [$L^3T^{-1}$], $t_{III}$ is the duration of phase III [T], $WC_{II}$ is the water column during phase II [L], $WC_V$ is the water column in phase V [L] and $\varphi$ the porosity of the waste [-].

Phase IV was used to calculate the hydraulic conductivity of the waste around the aeration well. Applying equation 3.12 gives the transmittivity of the waste, and since the water level is known, the hydraulic conductivity can then be calculated by dividing the transmittivity by the water column. There are however a few things that must be taken into account before applying the Theis solution. The waste aquifer is not a confined aquifer and the well is likely not penetrating the full aquifer, two things that are assumed by the Theis solution. Krusemann et al. (2000) mentions that also for an unconfined aquifer the Theis solution can be used, but that the data just after the ceasing of pumping does not fall onto the expected curve and should therefore not be used to determine the hydraulic conductivity. The same is mentioned for wells that are not penetration the full aquifer, if plotting the drawdown against the time factor gives a straight line it can be used to calculate the hydraulic conductivity, which should also occur for later times and not immediately after the ceasing of pumping. Also if there is a really large difference between the water column before and after pumping, the Theis solution is not valid and for those wells no hydraulic conductivity can be calculated.

## 5.4 Laboratory analyses of leachate

The possibility to sample leachate from the densely spaced aeration wells provided a unique opportunity to analyse the spatial variability of leachate properties, whereas usually these properties are only known for the bulk leachate leaving each landfill compartment. The lab leachate measurements have been performed to quantify the properties of the leachate from the aeration wells. These data were also compared with the biweekly measurements performed by Afvalzorg on the bulk leachate that is sampled from the leachate collection pit (PP in figure 2.2).

### 5.4.1 Sampling procedure

There is no standard sampling protocol to sample landfill leachate (Kjeldsen et al., 2002), and in addition to that, landfill leachate is almost solely sampled from drainage systems, and not directly from the waste. As in this study the leachate is sampled from the aeration wells and the leachate thus comes directly from the waste a consistent way of sampling was needed. The leachate was removed from the aeration wells with the jiggle pump shown in figure 5.3. Below the sampling method is described.

1. First the well was opened and the jiggle pump was inserted in the well. Then the pump was moved up and down for five strokes and the pump was removed from the well.

2. The leachate was removed from the jiggle pump. This leachate was not yet sampled, but discarded such that the inner part of the jiggle pump was flushed.
3. The jiggle pump was inserted again into the well, and the leachate was collected into a bucket. The pumping stopped after either leachate flowed out on the top of the pump or when was felt that the well was pumped dry. The pump was then removed from the well and the content was poured in the bucket.
4. The leachate in the bucket was mixed properly by rotating the bucket such that a homogenous sample could be taken. Then with the aid of a funnel two samples were taken: first one 50 millilitre tube and then a 200 millilitre bottle. Unless this was not possible because there was not enough leachate available, both were completely filled.
5. Lastly the bucket and funnel were rinsed with distilled water and the well is closed, the samples were kept cold until they could be stored. The tube was stored in a freezer and the bottle in a fridge.

Broken wells were not sampled as for those wells it was considered unlikely that the sample would be representative of the waste around the well.

### 5.4.2 Analysis of electrical conductivity, redox potential and pH

The electrical conductivity, redox potential and pH were all measured with electrodes connected to an electrochemical analyser (Consort, C6010). For these measurements the 200 millilitre samples stored in the fridge were used. The samples were taken out of the fridge 24 hours before they were analysed, such that all the samples had the same temperature and all the solid particles could settle fully after the samples had been moved to the measurement location. The electrochemical analyser can measure all three properties if the specific electrodes are used. The electrodes are inserted directly into the bottles.

The EC-electrode that measured the electrical conductivity was calibrated with a 0.01M KCl solution, the pH-electrode was calibrated with two buffers, one of pH 4 and one of pH 7, and the Redox-electrode, which is a Ag/AgCl reference electrode that uses a 3M KCl solution as the reference electrolyte, was calibrated with a special calibration fluid that has a known redox potential of 220 mV. All the measurements are corrected by the electrochemical analyser such that the reference temperature is 25 degrees Celsius.

### 5.4.3 Analysis of DOC

The DOC concentration in the samples was determined with an UV-spectrophotometer (DR6000, Hach-Lange). The UV-spectrophotometer cannot measure the DOC directly, but measures the absorbance of UV light with a wavelength of 254 nanometres which is often used as a proxy for the DOC concentration in aqueous solutions (Brandstetter at al., 1996). The measurements were performed on the samples stored in the fridge. The samples were taken out of the fridge one day before the measurements such that the sample temperature equilibrated with the lab temperature. As the DOC is the dissolved organic content in the sample, first the particulate organic carbon was removed by using a 45 micrometre filter. Then the filtered sample was placed into a cuvette and the absorbance was measured. If the absorbance was above the value of two, the sample was diluted five times and the absorbance was measured again. Equation 5.11 gives the expected relationship between measured UV-absorbance and DOC in the sample.

$$DOC = \alpha \cdot A_{254} \cdot DF + \beta \qquad 5.11$$

Where $DOC$ is the dissolved organic carbon [$L^{-3}M$], $\alpha$ and $\beta$ are scaling parameters [$L^{-3}M$], $A_{254}$ is the measured absorbance for UV light with a wavelength of 254 nanometres [-] and $DF$ is the used dilution factor [-].

The scaling parameters can be determined by linear regression between known concentrations and absorbance. For some samples the DOC has been directly measured by a commercial laboratory and in combination with the measured absorbance values the scaling parameters given in equation 5.11 have been determined.

### 5.4.4 Analysis of ammonium

Also the ammonium concentrations have been determined using the UV-spectrophotometer (DR6000, Hach-Lange), with the addition of an ammonium kit (LCK303, Hach-Lange). This kit contains a reagent that forms a complex with the ammonium ions, for which the relation between the absorbance and complex concentration known. The ammonium concentration is then calculated automatically by the UV-spectrophotometer. For this measurement, the samples stored in the freezer were used. The samples were taken out of the freezer a day before the measurements took place. The test is valid if the pH of the tested sample is between 4 and 9. First the samples were filtered with a 45 micrometre filter and then 200 microlitre of the sample was mixed with the reagent and after fifteen minutes the ammonium concentration was measured with the UV-spectrophotometer. If the concentration was above the limit of the cuvette test kit, the sample was diluted five times and tested again.

Table 5.1 gives an summarizing overview of the performed lab measurements.

*Table 5.1: Summary of lab measurements*

| Property | Sample storage | Measurement device |
|---|---|---|
| **Electrical conductivity** | Fridge | EC-electrode |
| **Redox potential** | Fridge | Redox-electrode |
| **pH** | Fridge | pH-electrode |
| **DOC** | Fridge | UV-spectrophotometer |
| **Ammonium** | Freezer | UV-spectrophotometer |

## 5.5 Long term monitoring of water columns and electrical conductivity

The goal of the long term monitoring is to analyse the temporal variation of water levels and electrical conductivity of the leachate in the aeration wells, especially in relation to the precipitation events. The divers shown in figure 5.3 were used, the Baro-diver was installed in an open container next to compartment 11Z and the CTD-divers were installed in fifteen selected aeration wells. As the CTD-diver remains in the aeration well for a longer duration, the connection between the aeration well and the divider system had to be changed. Initially on most wells a L-piece connection, shown in figure 5.6, was present between the wells and the tubing towards the divider system. For the monitored wells this was changed to a T-piece connection, also shown in figure 5.6. A 3D-printed part was designed by lab technician Roland Klasen which fits exactly into the T-piece and to which with a fishing wire the diver could be connected. Figure 5.7 shows the 3D-printed part as well as how the closed well looks like with the T-piece fully installed.

The divers were programmed to take a measurement each 15 minutes. The rainfall is measured on the landfill, as a small weather station is present on the east side of compartment 11Z. Each quarter hour is monitored how much rain has accumulated. The closest official KNMI weather station is in Lelystad, at roughly 30 kilometres distance from Braambergen. Figure 5.8 shows the cumulative rainfall measured since the installation of the divers for both the rainfall measured at Braambergen and by

the official KNMI weather station in Lelystad (KNMI, 2021) and show that the data from the Braambergen weather station and the official KNMI station are similar. Figure 5.9 shows the hourly rainfall measured on Braambergen that will also be used to compare with the diver measurements.

*Figure 5.6: L-piece connection pipe (left) and T-piece connection pipe (right)*

*Figure 5.7: 3D printed connection piece (left) and closed well after installation (right)*

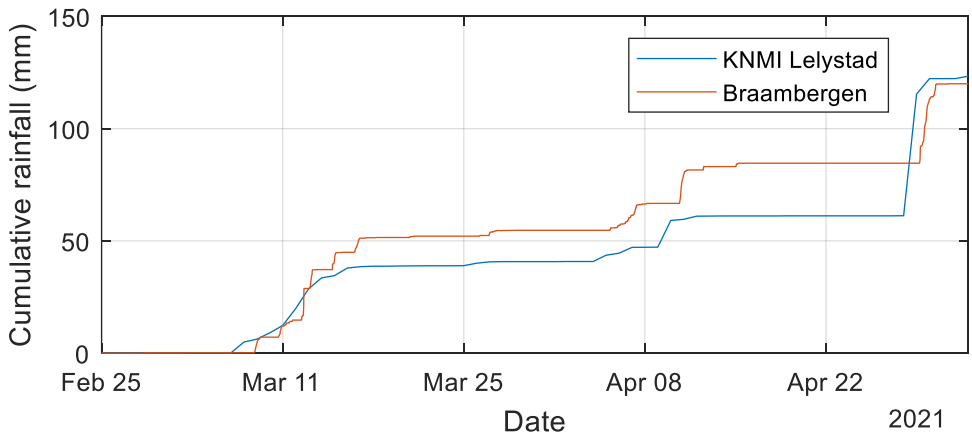


*Figure 5.8: Cumulative rainfall measured at the Lelystad KNMI weather station and on the Braambergen landfill during the investigation period*

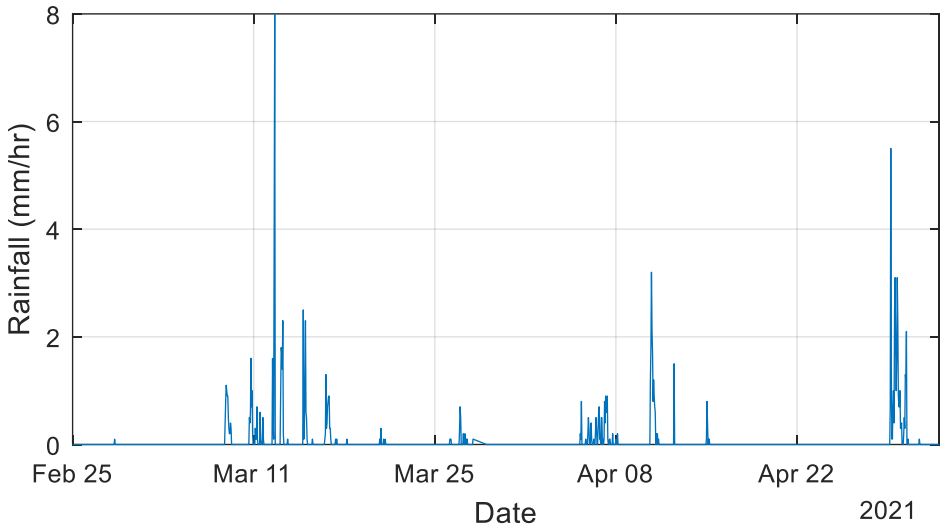


*Figure 5.9: Hourly rainfall measured on the Braambergen landfill during the investigation period*

# 6. Results and discussion

In this chapter the results and discussion of the experimental work are presented. First the results of the measurements are given and discussed (section 6.1 to section 6.4), after which the concept of the water distribution model is given (section 6.5).

## 6.1 Variability of water tables

The water tables in all aeration wells have been measured twice, once in December of 2016 (by Afvalzorg) and once in March of 2020 within the framework of this thesis (figures 6.1 and 6.2, respectively). In the figures, the white dots represent dry wells and the black dots represent broken wells for which the water level could not be measured.

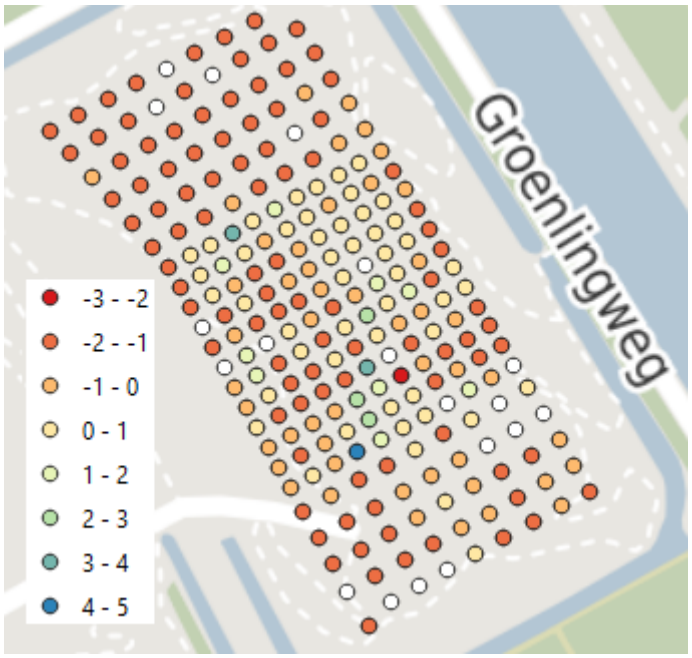


*Figure 6.1: Water levels in the aeration wells measured December 2016 (in m+NAP)*

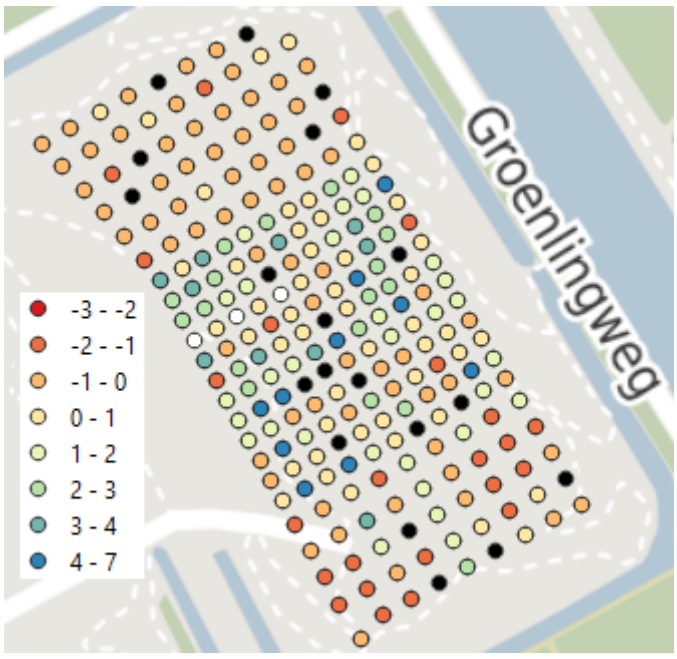


*Figure 6.2: Water levels in the aeration wells measured March 2020 (in m+NAP)*

As can be seen clearly in figures 6.1 and 6.2, the water levels are highest in aeration well rows G to R. This corresponds to compartment 11Z, and rows G and R (figure 2.5), which are according to the technical drawings just outside of compartment 11Z. It was therefore decided to focus during this thesis mostly on this compartment, as the problem of high water levels is most apparent in compartment 11Z. Figure 6.3 shows the water levels that were measured in November 2020 for rows G to R.

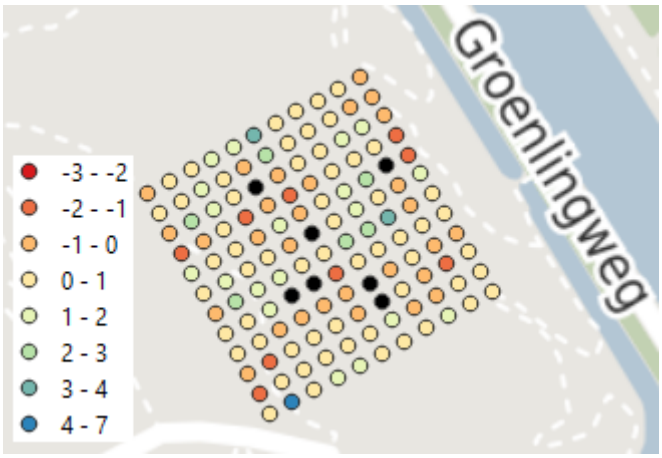


*Figure 6.3: Water levels in the aeration wells measured November 2020 (in m+NAP)*

The measurements can be interpolated such that also a water level can be given between to the locations of the measurement points. The advantage of this is that if spatial patterns are present these can visually be easier detected. Figure 6.4 gives the interpolation of the water levels for the November 2020 measurements. The interpolation has been done with TIN interpolation and the wells where no water level was measured have been excluded from the interpolation. Appendix C contains an explanation of how the TIN interpolation works and in appendix D the interpolations for the December 2016 and March 2020 measurements can be found. The interpolations do not show any clear high and low water level zones, only it is even more clear that the water levels in 11Z are higher than in 11N and 12, and especially the distinction between 11Z and 11N is really apparent in figures D.1 and D.2. The highest hydraulic gradient between to wells measured in November 2020 is 0.28 (-). According to Darcy's law one would expect flow to occur and the hydraulic gradient to disappear with time and the water level to equilibrate, unless there is a strong unequal distribution of rainwater or if the water bodies around the aeration wells are not connected to each other. The last seems be case, meaning that the interpolated water levels should be carefully interpret as they do not represent reality.

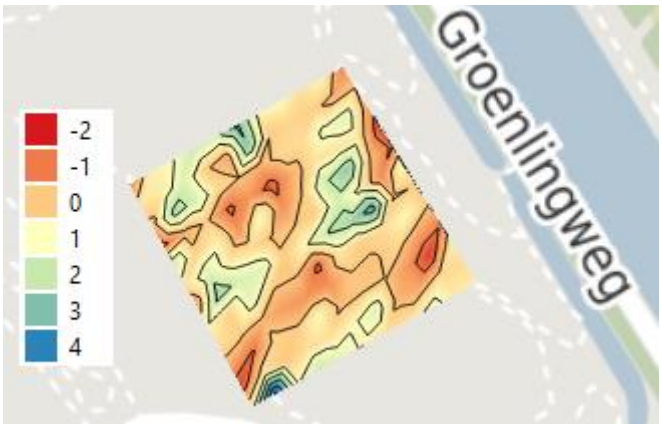


*Figure 6.4: Interpolated water levels in the aeration wells measured November 2020 (in m+NAP)*

The spatial variability of the measured water levels is large. In soils these large differences in water levels would not occur and since the waste in compartment 11Z consists for more than 95% out of soil and soil residues, the high variability in water level is likely to exist because the poor connectivity of the water bodies within the waste, which could for example be caused by the presence of plastic sheets, or differences in compaction.

### 6.1.1 Temporal variability of water tables

From figures 6.1 and 6.2 it is clear that in March 2020 the water levels measured in the aeration wells where generally higher than in December 2016. It is not possible to say whether generally the water level in the waste is increasing or not, as the measurements where not taken in the same period of the year and one could argue that the water level in the well does not necessary has to be the water level in the waste. Table 6.1 shows the average measured water levels in the different parts of the landfill during the three measurement campaigns. The division of the well rows is based on the spacing between the wells, if the average is taken of the entire landfill 11Z would be overrepresented as there is spacing between the wells is smaller. Table 6.1 shows that over the entire landfill the water level in the aeration wells was higher on March 2020 compared to December 2016, and also that it seems that for well rows G-R there is an increase in water level with time visible even when considering the seasonal variations. Figure 6.5 shows for well rows G-R the histogram of water level measurements for the three measurement campaigns, to get slightly more insight than is provided by just the averages.

*Table 6.1: Average water levels in the aeration wells (in m+NAP)*

| | Well rows A-F | Well rows G-R | Well rows S-W |
|---|---|---|---|
| **December 2016** | -1.20 | -0.14 | -0.78 |
| **March 2020** | -0.57 | 1.41 | -0.37 |
| **November 2020** | Not measured | 0.47 | Not measured |

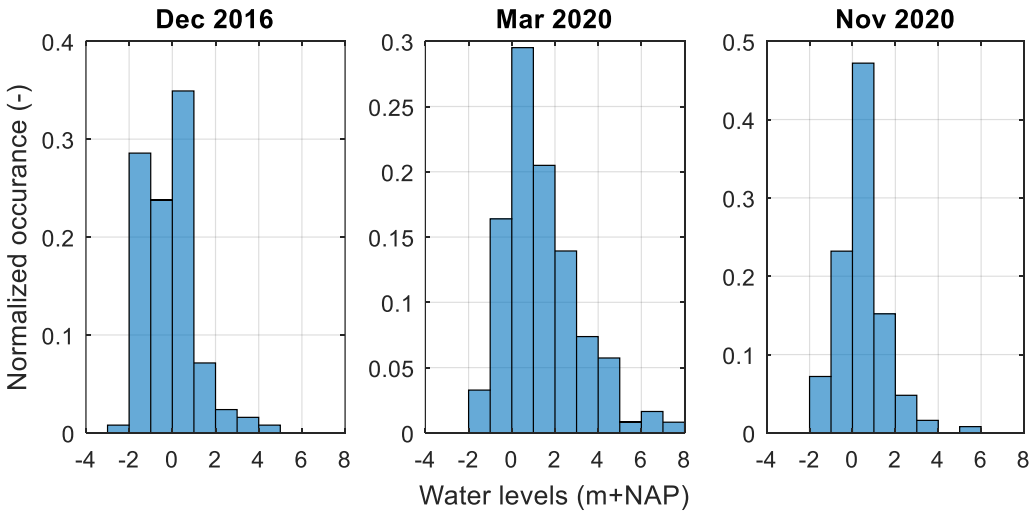


*Figure 6.5: Water level histograms for aeration well rows G-R*

Figure 6.6 contains a histogram that shows for all the wells from rows G-R which difference in water level is obtained when subtracting the March 2020 water level from the November 2020 water level. On average, the water level in these wells dropped 0.94 meters, but this average drop is simplifying too much the drop in water level over the entire compartment. Figure 6.6 shows that are wells for which the reduction of water level is only very minor or there is even an increase in water level, and that there are many wells which show a drop in water level much larger than the average.

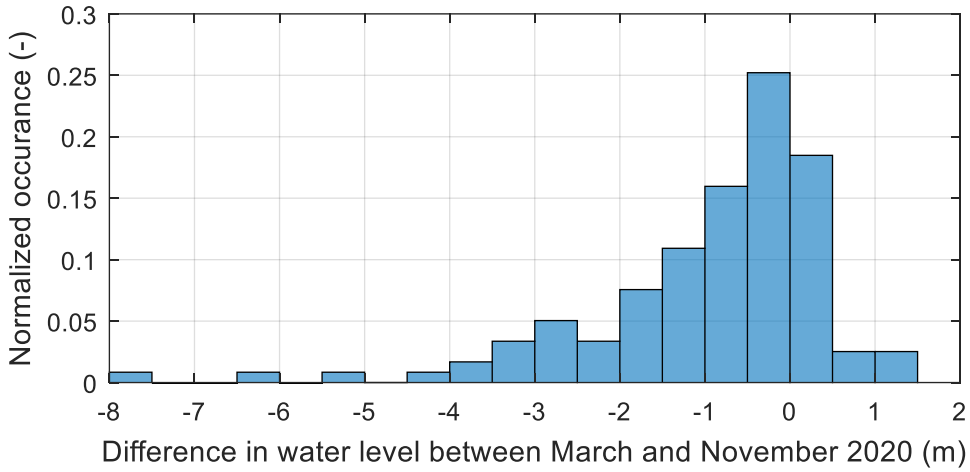


*Figure 6.6: Change in water level between March and November 2020 (November – March)*

To really capture the temporal variability of the water levels in the aeration wells more frequent measurements are needed. Figure 6.7 shows the results of the water level measurements that have been performed more regularly on a few aeration wells in 11Z by Afvalzorg in the period from October 2018 to August 2019. The variability seems to be large for some wells, while other wells only show very little variation in water level over time. It is clear that the water retention in the waste around the wells behaves very differently over the compartment.

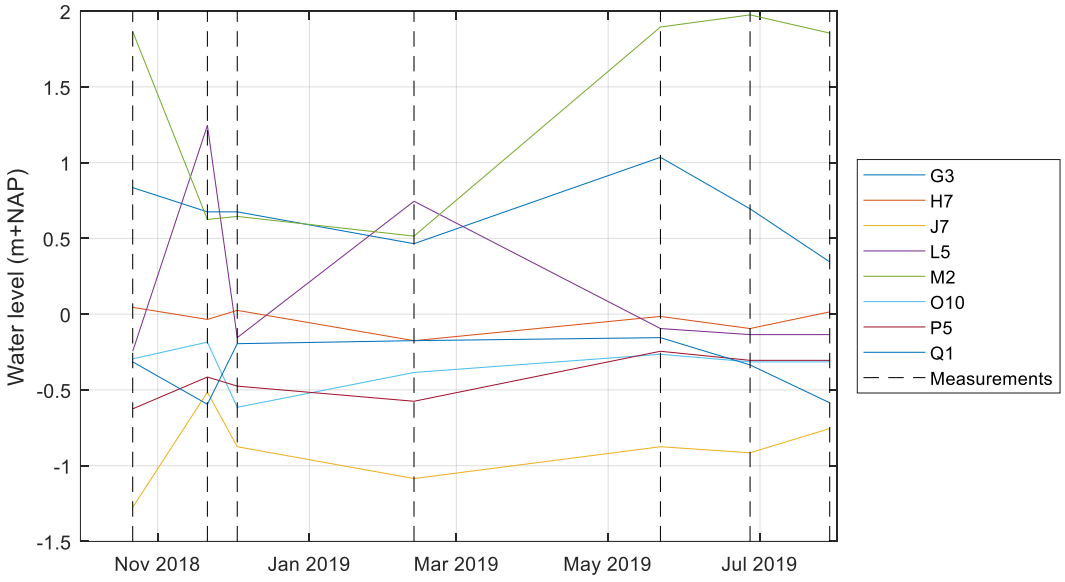


*Figure 6.7: Temporal variability in water level for a few wells in 11Z*

### 6.1.2 Influence of the old gas wells

Given how the old gas wells are constructed, which is illustrated in section 2.4, it was suspected that the old gas wells could provide a flow path for the leachate towards the basal drain. In October 2020, the water levels and states of the old gas wells have been measured and observed by Afvalzorg, and the summary of those measurements can be found in appendix E. The water levels in the old gas wells are lower than in the aeration wells, agreeing with the idea that water can flow towards the drainage system and does not accumulate in the wells. Figure 6.8 shows the water levels measured in the aeration wells against the distance to the nearest old gas well. The fact that there is no apparent

correlation visible in figure 6.8 is an indication that there is very little horizontal connectivity, as otherwise the water levels would be relatively lower in aeration wells close to the old gas wells.

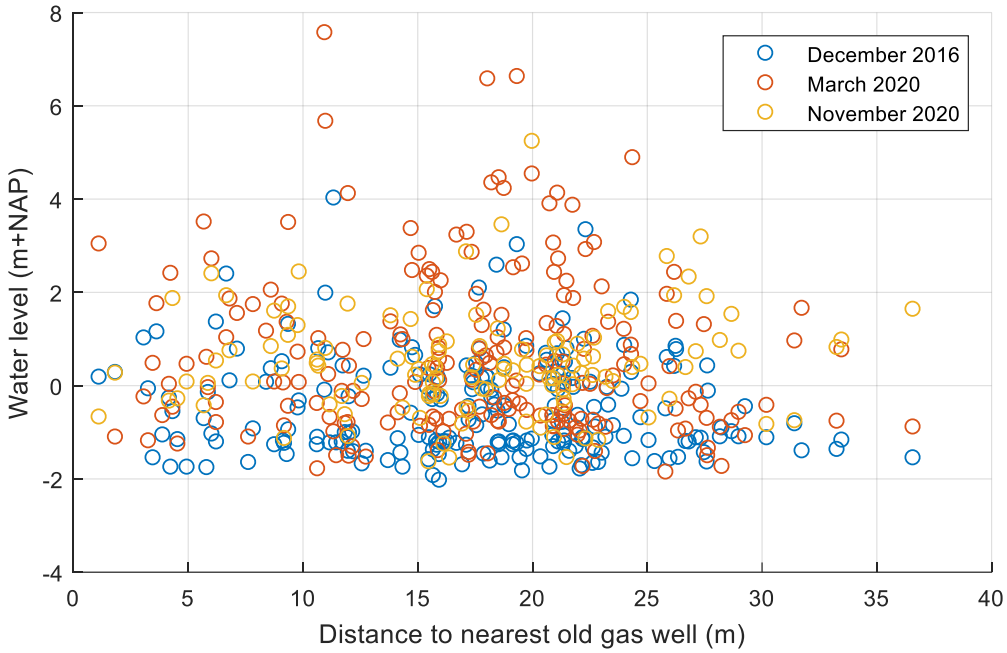


*Figure 6.8: Influence of old gas well on the water level in the aeration wells*

## 6.2 Velocity of landfill gas flow

Figures 6.9 and 6.10 shows the LFG flow velocity through the piping that is connected to the aeration wells against the water column observed in the aeration wells. Figure 6.8 contains the water column data measured in March 2020 and the flux measurements of two campaigns surrounding the water column measurements, one from February and one from March 2020. Both the water column and gas velocity measurements shown in figure 6.9 are from November 2020, but from different campaigns.

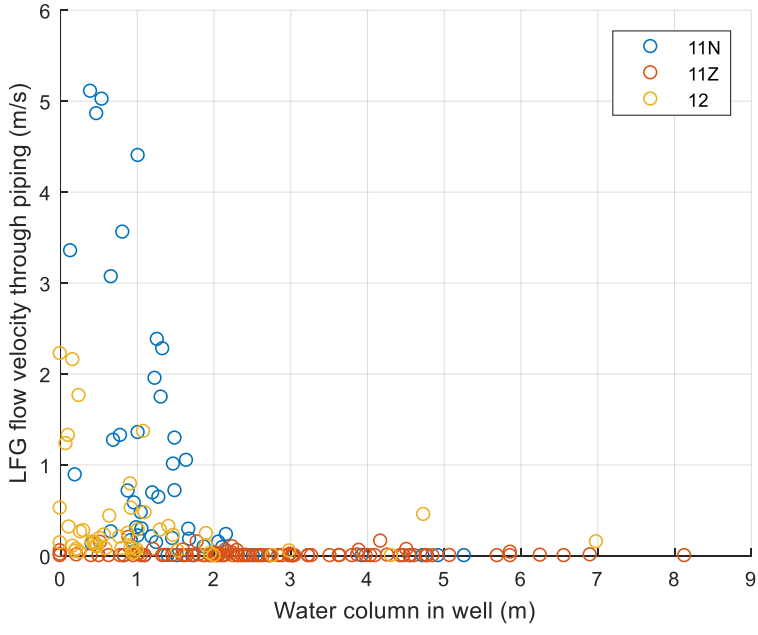


*Figure 6.9: LFG flow velocity in aeration wells in February/March 2020*

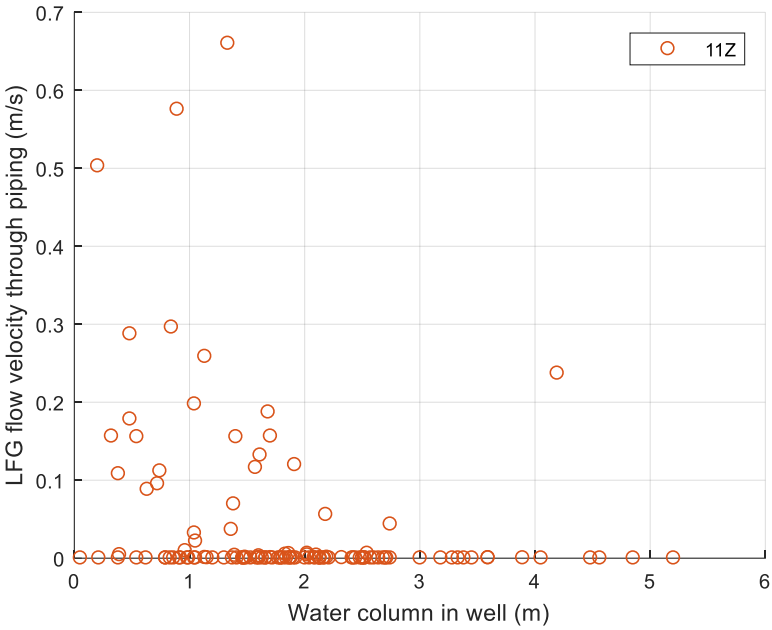


*Figure 6.10: LFG flow velocity in aeration wells in November 2020*

The reason that for figure 6.9 two flux measurement campaigns have been used is because of the alternating injection-extraction aeration method. For the extracting wells the fraction of flow coming from the waste can be determined based on the volume fraction of $CO_2$ and $CH_4$ in the measured flux. Comparing only the uncorrected flux values for both injection and extraction not be representative as different pressure differences are applied for injection and extraction. Therefore the data of two campaigns has been used, such that for all wells the extraction could be taken into account. For figure 6.10 all the flux measurements were taken on the same date, as due to a defect in the aeration system all wells were in the extracting mode.

The flux and water column measurements are thus not taken on the same day, but the temporal variability of the water level that is presented in figure 6.7 shows that the general trend of the water level in the wells is that there is little variation within a month and therefore it is justified that the measurements taken on different days are used in the same plot.

Figure 6.11 shows the expected relationship between the flow velocity of the LFG and the water column measured in the wells. This relationship comes from Darcy's law and the design of the perforated part of the aeration wells, which is the bottom 1.8 meter of the well. If the water column is therefore more than 1.8 meter, there can be no gas flux through the filter screen. Darcy's law then predicts that there is a linear relationship with the water column and LFG flow velocity for lower water columns. In reality the aeration wells are all on their own line as shown in figure 6.11, but with a different slope for each well, as the flow velocity is also depended on the permeability of the waste.

As can be seen in figure 6.9, for compartments 11N and 12 this predicted relationship is clearly visible. For compartment 11N the slope of the line capping the measured datapoints is larger than for compartment 12. However for compartment 11Z this relationship is not visible. In compartment 11Z the most wells had a water column of above two meters, but also in the wells with a lower water column barely any flow was measured. From figure 6.10 it is clear that with the lower water columns in November compared to March, the flow increased slightly, but still not to the magnitude that was measured in compartments 11Z and 12. The gas flow is thus not only restricted by the water levels, and Darcy's law then shows that the reason for the lower flow is also the lower permeability in the

waste in compartment 11Z compared to compartments 11N and 12. This is likely to be the case because of the large amounts of soil and soil residues present in compartment 11Z compared to compartments 11N and 12. Another possibility would be that there is just very little LFG produced in compartment 11Z and that the LFG flux is low because of that, but if that was the case there would be a similar amount of total extracted flux, but just a smaller percentage of LFG, but this is not what is observed. Soil residues can have very low absolute permeabilities compared to other waste types. Also is the relative permeability just above the water table small due to capillary action.

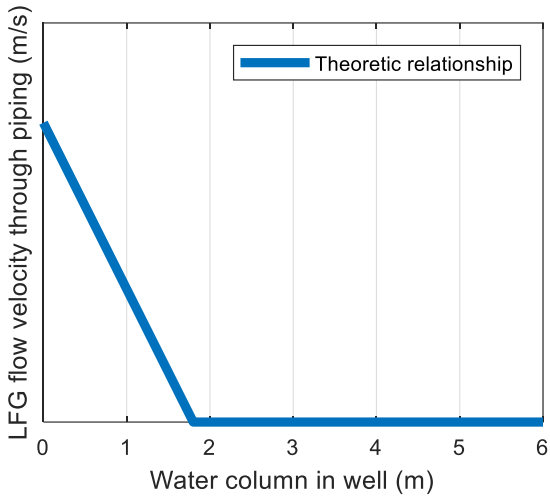


*Figure 6.11: Theoretic relationship between the LFG flow velocity and water column*

As figure 6.9 and 6.10 show that the theoretical relationship seems to hold, therefore the definition of the efficiency of the wells given in equation 5.6 can be extended. Equation 6.1 gives the efficiency of the aeration wells in terms of the water column measured in the well.

$$\eta = \frac{v_{LFG}}{v_{LFG,max}} = 1 - \frac{\min(WC, PL)}{PL} \qquad 6.1$$

Where $WC$ is the water column [L] and $PL$ is the perforated length of the aeration wells [L], which is 1.8 meter.

From equation 6.1 follows that the efficiency of the aeration wells increases linearly with a reduction of the water column if the water column is lower than the perforated length, and if the water column is larger than the perforated length the efficiency is zero.

## 6.3 Waste hydraulic conductivity

First an example is given of how results are obtained from the raw data gathered by the divers, then the different observed responses of the wells and the long term hydraulic response are given.

### 6.3.1 Example of evaluation of the pumping test

Figure 6.12 shows data obtained for a typical pumping test, performed on well R2. The five expected stages of the water column during the pumping test that are described in section 5.3 are clearly visible. The fact that the water level restored proves that the water is not only present in the well, but also in the waste surrounding the well. The measured temperature increased rapidly once the diver is was the well, as the equipment needs some time to equilibrate, but does not change during pumping or recovery. This is as expected as the temperature of the leachate is in equilibrium with the waste and the leachate that flows into the well should not have a temperature that is different than what is inside

the well. Therefore when evaluating the pumping test data, the temperature at the well location is considered to be the maximum observed temperature. The conductivity seems to decrease slightly after a few seconds and then increases again at the very end of the test. This is observed for all the pumping tests and is likely a distortion in the measurements due to movement of the diver. During the recovery phase of the pumping test the conductivity remained nearly unchanged. This means that the leachate that flows into the well from the waste has a conductivity that is the same as the stagnant leachate that is initially in the well. This proves that the water in the well is connected to the water in the waste and not, for example, just condensate or rainwater that is present only in the well. The conductivity at the well location is considered to be the median of the observed conductivities. Appendix F gives the water column measured during the pumping tests of all the wells as well as the considered temperature and electrical conductivity value.

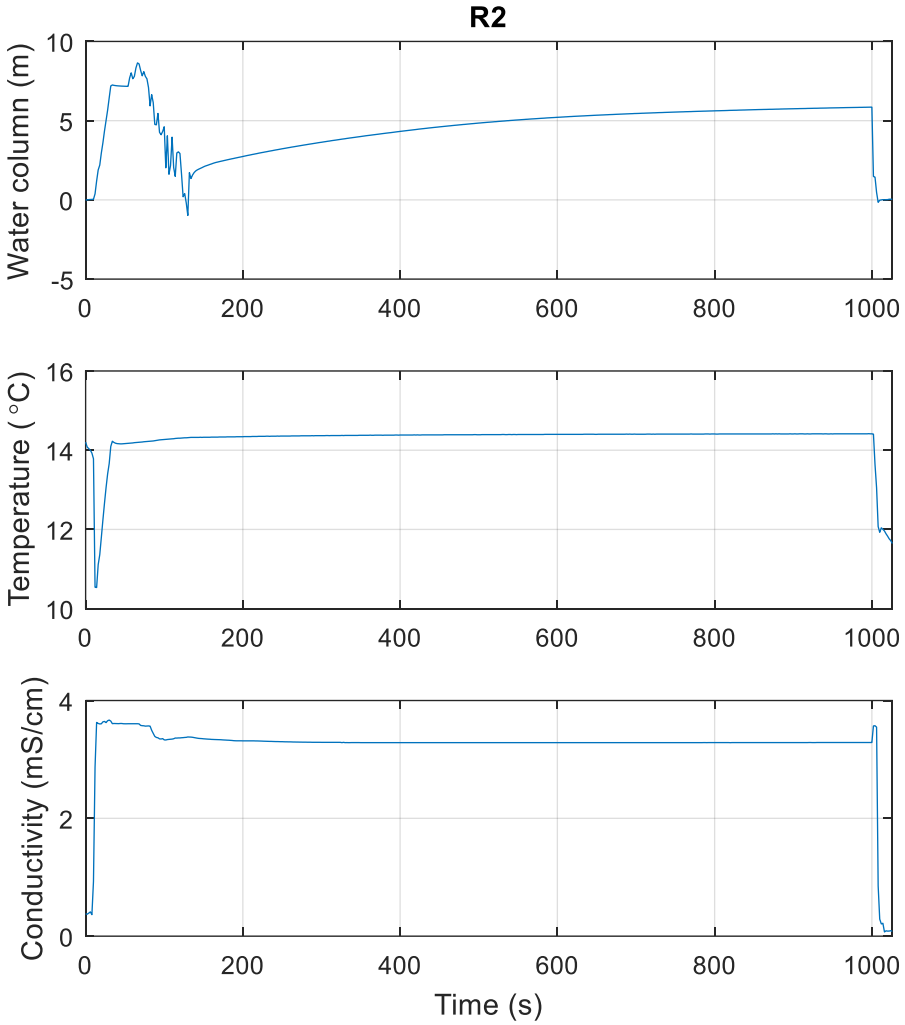


*Figure 6.12: Time course of water column, temperature and electrical conductivity during a pumping test on well R2*

The change in the water column over time can be used to determine the hydraulic conductivity of the waste around the aeration well using equation 3.12. Figure 6.13 shows the water column during the recovery phase, plotted as residual drawdown against the time factor, the logarithm of the ratio of time since the start of pumping and the time since the ceasing of pumping. The plot also shows two straight lines fitted through the data, one that takes into account all the data points collected by the

diver during the recovery phase, and one that only takes into account the second half of the data points for which the curve shows a clear linear relationship. The fit to the full data set is not valid as the fit does not correspond to any straight line segment in the data. The fit to the second half of the data is valid as the fit falls onto the straight line segment of the later data points. The hydraulic conductivity calculated is $1 \cdot 10^{-7}$ meter per second.

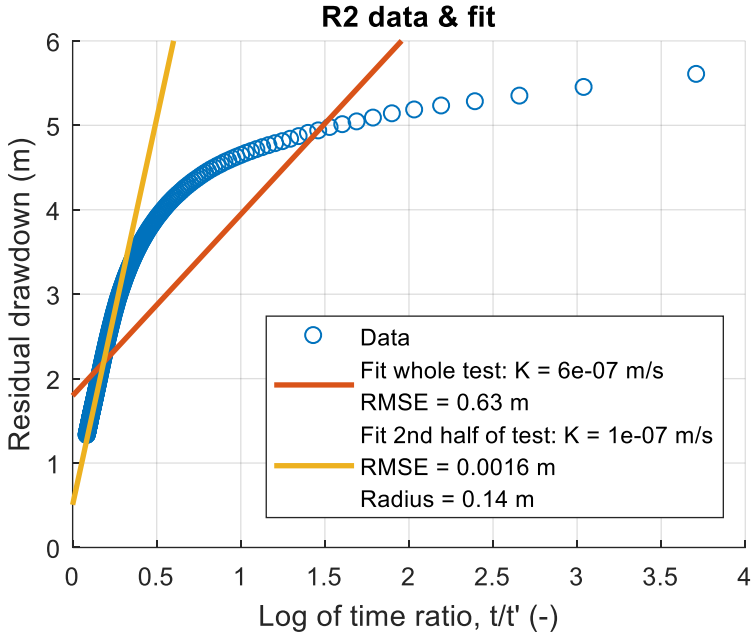


*Figure 6.13: Water column data processing for well R2. t = time since start of pumping, t' = time since ceasing of pumping*

The valid fit of the second half of the data points of the recovery phase does not intersect the y-axis at the zero point, which means that given the recovery so far and the shape of the Theis solution, after an infinite amount of time the water column is not the same as before the pumping test. The average pumping rate during all the pumping tests was 2.8 litres per minute. Applying equation 5.10 then yields that the radius of this cylindrical water body is only 0.14 meters. This means that the water flowing towards the well during the test is locally present around the well and the water further away is less or not mobile. The found hydraulic conductivity is only representative for this small part of the waste around the well.

### 6.3.2 Classification of hydraulic behaviour

The example given in section 6.3.1 is a perfect example of how the pumping test can be used to determine hydrological properties of the waste around the aeration wells. However not every well has this perfect recovery curve. The wells are therefore divided in six classes based on the recovery curve. Table 6.2 shows the classes and which parameters can be obtained for the class.

*Table 6.2: Pumping test classes*

| Class | Description | Parameters (* maybe) |
|---|---|---|
| **1** | Instant recovery | Radius*, $K$*, $T$, $EC$ |
| **2** | Slow recovery | Radius*, $K$*, $T$, $EC$ |
| **3** | No recovery | $T$, $EC$ |
| **4** | Different behaviour | $T$, $EC$ |
| **5** | Well too dry to test | $T$*, $EC$* |
| **6** | Well broken and not tested | - |

Figure 6.14 gives an example of each of the different classes, except for classes 5 and 6 for which no recovery curve can be obtained. In class 1 are the wells for which the recovery is so quickly, that the inflow of leachate from the waste is the same as the removal of water with the jiggle pump. There is maybe a recovery curve that can be fitted to the Theis solution, but if there is a reduction in total water level due to the removed leachate, a radius of influence of the water body can be given. The wells that are in class 2 show a slow recovery, and thus can be used to determine the hydraulic conductivity and the radius of influence, but only if the conditions to apply Theis solution are met. In class 3 there is no clear recovery present, this can be because the recovery is either too slow, and not measured during the time that the diver is in the well, or because the leachate is only present in the well and not in the surround waste, however if that is the case then the conductivity in the well should also be really low. Class 4 are the wells that do show a recovery, but the shape of the recovery curve is not as expected according to the Theis solution, in most of the cases this corresponds to a decreasing water column even after the ceasing of pumping. In class 5 are the wells for which the water level was too low, and no water could be pumped out of the well. Class 6 contains the wells that were known to be broken and therefore not opened, the wells for which it was impossible to lower the diver due to some narrowing in the well and the wells that where too deep to be pumped.

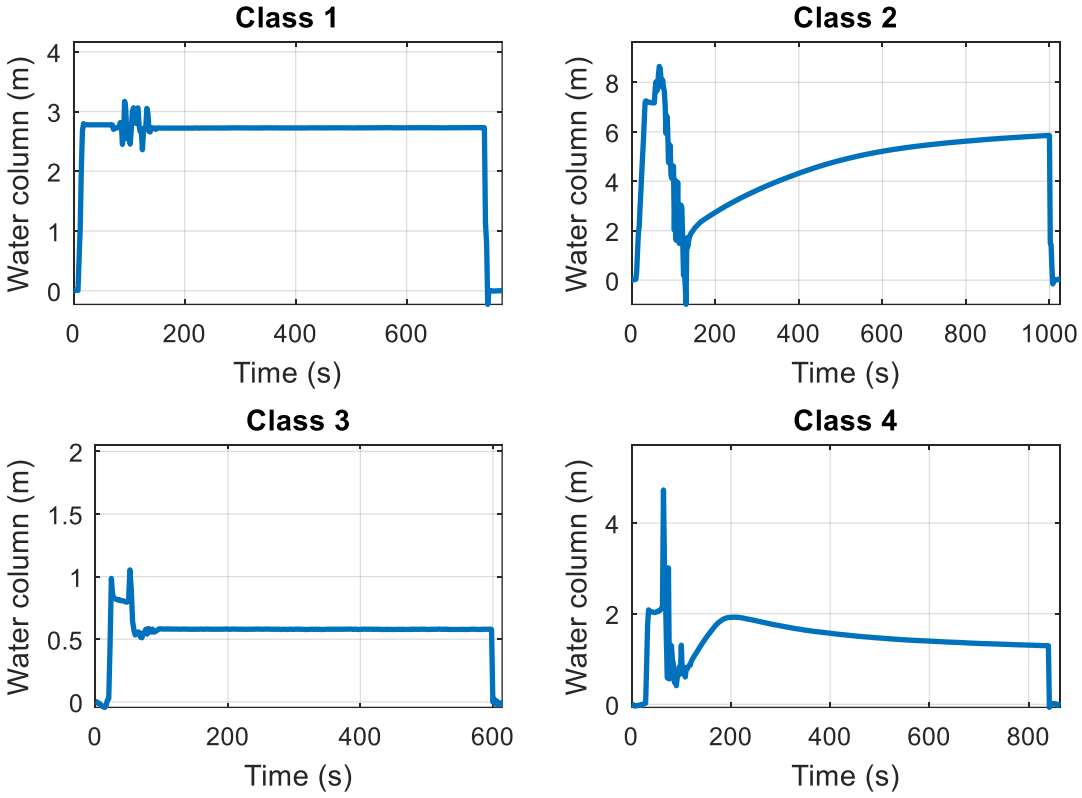


*Figure 6.14: Different pumping test response classes examples*

Figures 6.15 and 6.16 show how the classes are spatially scattered in the landfill, and a pie chart showing the relative size of the classes. Figure 6.15 shows that the different classes are widely spread over the compartment. From figure 6.16 can be concluded that there is not a class of response to the well test that is predominant. In the north-eastern part the compartment the wells tend to show a faster recovery than in north-western part, but overall there is not a part of the landfill where one class is really dominant. For some wells the applied pumping rate could be applied longer to remove more leachate, but using a single pump to lower the water level in the entire landfill does not seem to be a realistic solution.

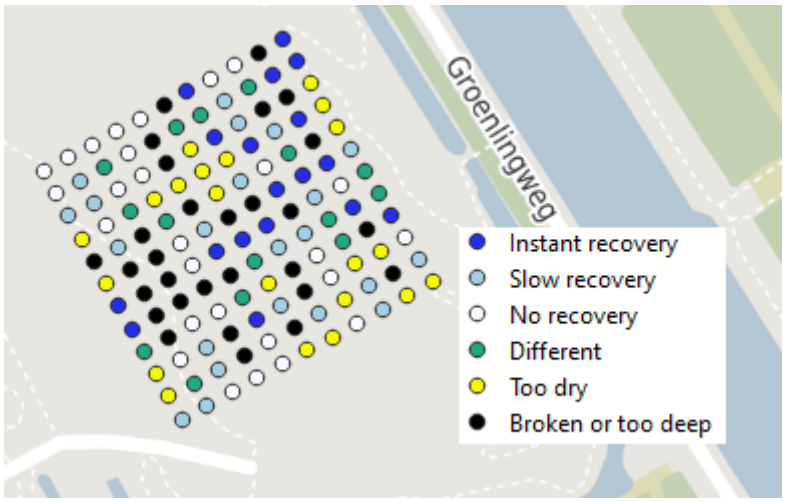


*Figure 6.15: Spatial graph of pumping test well classes*

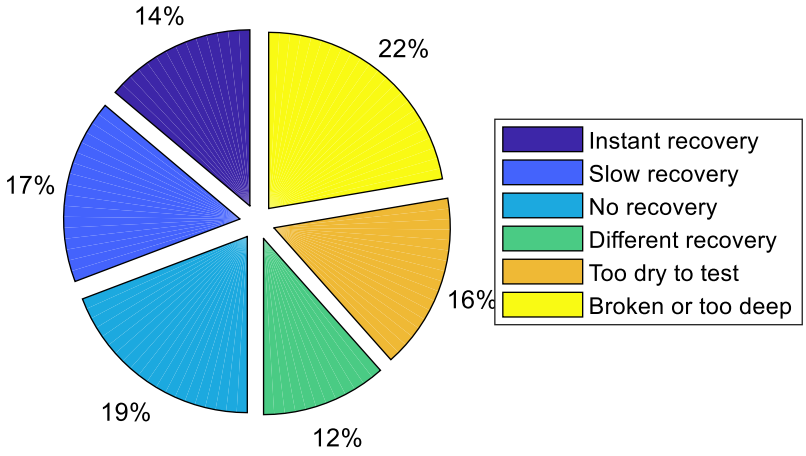


*Figure 6.16: Pie chart of pumping test well classes. Total number of wells = 132*

### 6.3.3 Wells showing fast supply of leachate

With the manual pumping of the jiggle pump it is hard to keep a constant pumping rate for over a minute, because once the pump is filled with leachate the pump is heavy and it takes quite some physical effort to keep pumping. With the mechanical driver shown on figure 5.3 it is however possible to keep a constant pumping rate for a longer duration. Therefore five wells for which during the manual pumping it seemed that it would be possible to extract leachate for a much longer duration, were tested again with the aid of the mechanical driver. Figure 6.17 shows for well L8 the pumping test data while the results for the other tested wells, G1, G7, M6 and P5 can be found in appendix G. During the pumping with the mechanical river in well L8, roughly 30 litres of leachate was removed, reducing the water level with about 0.5 meters. Even for this well which shows really fast recovery, the size of the free standing leachate body surrounding the well is relatively small compared to the size of the compartment. For the other four wells that were pumped with the mechanical driver, three of them recovered so fast that no clear recovery curve was obtained, and one of them was pumped dry and did not show any recovery. Table 6.3 shows an overview of the results of the pumping tests performed with the mechanical driver. The results showed that for most of the wells the mechanical driver did not succeed in lowering the water column a lot, and therefore it was decided to not retest the other instant recovery wells besides these five.

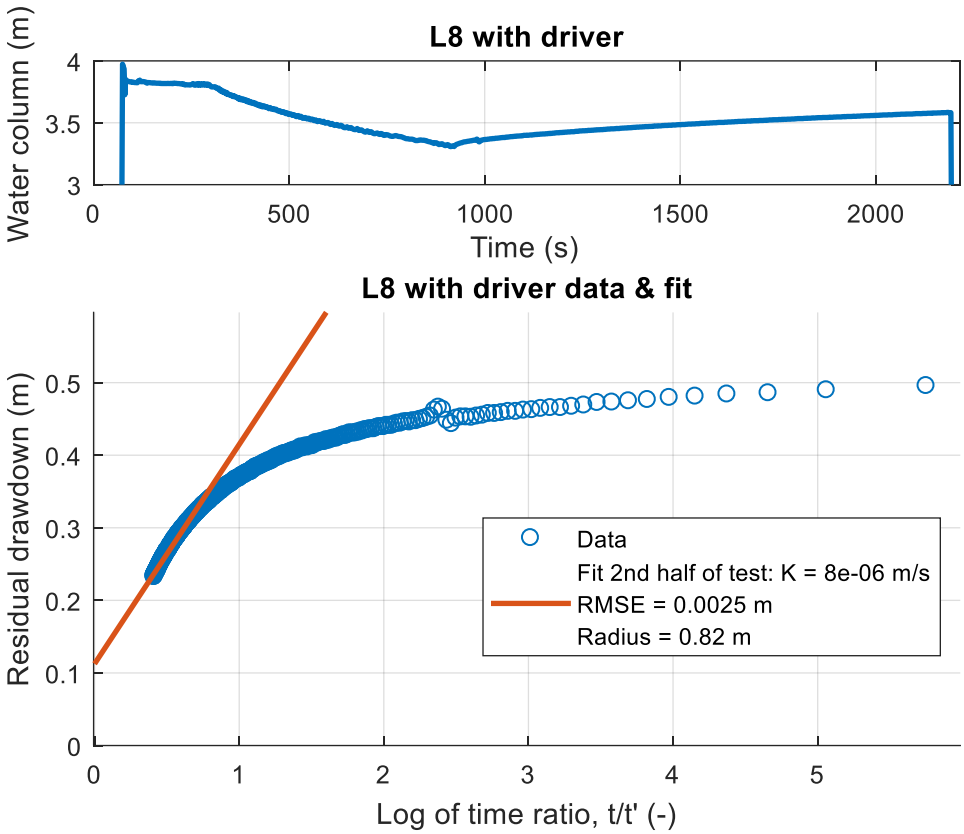


*Figure 6.17: Pumping test results for 'instant recovery' well L8*

*Table 6.3: Summary of parameters obtained from the pumping test performed on five selected fast supplying wells*

| Well | Volume pumped (L) | Radius (m) | $K$ (m/s) | EC (mS/cm) | Temperature (°C) |
|---|---|---|---|---|---|
| **G1** | 5 | - | - | 3.47 | 14.9 |
| **G7** | 38 | 1.37 | $3 \cdot 10^{-4}$ | 4.63 | 14.3 |
| **L8** | 31 | 0.82 | $8 \cdot 10^{-6}$ | 9.69 | 14.6 |
| **M6** | 49 | - | - | 4.18 | 14.5 |
| **P5** | 57 | 1.45 | $6 \cdot 10^{-4}$ | 11.44 | 14.3 |

### 6.3.4 Waste hydraulic conductivity

The hydraulic conductivity and radius of the hypothetic water bodies must be interpreted carefully. Only a few of the hundred wells on which the pumping test was performed gave recovery curves that could be interpret with the Theis solution. A lot of assumptions have been made to simplify the Theis solution, and based on the fact that almost all the wells did not show full recovery to the level before pumping, it can be concluded that the assumption that the leachate body is infinite in size is not at all met. Therefore the calculated hydraulic conductivity values should be seen as rough estimates. Also the method used to determine the radius of the water body is biased towards a certain range of radii, and should therefore be interpreted qualitatively. Figure 6.18 shows a boxplot with the spread of the hydraulic conductivities and radii calculated. For thirteen wells the hydraulic conductivity could be estimated, and for 25 wells an estimate of the radius of the water body could be given. Based on the hydraulic conductivity values can be concluded that there is a large spread of hydraulic conductivities that corresponds to values that are observed from silty soils to more coarser sands, which is not unexpected given that most of the waste in compartment 11Z are soils and soil residues. The values

are rough estimates, but represent the order of magnitudes of horizontal hydraulic conductivities that could be expected in the landfill.

As mention before, the calculated radii should be interpret qualitatively, as the really large and really small radii cannot be reliably calculated. What the values do show, is that there are bodies of leachate present in the landfill that are isolated from the rest of the of the landfill. This also partly explains the enormous differences in water levels measured in the aeration wells.

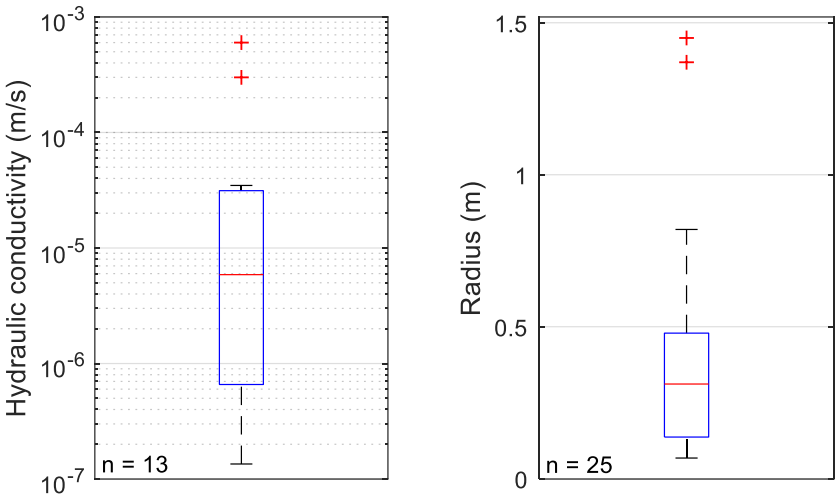


*Figure 6.18: Boxplot of calculated hydraulic conductivity (left) and radius (right). Box = interquartile range, line = median, whiskers = extremes, red crosses = outliers*

### 6.3.5 Long term hydraulic response

Based on the results of the previously performed measurements, a selection of fifteen aeration wells was made which were monitored with the CTD-diver for a longer duration. The long term monitoring took place from the 25th of February 2021 until the 5th of May 2021.

Typical cause-response relationships that were expected to be encountered are the slow increase of the water column after a large rainfall event. Or in case of preferential flow paths around the wells an instant increase in water column and an instant decrease in electrical conductivity due to addition of poorly conducting rainwater. If there is no response from the rainfall then this is either because the rainwater is retained in the soil, which can occur if the soil is dry, because the rain does not get to the well as a result of preferential flow or the permeability is high enough to instantly drain the rainwater. The potential evapotranspiration on average increased roughly linear from 1 to 3 millimetres per day throughout the measurement duration.

As the pumping tests and the chemical analyses showed large variability in hydraulic and chemical properties, the goal was to make a selection of aeration wells that represents as best as possible the range of hydraulic properties found for compartment 11Z. For the selection, the electrical conductivities measured in the lab (section 6.4.2.2), the water levels measured in March 2020 (section 6.1) and the response to the pumping test (section 6.3.2) are taken into account. The goal was to make a balanced selection that included wells with high and with low water levels, and wells with low and with high electrical conductivities. As a pilot 16 of the aeration wells on compartment 11Z were lifted in February 2021 to move the aeration filter screen out of the saturated zone. Also two of these wells have been included in the selection. Table 6.4 shows the wells that have been selected and the reasoning for the selection.

*Table 6.4: Wells selected for long term monitoring*

| Well | Reason |
|---|---|
| **G1** | Low conductivity (3.51 mS/cm) |
| **G8** | Aeration well lifted |
| **H2** | Low conductivity (3.24 mS/cm) |
| **J2** | Low conductivity (2.88 mS/cm) |
| **J9** | Aeration well lifted |
| **K9** | High water level (2.76 m + NAP) |
| **L8** | Interesting response to the pumping test |
| **M10** | Low conductivity (3.53 mS/cm) |
| **N1** | High conductivity (12.3 mS/cm) |
| **N6** | Low water level (- 1.12 m + NAP) |
| **O9** | Interesting response to the pumping test |
| **P5** | High conductivity (11.5 mS/cm) |
| **P10** | Low water level (-1.64 m + NAP) |
| **Q2** | High conductivity (13.2 mS/cm) |
| **R2** | High water level (5.23 m + NAP) |

Some of the monitored wells show a very interesting response to the rainfall, and those are discussed individually in the following subsections. The results of the other monitored aeration wells that show less response as well as the measurements of the Baro-diver can be found in appendix I. All the figures also contain the water columns measured in March and November 2020, and the electrical conductivity measured in the lab from the samples taken in December 2020 for comparison.

#### 6.3.5.1 Well H2

Figure 6.19 shows the measured water column and electrical conductivity in aeration well H2 during the long term measurements. In the first month, the water column dropped by more than 2.5 meters, after which the water level still fluctuated, but only in the range of a meter. This well shows that within a month the water column can drastically change. In March 2020 the water column observed was 5.27 meters and in November 2020 the water column measured was 2.43 meters. This large seasonal variation is also visible in the long term monitoring results. The electrical conductivity measured in the lab was 3.24 mS/cm. For both the water column and electrical conductivity the influence of the rainfall is not clear, but it seems that there is some negative correlation between the water column and the electrical conductivity, indicating dilution plays an role for this well. Figure 6.20 gives the water column plotted against the electrical conductivity.

Figure 6.20 shows that there is indeed some negative correlation between the water column and the electrical conductivity, but the exact relation is not apparent. The electrical conductivity is a measure of the concentration of solids dissolved in the leachate. Knowing this, an expected relation could be as is shown in equation 6.3. The reality is more complex, as infiltrating rain could also bring dissolved solids from higher up in the waste, and if water drains away the conductivity does not change. However there will be a point in time at which the waste has almost fully leached and the water which enters through the waste body will only dilute and not bring more solutes, in which case equation 6.2 is the expected behaviour. The fact that the relationship is visible for a decrease in water level as well, which is not the case for all the other monitored wells, could indicate that the observed drop in water level is also caused by evaporation of the leachate.

$$Water\ level \cdot Electrical\ conductivity = Constant \qquad 6.2$$

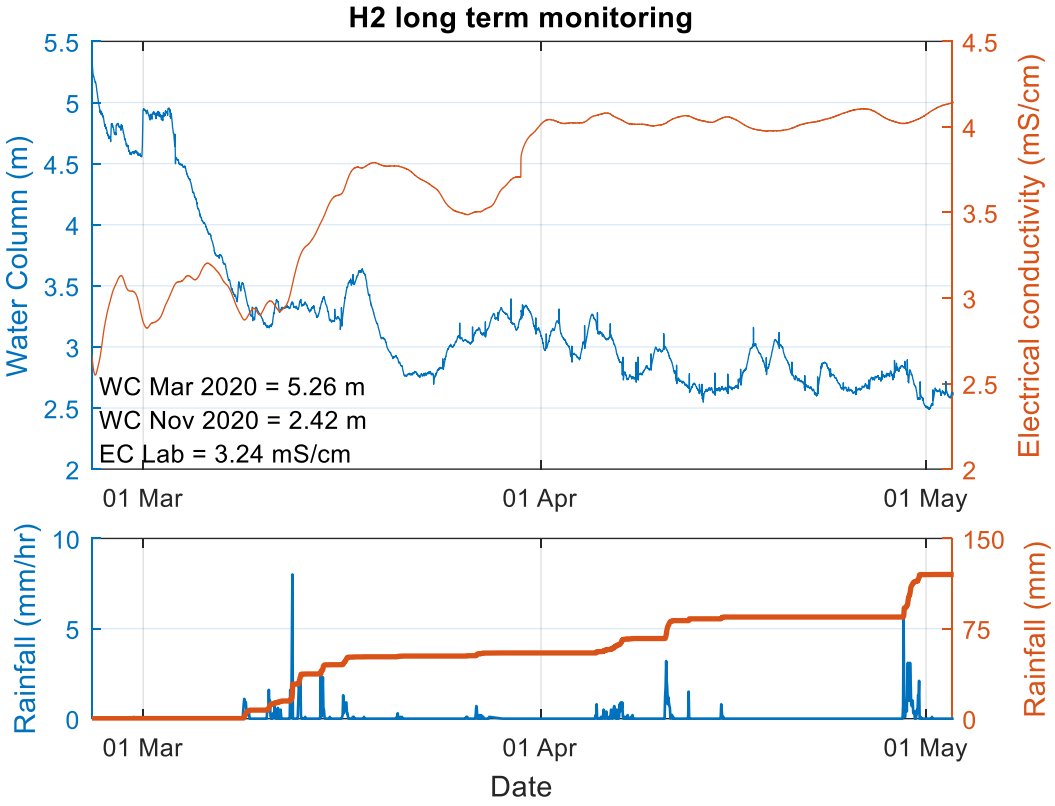


*Figure 6.19: H2 long term monitoring of water levels, electrical conductivity and rainfall*

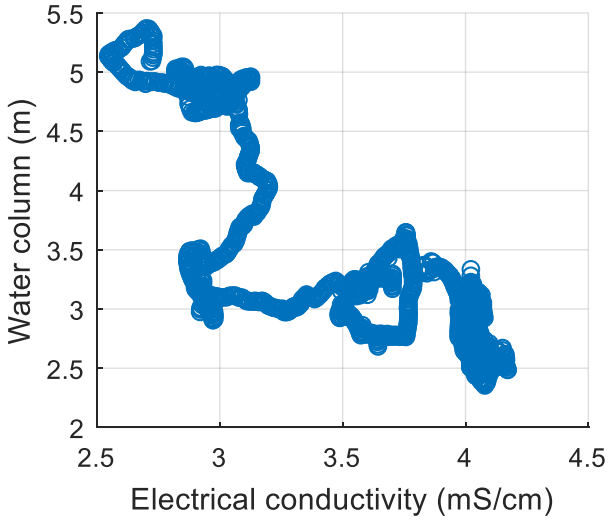


*Figure 6.20: Water column against electrical conductivity for well H2*

#### 6.3.5.2 Well J2

Figure 6.21 shows the measured water column and electrical conductivity in aeration well J2 during the long term measurements. This well showed a clear instant response in water column to the rainfall. Interesting is that there is no decrease in electrical conductivity with the increase in water column, while it is clear that the increase in water column is directly caused by the rainfall. The fact that the response in water column is instant, indicates that this well is connected to the top of the landfill with a preferential flow path, as it is otherwise unlikely that the rainfall could move through eight meters of waste and cover soil so quickly. The rise in water column is not one to one related to the amount of

rain that has fallen. If for example the rainfall peak at the 10th of April is evaluated, the following is obtained: the total rainfall was 14.2 millimetre, and the rise in water column is 49.5 centimetre. Assuming that there is a porosity of 0.35, the average rise in water column over the entire compartment would be 4.0 centimetre. Meaning that the rain has a preferential path towards the stagnant water surrounding this well that attracts rain from a larger area.

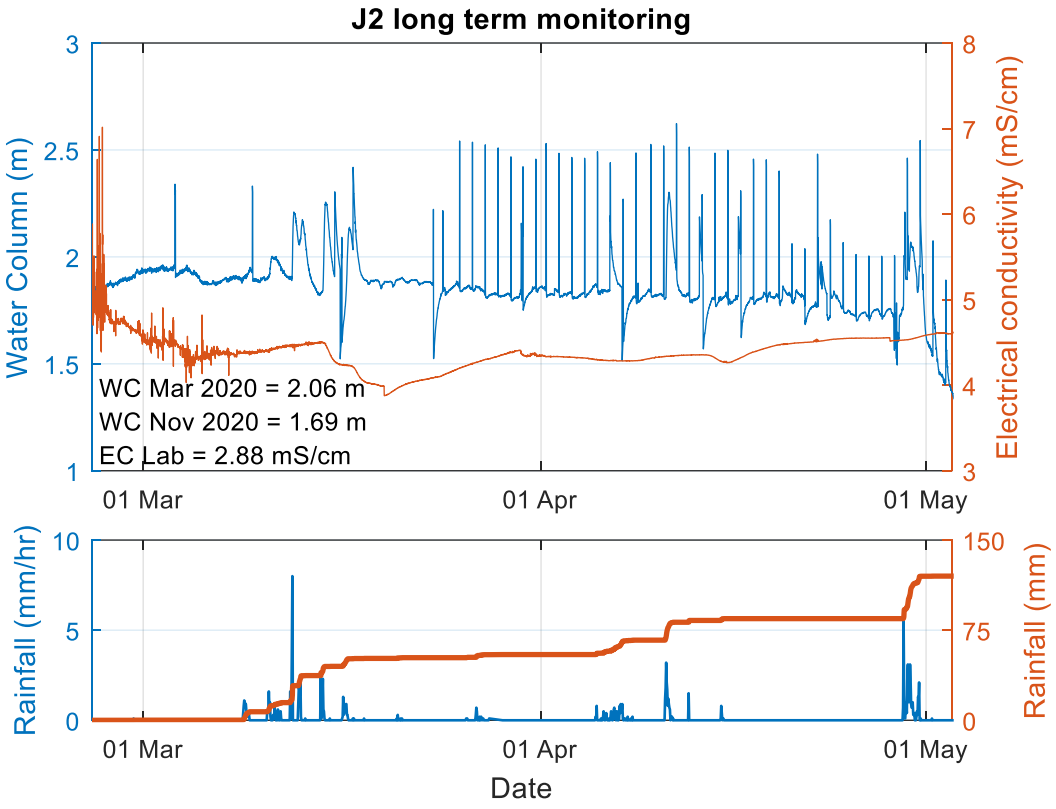


*Figure 6.21: J2 long term monitoring of water levels, electrical conductivity and rainfall*

#### 6.3.5.3 Well M10

Figure 6.22 shows the measured water column and electrical conductivity in aeration well M10 during the long term measurements. For this well the response in water column due to the rainfall is not at all clear, but there is a clear drop in electrical conductivity measured after the two largest rainfall events, in the middle of March and the end of April. Assuming that the added rainwater has a near zero electrical conductivity, then equation 6.3 holds, giving the ratio between the volume of the rainwater added to the system and the volume of the water body.

$$DF = 1 + \frac{V_r}{V_{wb}} = \frac{EC_{br}}{EC_{ar}} \qquad 6.3$$

Where $DF$ is the dilution factor [-], $V_r$ is the volume of rain added to the water body [$L^3$], $V_{wb}$ is the volume of the water body [$L^3$], $EC_{br}$ is the electrical conductivity before the rainfall [$L^{-3}M^{-1}T^3I^2$] and $EC_{ar}$ is the electrical conductivity after the rainfall [$L^{-3}M^{-1}T^3I^2$].

At the first large rainfall event the electrical conductivity dropped from 3.78 to 3.26 mS/cm. This correspond to a volume of rainwater to volume of the water body ratio of 16 percent, while there was only 44.1 millimetre of rain in this period. During the second large rainfall event 35.3 millimetre of rain was measured, and a drop in conductivity from 4.80 to 4.14 mS/cm, corresponding to a dilution factor of 1.16, the same volume of rainwater to volume of the water body ratio of 16 percent. The numbers

of both rainfall events are similar, and suggest that either the water body surrounding the well is really small, or that there is a lot of preferential flow leading towards the well, or most likely both.

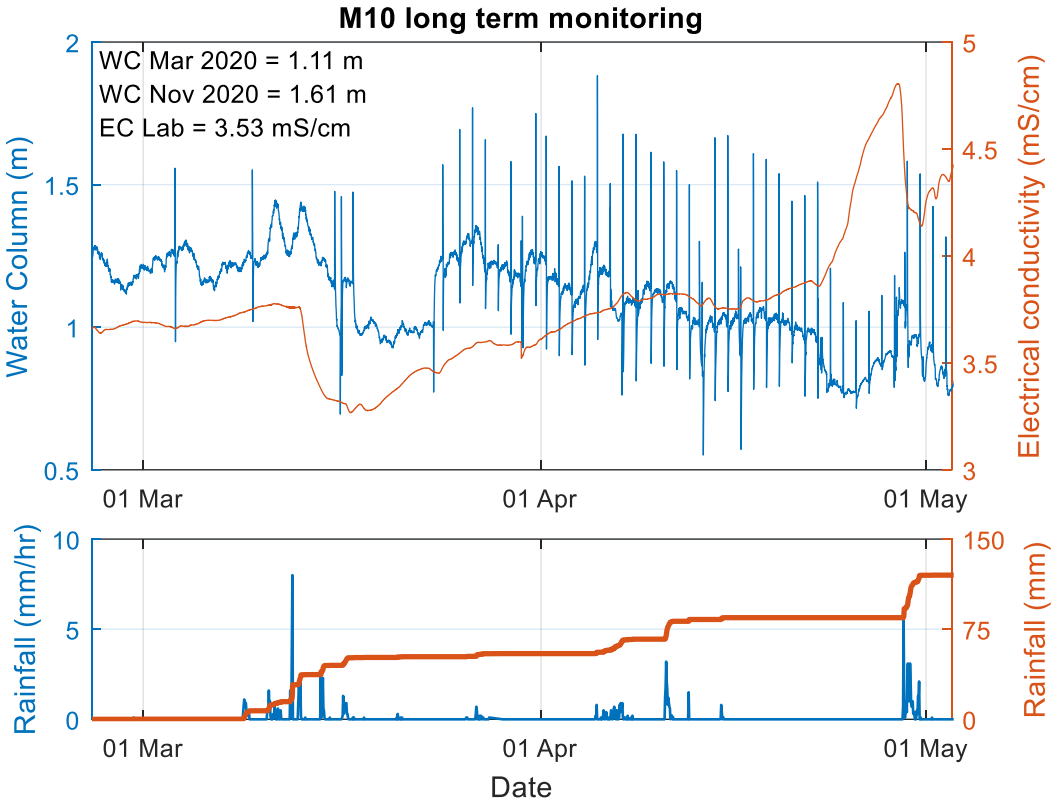


*Figure 6.22: M10 long term monitoring of water levels, electrical conductivity and rainfall*

#### 6.3.5.4 Well R2

Figure 6.23 shows the measured water column and electrical conductivity in aeration well R2 during the long term measurements. The data is slightly influenced by the fact that a pumping test was performed on this well during the long term measurements. The previous water table measurements seem to show that the water column in this well is consistently much larger than in the surrounding wells, however the long term measurements show a different picture, the water table is changing rapidly over time and is at a certain point even below two meters. The most remarkable about the data is that in an 18 hour period during the first heavy rainfall event, the water column rose with almost 4 meters, while only 44.1 millimetres of rain was measured, but the second large rainfall event is not visible in the data. The strong rise in water column did not translate into an immediate drop of electrical conductivity. A possible explanation for this is that the water does not flow immediately to the well, but through the waste and cover layer, and the rainwater picks up dissolved solids on the way to the well. The lack of response for the second rainfall event could then be caused by the fact that the cover layer and waste was too dry, due to evapotranspiration, holding on the rainwater.

Looking at the large increase in water column during the first rainfall event, it might be tempting to think that this increase is only present inside the well itself. However during the pumping test the water column in the well was reduced by two meters, after which the water column restored mostly, showing that the free standing water was is present in the surrounding waste as well.

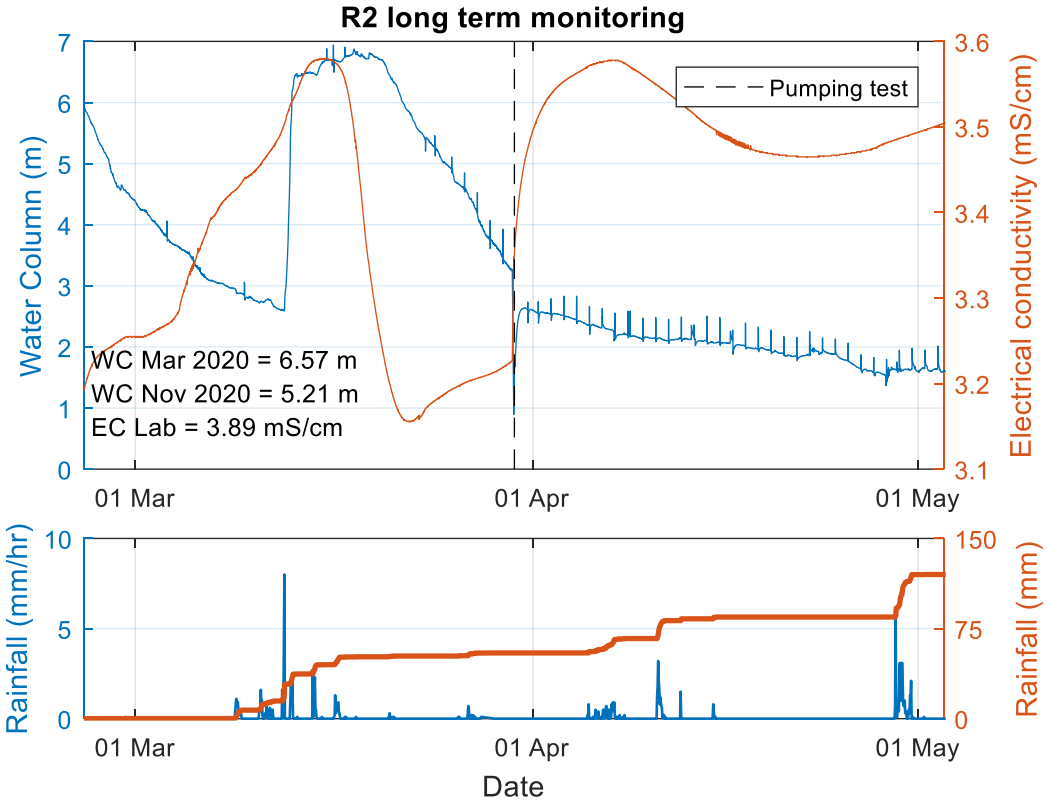


*Figure 6.23: R2 long term monitoring of water levels, electrical conductivity and rainfall*

#### 6.3.5.5 General response

In general, did the wells under long-term monitoring for these measurements not show uniform behaviour. In most wells, the rainfall cannot be related to changes in electrical conductivity or water column. This is also the desired situation, as it shows that there is no short circuiting of rainwater along the well-waste interface. In one well an immediate drop of electrical conductivity was seen with the rainfall events, and in some a delayed response. Unfortunately, in some of the wells the measurements of the electrical conductivity were not stable, and in those wells the obtained values are not valid. For most wells, the rain seems to influence the water column slightly, but often it is not fully clear how much the fluctuations in water level are caused by the rainfall events, as some responses are delayed, which is what is expected if the rainwater slowly infiltrates the waste body.

In many of the monitored wells, a periodic pattern in the water column could be observed which is shown in figure 6.24. There is a sudden jump and drop in the water column, after which the water column was even lower than before the jump. The explanation for this can be found in how the aeration system is operated. From 23 March 2021 onwards, a daily high injection pressure was put on the divider that brings the pressure to the aeration wells. The pressure put on the system is about 30 millibar, which corresponds to 30 centimetres of water, which is for most wells indeed the magnitude of the peaks. The peak in water column is thus only apparent, the signal reflects an increase in pressure which is not recorded by the Baro-diver and therefore not compensated, which in the data looks as an increase in water column. The drop in water level however is really present, which is caused by the high pressure applied. It then it takes up to a few hours before the water level is restored to the level before the pressure was applied.

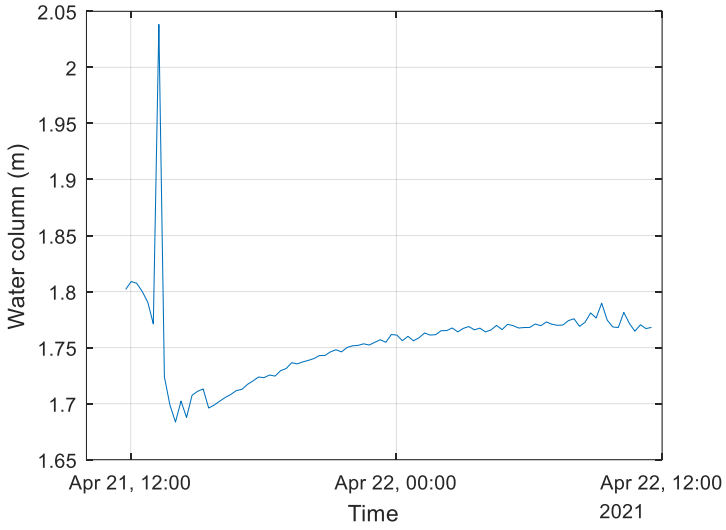


*Figure 6.24: Common sudden jump in water column (example from J2)*

## 6.4 Leachate properties

This section is subdivided into two subsections, first the results from the measurements performed in the field are given. These measurements have been taken with the CTD-diver during the pumping tests. The second subsection contains the results of the measurements that have been taken in the laboratory on the samples from the aeration wells that were sampled in December 2020.

### 6.4.1 Field measurements

Figure 6.25 shows the spatial graphs of the temperature and specific electrical conductivity measured with the divers. Visually can be seen that for the temperature and less for the specific electrical conductivity neighbouring wells seem to have similar values, meaning the difference in measured value for neighbouring wells is smaller than the average difference between all the wells. To quantify this spatial variability the absolute difference in measured value between all the wells and the distance between the wells is fitted to equation 6.4, which is the exponential semivariogram model. Figures 6.26 and 6.27 show the data points and the fit for the measured specific electrical conductivity and temperature. From the fitted curves can be seen that both parameters show no correlation between the difference between measured values and the distance between the wells.

$$AD = a \cdot \left(1 - e^{-\frac{Distance}{b}}\right) \qquad 6.4$$

Where $AD$ the is absolute difference in the measured value [X], which can have any dimension, $a$ is a scaling parameter [X], that is a measure of how large the spread in measured values is and $b$ is a scaling parameter [L], that is a measure for the spatial variability.

The curve fitted for the temperature does seem to have a larger range (distance at which 95% of the asymptotic value has been reached). This is also what could be expected, the temperature can equilibrate due to radiation through both solids and fluids, and therefore is expected that neighbouring wells have a similar temperatures, while electrical conductivity can only equilibrate because of the movement of ions trough liquids. The fit is however so poor that also for the temperature can be stated that even the small spacing between the aeration wells is too large to accurately show the correlation between distance and measured values.

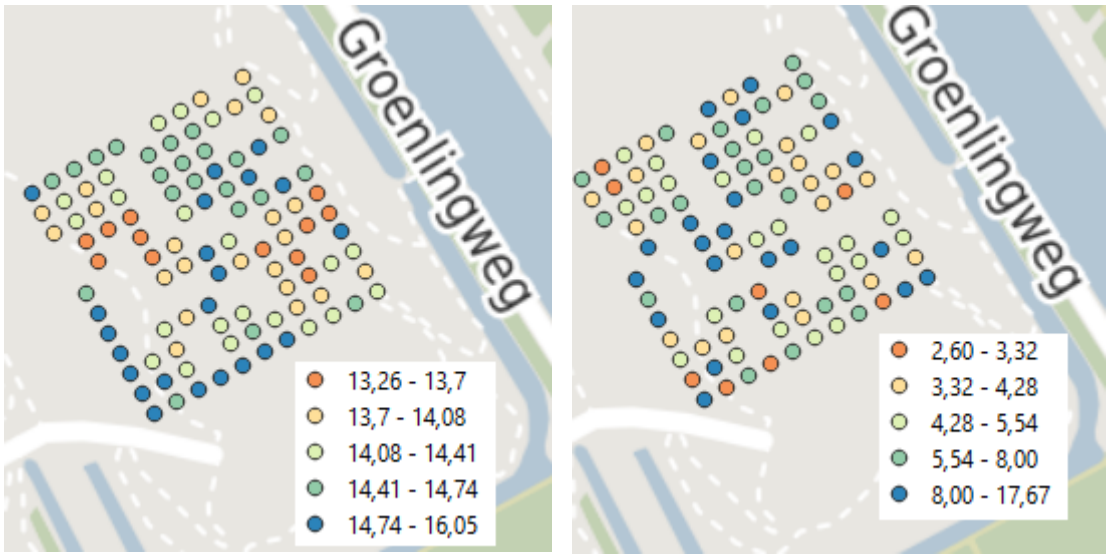


*Figure 6.25: Spatial variability of temperature in $^{o}C$ (left) and electrical conductivity in mS/cm (right)*

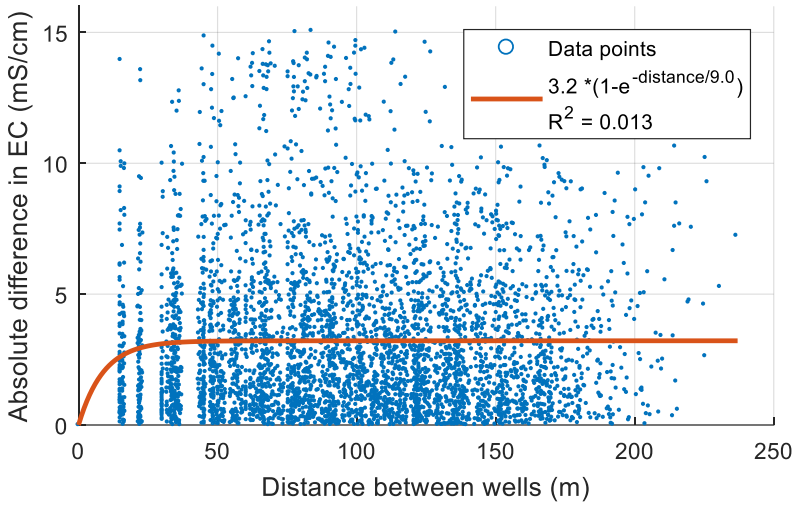


*Figure 6.26: Semivariogram of electrical conductivity measured in the field*

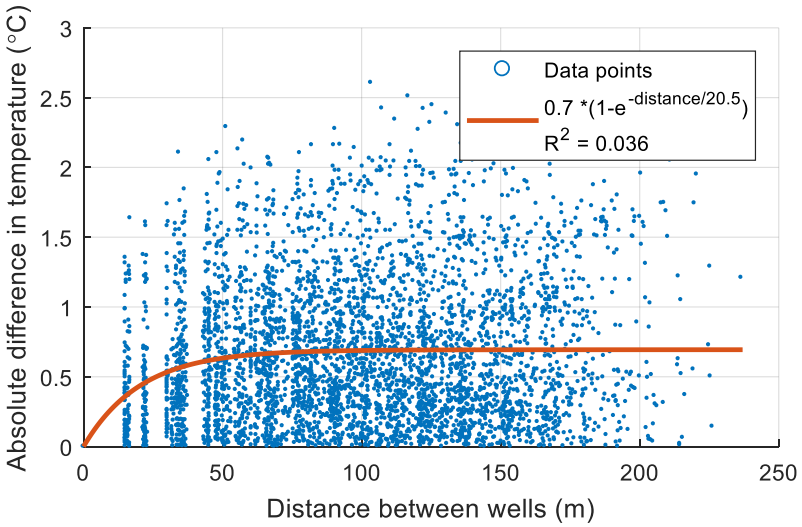


*Figure 6.27: Semivariogram of temperature*

The temperature and specific electrical conductivity values are representative for compartment 11Z as a whole since the data comprises of almost hundred measurement points. The average electrical conductivity measured was 6.2 mS/cm, and all the measured values were between 2.6 and 17.7 mS/cm. All the measured electrical conductivities fall within the range that can be expected for landfill leachate (as given in section 3.2.2). The average temperature measured was 14.4 $^{o}$C, and all measured values were between 13.4 and 16.0 $^{o}$C.

The spread of electrical conductivity values is large, showing that there is a large range of waste solute content present in the compartment. The temperature range is rather small and not much larger than the temperature below surface level at a non-landfill location. This indicates that there is not so much biodegradation occurring. For comparison, in compartment 11N temperatures above 40 $^{o}$C have been observed.

### 6.4.2 Laboratory measurements

From all the aeration wells in rows G to R for which this was possible two leachate samples have been taken according to the procedure described in section 5.4. The wells that have not been sampled, were either too dry to sample or it was not possible to sample because the wells were too deep. The samples have been taken on the 9$^{th}$, 18$^{th}$ and 21$^{st}$ of December 2020, so not all the samples are taken on the same day, but it is assumed that the leachate samples can still be compared, especially because during this twelve day interval only 11 millimetres of rain have fallen at the Braambergen landfill. Appendix H shows a few pictures of the samples that have been taken to show that the variability is also apparent visually. For the five properties that have been measured, pH, EC, redox potential, DOC and ammonium concentration, the results from the samples taken from the aeration wells are compared to the biweekly measurements that are performed by Afvalzorg on the leachate collected from the pumping station which removed leachate from the basal drain of compartment 11Z. The leachate from the aeration wells and from the basal drains can be used for comparison, but it must be made clear that these samples are taken from different parts of the landfill.

#### 6.4.2.1 pH and redox potential

Figure 6.28 shows a boxplot of the pH values measured on the aeration well samples and the measured pH values on the samples taken from the basal drain that have been analysed by Afvalzorg. The average pH measured with 82 aeration wells samples was 7.1, which is for a landfill a typical value (section 3.2.1). This value is similar to what is observed over the years in the basal drain. The spread of measured pH values is relatively small, however there are a few wells that show an elevated pH. It is likely that this high pH is caused by the local characteristics of the waste, for example if construction waste with calcite is present, and not by microbial activity. Two samples show a pH higher than 9, which means that for those samples the ammonium concentration cannot be determined using the ammonium kits.

Figure 6.29 shows a boxplot of the redox potential measured on the aeration well samples and the measured redox potential on the samples taken from the basal drain that have been analysed by Afvalzorg. All the 82 aeration well samples give a negative redox potential, while the basal drain samples are in general positive. There is a large spread of measured values, but the general trend is that the redox potential is largely negative. At these redox potential values, poorly soluble salts, which would otherwise remain in solution, can precipitate and carbon dioxide can be reduced to methane, however it must be noted that redox potential is hard the accurately measure and that the values should always be interpret qualitatively and not quantitatively. The negative values indicate that the aeration intensity is not sufficient to maintain aerobic conditions. The basal drain values are taken from the pumping station where the leachate might has been in contact with air, increasing the redox potential.

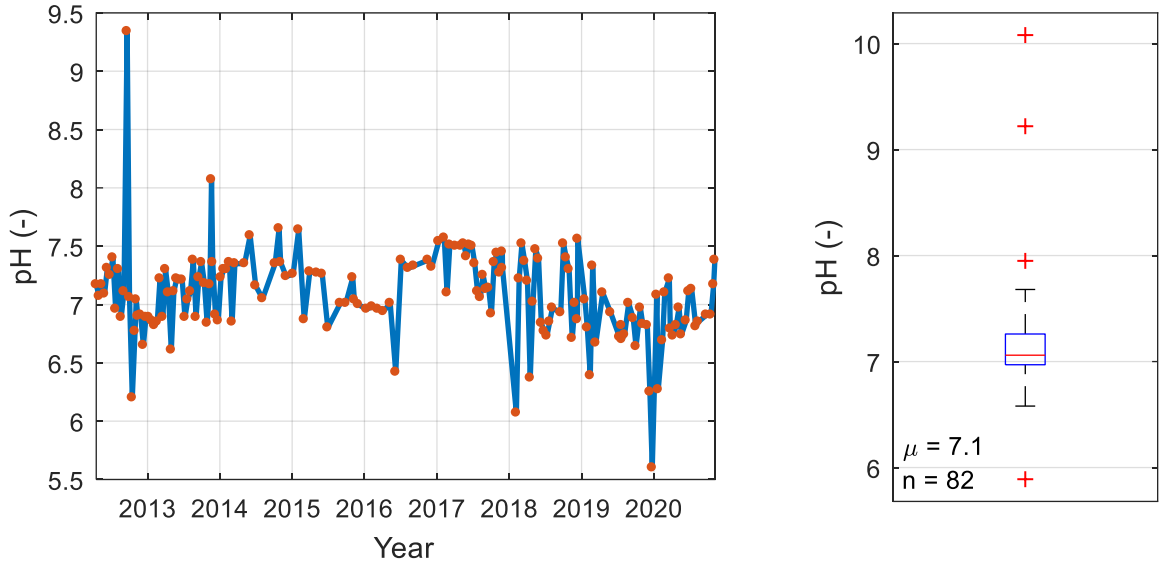


*Figure 6.28: Basal drain pH values (left) and pH values aeration well samples (right). Box = interquartile range, line = median, whiskers = extremes, red crosses = outliers*

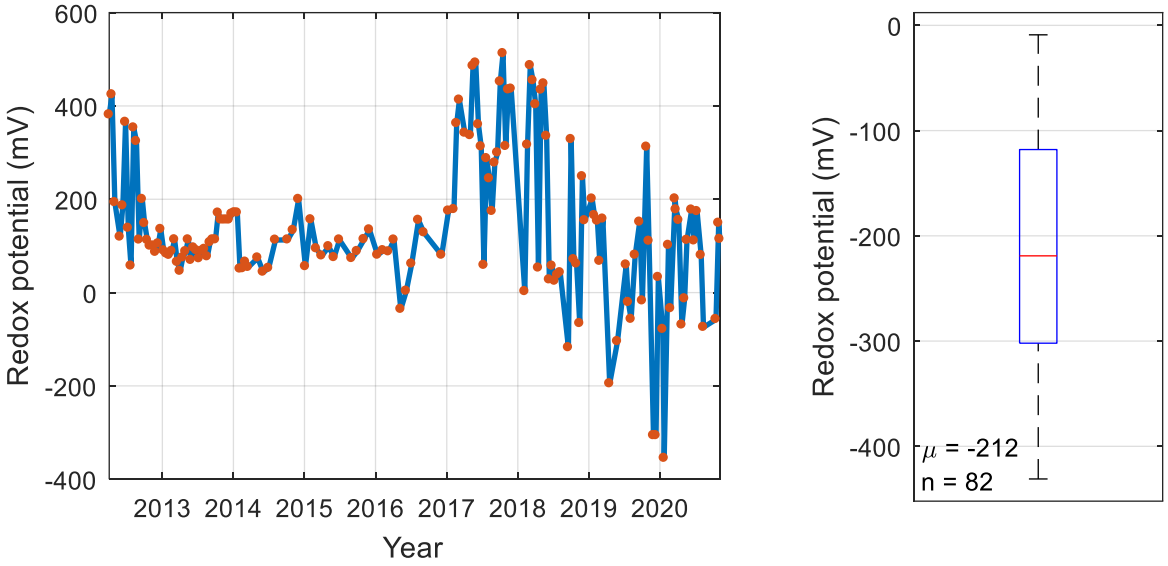


*Figure 6.29: Basal drain redox potential (left) and redox potential aeration well samples (right). Box = interquartile range, line = median, whiskers = extremes, red crosses = outliers*

#### 6.4.2.2 Electrical conductivity

Figure 6.30 shows a boxplot of the electrical conductivity measured on the aeration well samples and the electrical conductivity measured on the samples taken from the basal drain that have been analysed by Afvalzorg. The average value of the aeration well samples is very similar to the average value that was found in 2020 in the basal drain (6.17 mS/cm). If all the waste in the landfill would have a similar composition, a strong negative correlation between the water level measured in the aeration well and electrical conductivity would have been expected and been indicative of the addition of rainwater (i.e. dilution) to the leachate in wells with reduced electrical conductivity values. Figure 6.31 however shows that such a relationship is not present. To that must be added that the water levels have been measured in November 2020, and the samples have been taken in December 2020. Figure 6.32 shows a spatial graph of the electrical conductivities measured.

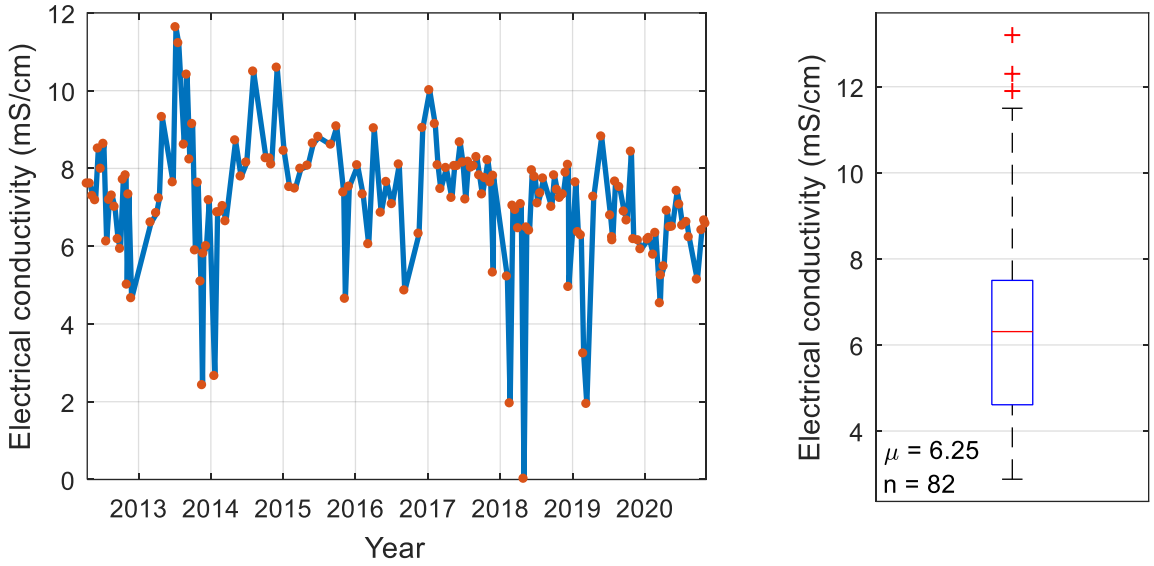


*Figure 6.30: Basal drain EC values (left) and EC values aeration well samples (right). Box = interquartile range, line = median, whiskers = extremes, red crosses = outliers*

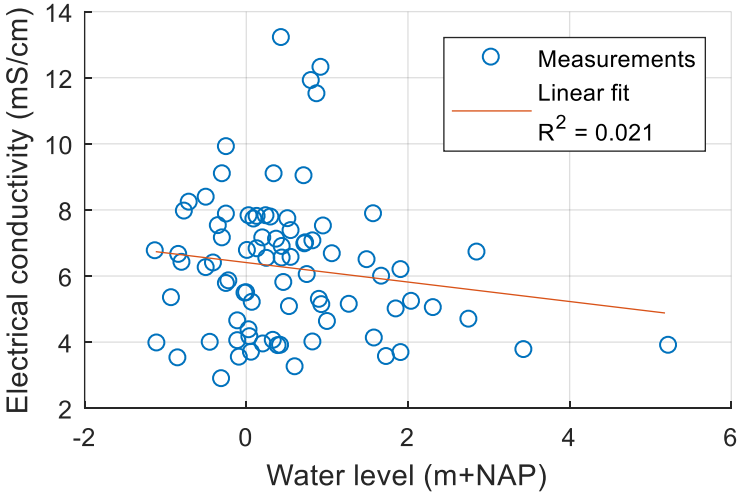


*Figure 6.31: Electrical conductivity against water level*

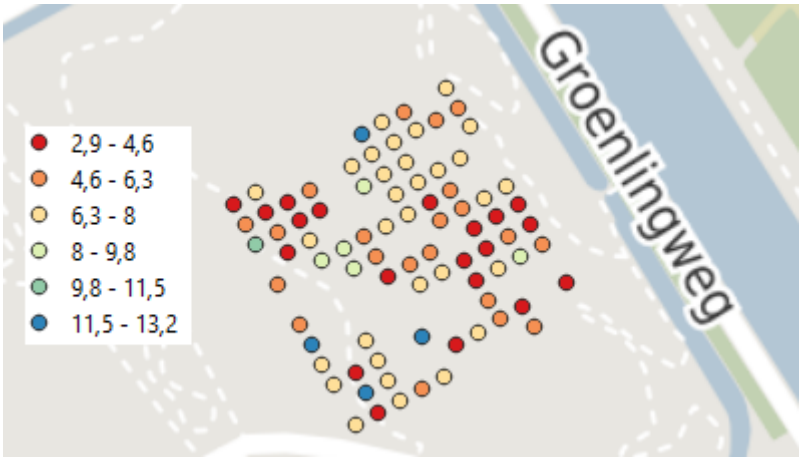


*Figure 6.32: Spatial variability of electrical conductivity in mS/cm*

Looking at figure 6.32, it might appears to be the case that in some areas of the compartment the measured electrical conductivities are correlated to the values from the neighbouring wells. However figure 6.33 shows a graph of the spatial variability of the measured electrical conductivity values and the fit of equation 6.4, which shows that there is very little correlation between the distances between the wells and the difference in measured values. The same conclusion was drawn from the electrical conductivity measured with the divers during the pumping test. Figure 6.34 shows that for some of the wells there were very large differences between the values measured with the divers and in the lab, but the linear fit is rather close to the expected relationship, which is that the measured values are the same in the field with the divers and in the lab with the electrode. A possible explanation for the large differences in some wells is that the samples are taken a month before the pumping tests took place and that in the time between the electrical conductivity of the leachate has changed locally. Most of the values obtained with the divers in the field are below the lab data, while if in the field more carbon dioxide was dissolved in the leachate higher values were expected instead.

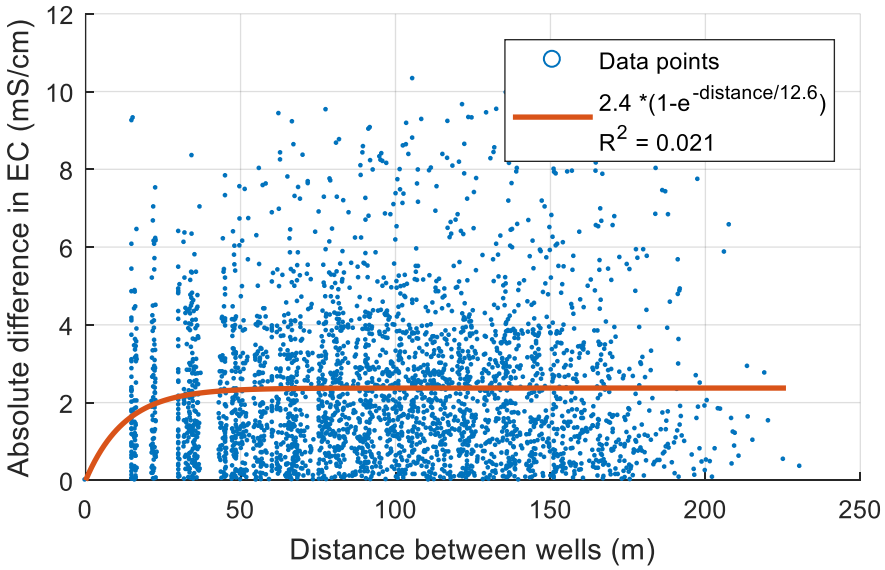


*Figure 6.33: Semivariogram of electrical conductivity measured in the laboratory*

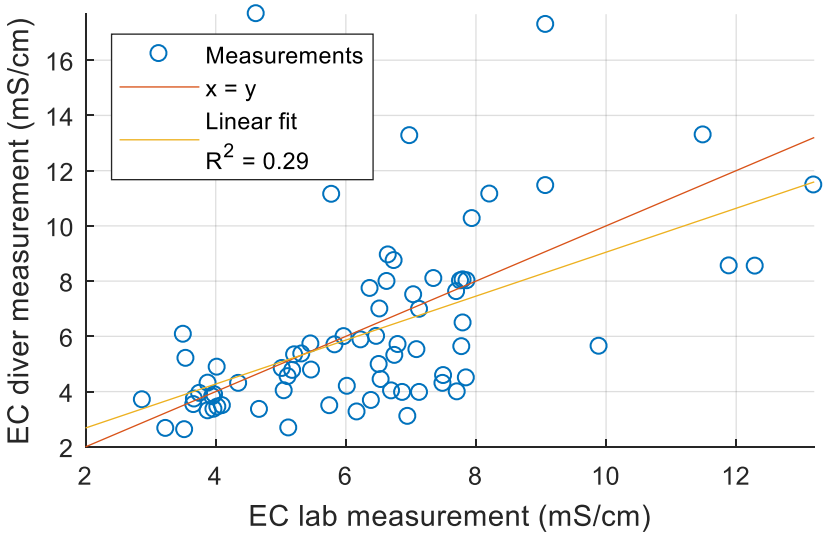


*Figure 6.34: Electrical conductivity measured in the field and measured in the lab*

#### 6.4.2.3 Ammonium concentration

Figure 6.35 shows a boxplot of the ammonium concentrations measured on the aeration well samples and the ammonium concentrations measured over time on the samples taken from the basal drain that have been analysed by Afvalzorg. The measured values are lower than what is typically reported in literature (section 3.2.5). There seems to be a yearly fluctuation in ammonium concentration and a small increase in concentration with the years. The four peaks present in the basal drain data are so far off that the most logical explanation is that those are measurement mistakes. The ammonium concentrations measured in the aeration wells are generally lower than what was measured in the basal drain. The enormous difference in ammonium concentrations between the wells is also striking, in the well with the largest ammonium concentration, the concentration measured was more than a hundred times larger than the well with the smallest ammonium concentration. This is an indication that the amount of biological activity is really diverse, as the ammonium concentration increases with the increased decay of organic matter, or that there is accumulation of ammonium in some wells. Figure 6.36 shows a spatial graph of the measured ammonium concentrations.

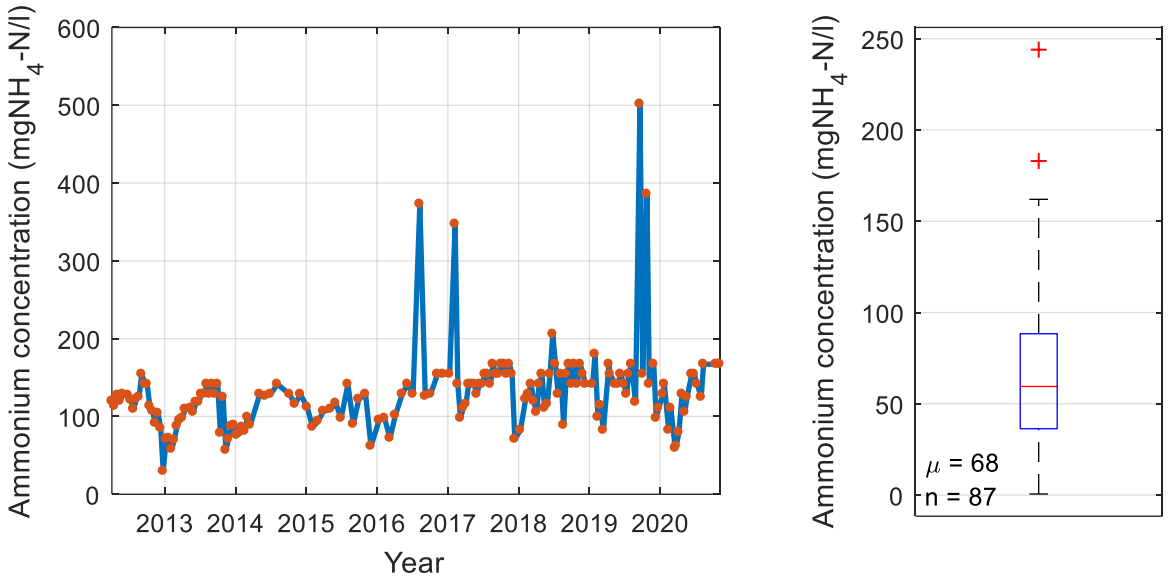


*Figure 6.35: Basal drain ammonium concentrations (left) and ammonium concentrations aeration well samples (right). Box = interquartile range, line = median, whiskers = extremes, red crosses = outliers*

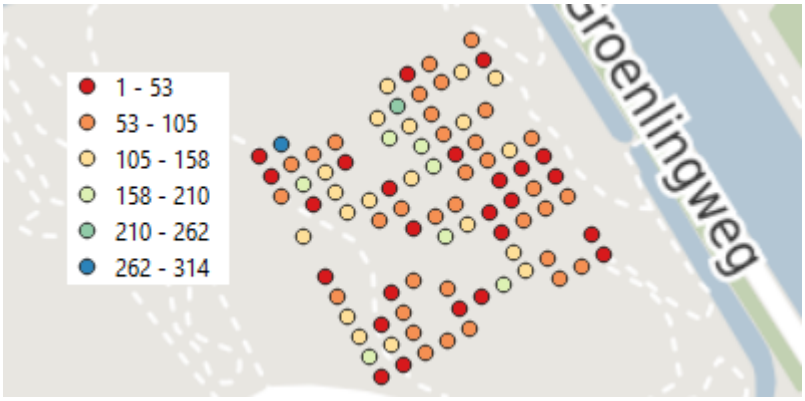


*Figure 6.36: Spatial variability of ammonium concentration in mg$N_{NH4}$/l*

Figure 6.37 shows a graph of the spatial variability of the measured ammonium concentrations and the fit of equation 6.4, which shows that there is no correlation between the distances between the wells and the difference in measured values. The range is only 20.3 meters, while the closest wells are already 15 meters apart, showing that in general the leachate in the wells in not related to neighbouring wells, which is the same as was found for the other parameters.

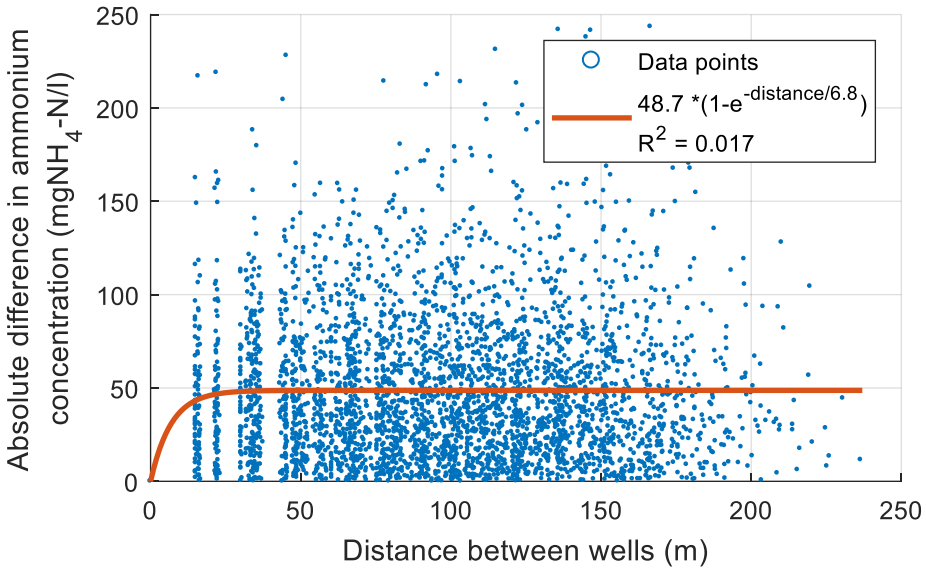


*Figure 6.37: Semivariogram of ammonium concentration*

Figure 6.38 shows for the measured electrical conductivity against the ammonium concentration for all the wells for which both measurements could be made. The general trend is that a well with a higher ammonium concentration also has a higher electrical conductivity, but there does not seem to be a clear relationship between the two. An explanation for this is that during degradation of organic matter, ammonium and other dissolved solids end up in the leachate, increasing both the ammonium concentration and the electrical conductivity. The electrical conductivity is however also a function of the non-biodegradable part of the waste, while the ammonium concentration is not.

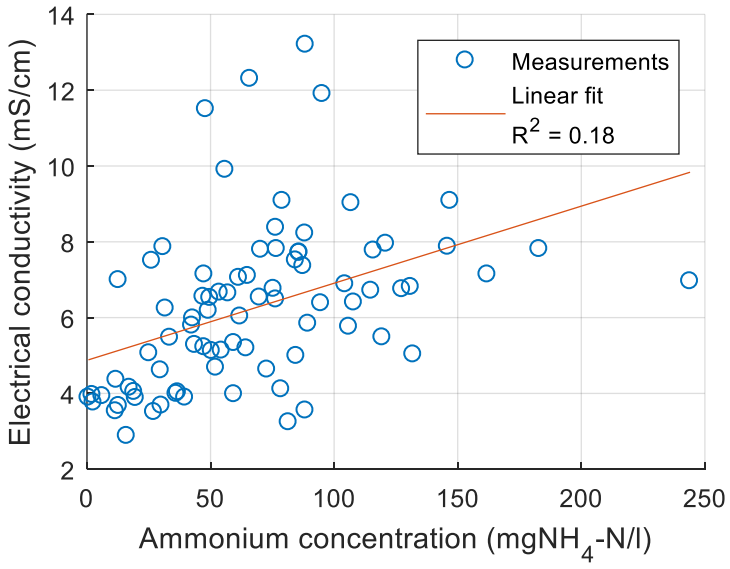


*Figure 6.38: Relation between measured electrical conductivity and ammonium concentration*

#### 6.4.2.4 Dissolved organic carbon (DOC)

The DOC is determined indirectly by measuring the absorbance of UV-light with a 254 nanometre wavelength and using this as a proxy. To get a DOC value from the absorbance, first a relationship between the two is quantities is established. For this samples have been taken from twelve different aeration wells in June 2021, and the absorbance of these samples has been measured in the lab, while the total DOC in the samples was determined with DOC fractionation performed by a commercial laboratory. The results used for the relationship and the linear fit can be found in appendix J.

For the samples taken in December 2020 the DOC was not determined directly, instead equation 5.11 is used to calculate the DOC from the measured absorbance, with the following scaling parameters: $\alpha$ = 30.1 mgC/l and $\beta$ = 14.9 mgC/l.

Figure 6.39 shows a boxplot of the DOC calculated from the absorbance measured on the aeration well samples and the DOC measured over time on the samples taken from the basal drain that have been analysed by Afvalzorg. The measured values are lower than what is typically observed in landfills (section 3.2.4). Similar as for the ammonium concentration, there is a yearly fluctuation present. The fluctuations are caused by the fact that during summer the supply of rainwater into the waste body is smaller and the dilution is less, giving larger concentrations. On avarage the samples from the earation wells have a slightly lower DOC compared to the basal drain, but given that the samples come from different parts of the landfill, the values are really similar. Figure 6.40 shows a spatial graph of the calculated DOC. Figure 6.41 shows the spatial variability of the calculated DOC values, and again there is no correlation between the distances between the wells and the difference in measured values. In figure 6.42 the DOC is plotted against the ammonium concentration for the wells for which both could be determined. There is not a strong relationship, but in general a higher DOC also corresponds to a higher ammonium concentration, which can be explained as during the degradation of organic material both DOC and ammonium are released. For electrical conductivity and DOC the same holds, wells with a higher electrical conductivity also tend to have a higher DOC.

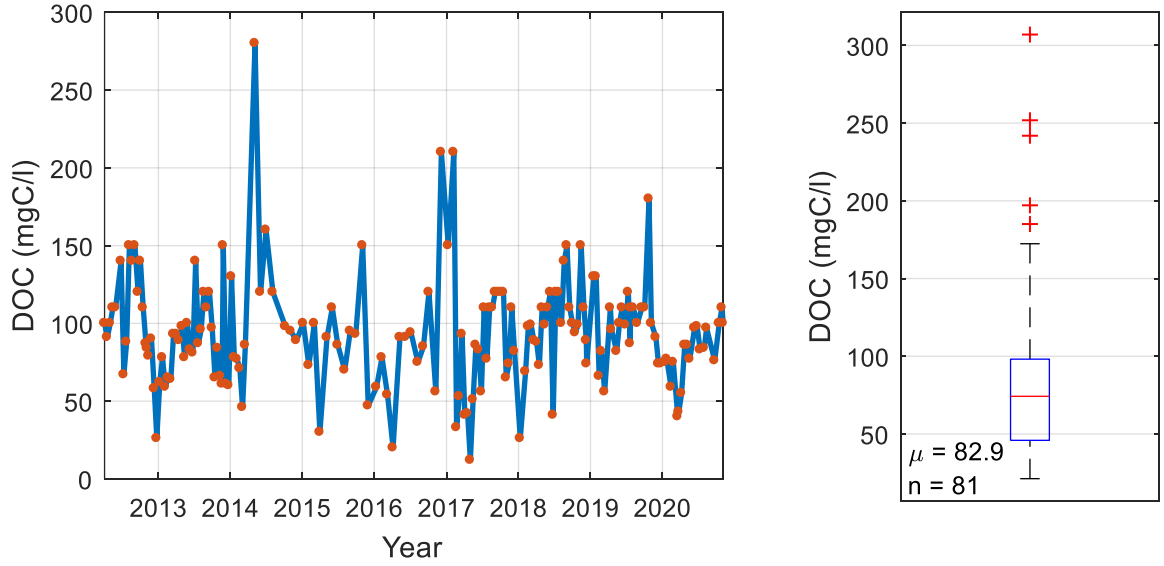


*Figure 6.39: Basal drain DOC (left) and DOC aeration well samples (right). Box = interquartile range, line = median, whiskers = extremes, red crosses = outliers*


*Figure 6.40: Spatial variability of DOC in mgC/l*

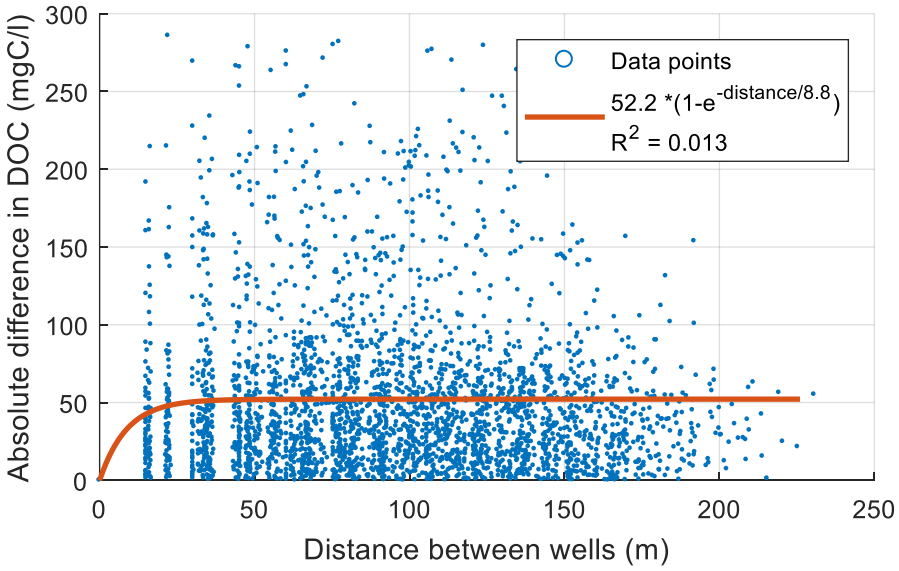


*Figure 6.41: Semivariogram of DOC*

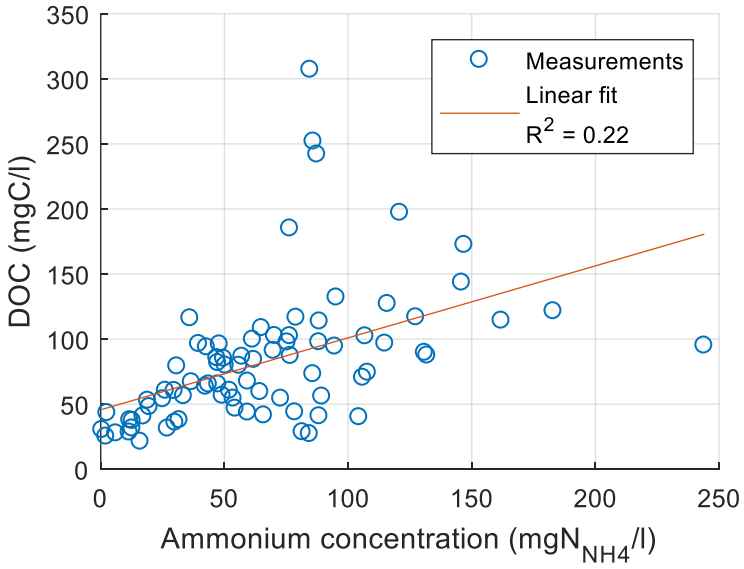


*Figure 6.42: Relation between calculated DOC and measured ammonium concentration*

## 6.5 Water distribution model

One of the research questions that has to be answered is how the water that is present within compartment 11Z is distributed. The water table measurements show that there is definitely free standing water present that does not drain towards the drainage system, meaning that there must be zones of very low vertical permeability. Also does the large variability in water levels suggest that there is limited horizontal flow as well. The pumping test results suggest that there are separate bodies of water present which are not connected, for which the calculated radius of the water bodies is often less than a meter. The large variability of chemical properties of the leachate present in the aeration wells are in agreement with the idea of water bodies that are not connected. Also do the chemical properties show that in none of the wells only rainwater is present, and that the water in the wells is only connected to the immediate surrounding water body, as neighbouring wells are not more likely to have similar properties than wells that are far apart. Then from the long term monitoring can be concluded that there are some wells for which the water level is really stable, and for other wells there seems to be a limit of how high the water level can be, but still large fluctuations can occur. All these measurements and observations seem to suggest that within the landfill there are 'buckets' of leachate present, which are demarcated by horizontal and vertical zones of relatively low permeability. Once a bucket is full, the addition of more leachate/rainwater will cause it to overflow. As the zones of relative low permeability can in some cases still drain, it is possible that the water level in the bucket reduces over time in these 'leaky' buckets. The water in the landfill cannot be seen as continuous water body. Figure 6.43 shows a representation of the described bucket model.

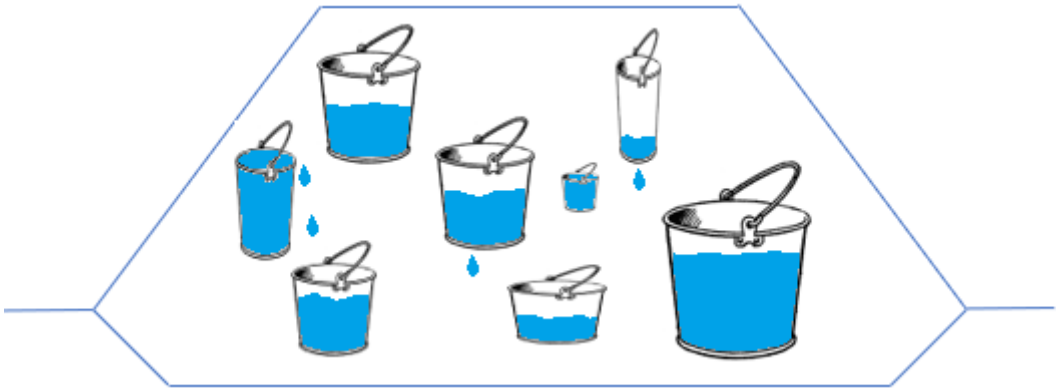

*Figure 6.43: The bucket model*

# 7. Conclusions on the lab and field measurements

This chapter gives a concluding overview of the measurements performed in the lab and in the field. The five types of measurements performed all contributed to finding an answer to the research question.

From the water table measurements can be concluded that there are large hydraulic gradients present within the landfill. Some of them are so large and stable over time that it is unlikely that there is flow occurring between some of the aeration wells. It is possible to interpolate the measurements to obtain water levels in between measured locations, but given that the scale at which the water level varies is seemingly smaller than the distance between the measurement locations, this does not give a realistic picture. Looking at the temporal variation of the water levels, between March and November 2020, the average water level has dropped with almost a meter. A closer look shows that in some wells the water level did not change at all, while others showed a drop in water level of multiple meters. This is a first indication that the water surrounding the aeration wells is not or only poorly connected. The fact that aeration wells that are close to an old gas well, which has a gravel layer that extends towards the drainage system, do not clearly have lower water levels then the wells further away also indicates that there is limited horizontal flow occurring in the landfill.

The gas velocity and composition measurements show why the water levels are problematic. For a particular well the amount of LFG extracted reduces linearly to zero when the water column rises towards 1.8 meter, the height of the filter screen. However, the extraction rates are so low in compartment 11Z that a lot of the aeration wells have a zero extraction rate even when the water column is lower than this 1.8 meter, making it likely that even if the water column in the aeration wells is reduced, still the amount of LFG extracted from 11Z will be low compared to compartments 11N and 12. In March 2020 was the average LFG extraction rate for the aeration wells in compartment 11Z was only 2.4% of the average extraction rate for wells in compartment 11N.

The pumping test performed on all the aeration wells showed that the response to lowering the water column was very diverse. Some wells show an instant recovery in water column, while others show no recovery at all. The free standing water bodies that surrounds the wells are found to be small in size, with most radii of influence being less than a meter. The estimates for the horizontal hydraulic conductivities found with the pumping test range from $1 \cdot 10^{-7}$ to $6 \cdot 10^{-4}$ meter per second, but these estimates only hold in the close proximity of the aeration wells in which they were measured. The results show that lowering the water level in the entire landfill by installing a pump will not be effective.

The results from the lab measurements performed on the leachate samples taken from the aeration wells show the same picture. For all measured properties it is clear that there is almost no relation between the distance between the wells and the measured properties of the leachate, indicating that most wells are not located in the same body of water as their neighbouring wells. Also do the measurements show that in none of the wells only rainwater is present. The average measured values for the electrical conductivity, ammonium concentration and DOC from the aeration wells are close to the values measured in the basal drain of compartment 11Z, which means that for these properties the water that flows into the basal drain is representative for the water present in the landfill.

Monitoring the water column and electrical conductivity of the leachate in fifteen wells for over two months showed again that the hydrological behaviour is highly diverse. Some of the wells showed a clear response to the rainfall, while others seemed to be not influenced by rainfall events at all. The water columns observed with the divers was for almost all the wells in line with the water columns

that were measured manually in March and November 2020, and for the wells where the seasonal variations seemed to be huge it was observed that the water columns can change very rapidly, where the largest variation observed was an increase in water column of almost four meters in only 18 hours.

Putting together all the measurements resulted in the concept that within the landfill multiple 'buckets' of water are present with different sizes, demarcated by zones of relatively low vertical and horizontal permeability. Once a bucket is full, adding more water to it will not give an increase in water level as the bucket will overflow. The relatively low permeability zones do not have to be fully impermeable, which is why for some buckets it is possible to lower in water level if the accretion of leachate is small.

# Part III – Numerical Evaluation

# 8. Introduction to the numerical evaluation

With the lab and field measurements knowledge about the temporal and spatial variability of the hydraulic behaviour and leachate composition is sufficiently gained to quantify the relation between the elevated water levels and the reduced aeration efficiency. It is also clear that installing a pump or gravel column in the waste body will not be able the solve the problem of the reduced aeration efficiency, as the water bodies that are present in the landfill are poorly or not connected. There is another possibility to increase the efficiency of the aeration system. Instead of lowering the water column in the wells by lowering the water level, the water column can also be lowered by lifting the aeration wells. The downside of this compared to the lowering of the water level is that the lifting has as a result that the lower part of the waste is abandoned for aeration.

Because of this risk of losing a part the waste for treatment, this method of mitigating the reduced aeration efficiency must be applied carefully. If a well is lifted too much, waste is left behind unnecessarily and if a well is not lifted enough the efficiency of the aeration is still unnecessarily below its potential. From the water table measurements performed it is known at a few moments in time what the water columns were in the aeration wells, but it is also known that the water columns are very variable and can in some cases change rapidly over time. Also, based on only the measured water columns it cannot be said how much of the fluctuations over time can be explained by the seasonal variation, and whether there is in the longer term a general increase or decrease of water level looking at the entire landfill. Because of the large spatial variability and large amount of unknowns, it is not feasible to model the spatial and temporal variability of water ponding and water flow through the landfill, however it is possible to determine the large scale general behaviour with a water balance model. In this part of the thesis the result of a water balance model that simulates the total water storage in compartment 11Z is used to predict the behaviour of the water levels in the landfill over time, answering the last sub question:

6. Can the observed temporal variability of water levels in compartment 11Z be explained with a water balance model?

An explanation of the utilized model and the method used to calculate the water level is given in chapter 9. Chapter 10 contains the results and the discussion of these results. The conclusions that drawn from the results are presented in chapter 11.

# 9. Method

In this section is the model developed by Liang Wang (Wang et al., 2021) presented and is explained how the model is used to relate the model to the on-site water table measurements.

## 9.1 The model

The water balance model developed by Liang Wang is a stochastic travel time distribution model, for which the conceptual model structure is shown in figure 9.1. Each water droplet has a travel time, the time it takes for the water for the water to travel through the waste body. The water is divided over a fixed amount of cells, and each timestep, which corresponds to one day, the water is moved to a cell closer to the drainage system and from the first cell to the drainage system, such that for the water in cell $\mathrm{Vm_n}$ it takes $\mathrm{n}$ days to enter the drainage layer. Only the last cell, which is in figure 9.1 shown as $\mathrm{Vim}$ and corresponds to the cell containing the water from the bulk waste, does not move all its water to the next cell, but only a part as some part of the water is retained and not mobile, which is in figure 9.1 shown as $\mathrm{q_{baseflow}}$. The model determines with a stochastic process the a density function of state variables, among which also the storage, which is a measure of how much water is stored in the landfill and can be used to calculate the water levels in the landfill.

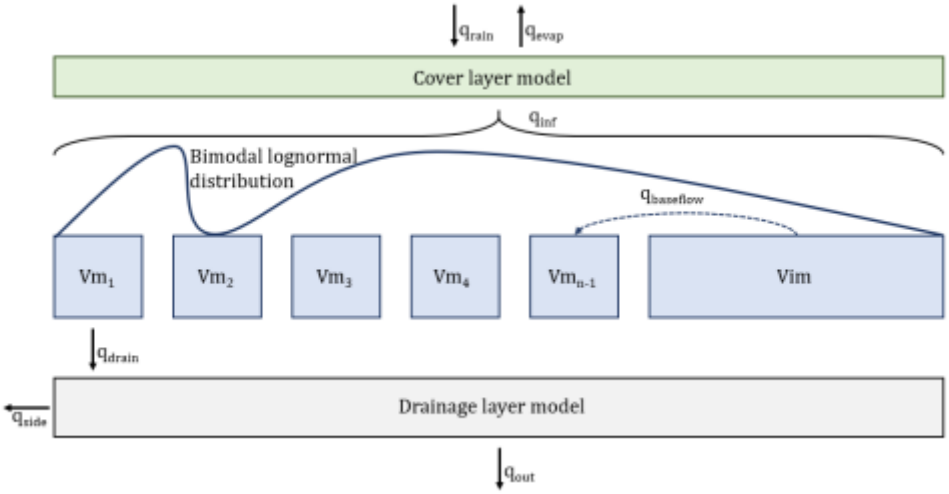


*Figure 9.1: Travel time distribution water balance model (Wang, 2021)*

## 9.2 Model input and output

The rainfall and potential evapotranspiration (pEV) are taken from the KNMI data measured at the Lelystad weather station. These are the input parameters for the model, in figure 9.1 noted as $\mathrm{q_{rain}}$ and $\mathrm{q_{evap}}$. Figure 9.2 shows the daily rainfall measured at the weather station and the 30 day average value. It seems that often in the autumn there is a slight peak in the rainfall, but further than that there is not a clear pattern. Figure 9.3 shows the daily potential evapotranspiration at the weather station and the 30 day average value. There is a clear yearly pattern, peaking in the summer at three to four millimetres per day. The actual evapotranspiration is depended on the potential precipitation, water content of the cover layer and the type of vegetation present. The actual evapotranspiration is a negative term (water is removed from the system) and the rainfall is a positive term (water is added to the system).

The measured daily outflow from the drainage layer is shown in figure 9.4, which is in figure 9.1 noted as $\mathrm{q_{out}}$. The 30 day average shows that there is often a peak in outflow at the end of winter, indicating that the storage is also higher then, as the outflow is a function of the water present in the waste body, which is larger in the end of winter as the precipitation is slightly higher and the potential

evapotranspiration reaches the yearly lowest values. The baseflow, the lowest average flow during the year, seems the be decreasing over the years when looking at the 30 day average, which would indicate that the storage is also decreasing. The 3000 day average is indeed slightly decreasing, meaning an expected reduction in storage over the years.

Figure 9.5 shows the most likely storage that is simulated by the model, which can be seen as the sum of all cells $\mathrm{Vm_n}$ and cell $\mathrm{Vim}$, and shows the lower and upper bound of the 95% confidence interval. The storage is given as total meters of water in the waste body, which is itself about 12.5 meters, given that the average height is 9.2 meters above NAP, the drainage system is located at -4.3 meter above NAP and there is a soil cover of a meter. The predicted patterns based on the outflow are also visible in figure 9.5.

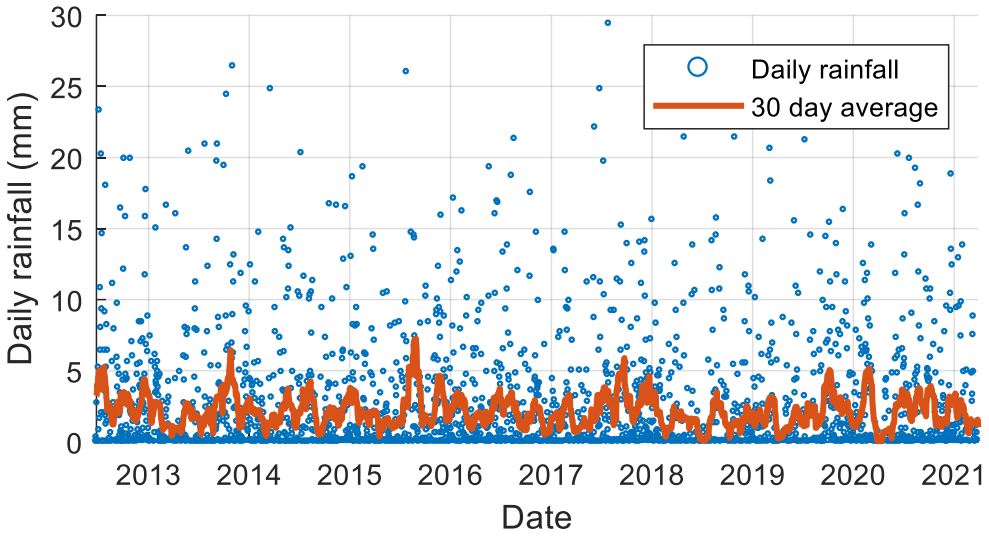


*Figure 9.2: Daily rainfall input ($q_{rain}$) for model (KNMI, 2021)*

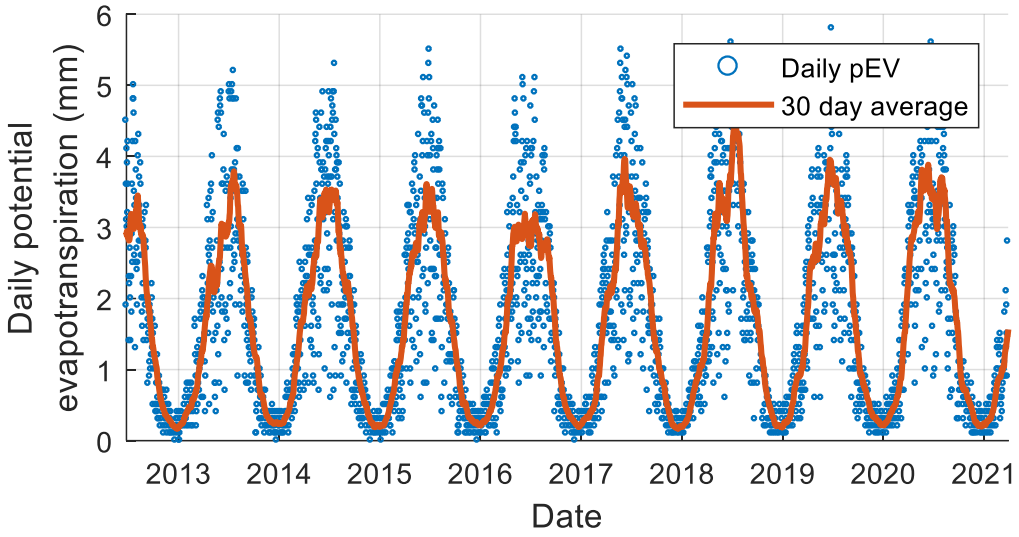


*Figure 9.3: Daily evapotranspiration ($q_{evap}$) input for model (KNMI, 2021)*

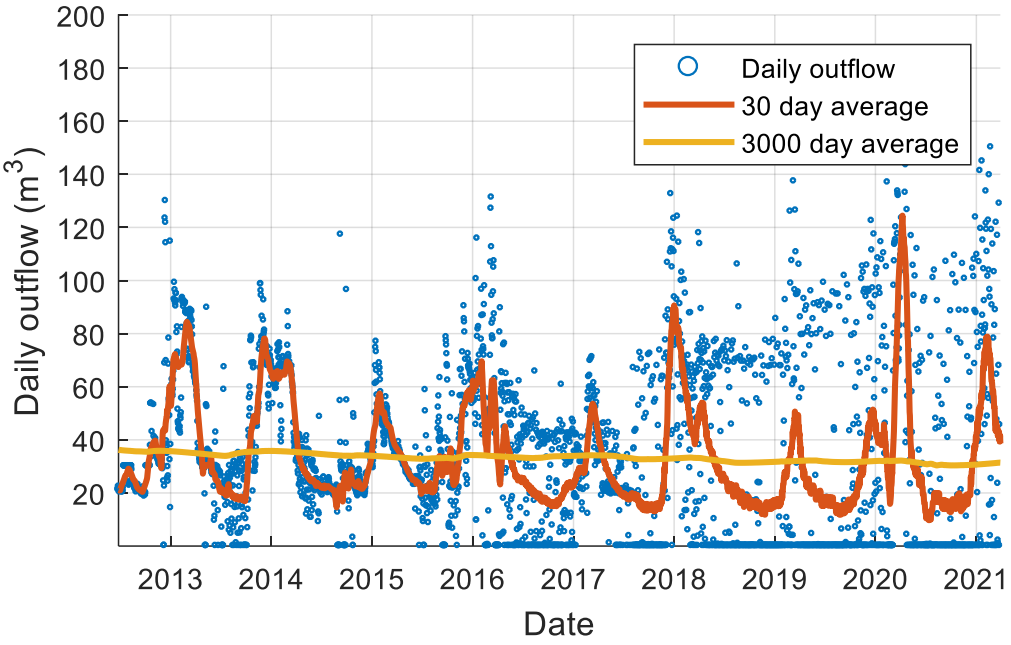


*Figure 9.4: Daily outflow ($q_{out}$) input for model*

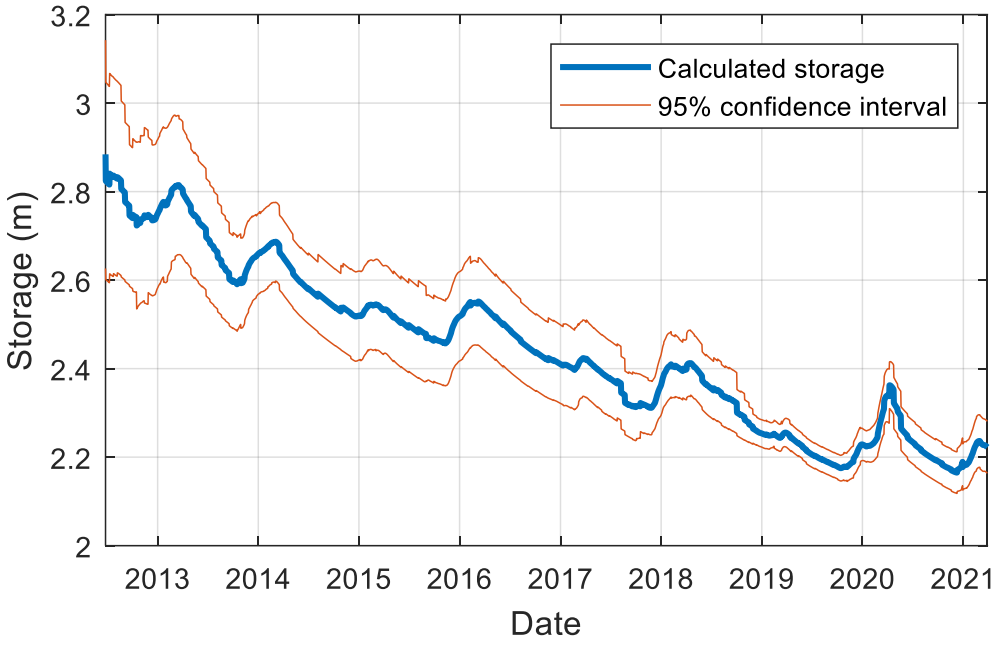


*Figure 9.5: Storage output from the model*

## 9.3 Van Genuchten parameters

With the van Genuchten equation (equation 3.17) the calculated storage can be translated to a water column. To do this the van Genuchten parameters are needed. As compartment 11Z is not a typical landfill waste body, because it contains almost only soils, both soil and waste van Genuchten parameters found in literature are compared. First the total amount of water present in the waste body was calculated, then this was be converted to a water level. The storage is not the total amount of water, as it does not take into account the residual water content, which is the water that will never flow due to gravity. The total water present is given in equation 9.1, which takes into account that the

landfill can be discretised into multiple layers with their own residual water content as the residual water content can be a function of depth. The storage is a function of time, but in the calculations is assumed that the residual water content and thickness of the waste body are constant. Equation 9.2 gives also the total amount of water present, as $\theta(l, WL)$ can be calculated with the van Genuchten equation presented in section 3.4. Setting equation 9.1 equal to 9.2 makes it possible to solve for the water level $WL$. For this thesis this was not solved analytically, but for each possible water level the total water was calculated and that relation was used to look up the water level corresponding to a certain storage.

$$TW = S + \int_0^L \theta_r(l)dl \approx S + \sum_{n=1}^{n=layers} {\theta_r}^n \cdot L^n \qquad 9.1$$

Where $TW$ is the total water in the waste body [L], $S$ is the storage [L], $\theta_r$ is the residual water content [-] and $L$ is the thickness of the waste body or the discretised waste body layers [L].

$$TW = \int_0^L \theta(l, WL)dl \approx \sum_{n=1}^{n=layers} \theta^n \cdot L^n \qquad 9.2$$

Where $TW$ is the total water in the waste body [L], $\theta$ is the water content [-], which is a function of the depth and the water level in the waste body and $L$ is the thickness of the waste body or the discretised waste body layers [L].

The water content can be calculated with a given set of van Genuchten parameters. The soil van Genuchten parameters that are evaluated are given in table 9.1. Figure 9.6 shows for these parameters the relation between the total water and the water level. The water level given is assuming that the standing water body already starts at the drainage system and that there are no spatial differences, which are both in reality not likely to be the case. Besides the soil parameters that were evaluated, gives table 9.2 the waste van Genuchten parameters that were evaluated. White et al. (2015) present ten sets of van Genuchten parameters obtained from landfills, of which the three with the lowest saturated water contents have been chosen to be evaluated. The reason for this is that because of the large amount of soil present the porosity in compartment 11Z is relatively low (0.3-0.4), while in landfills that contain different types of waste the porosity can get up to 0.77 (White et al., 2015).

*Table 9.1: Soil van Genuchten parameters (Hilberts et al., 2005)*

| Name | $\theta_s$ (-) | $\theta_r$ (-) | $\alpha$ (kPa$^{-1}$) | $n$ (-) |
|---|---|---|---|---|
| **Sand** | 0.26 | 0.01 | 3.24 | 6.66 |
| **Loam** | 0.37 | 0.05 | 1.61 | 2.66 |
| **Clay** | 0.47 | 0.16 | 0.66 | 1.86 |

*Table 9.2: MSW van Genuchten parameters (White et al., 2015)*

| Name | $\theta_s$ (-) | $\theta_r$ (-) | $\alpha$ (kPa$^{-1}$) | $n$ (-) |
|---|---|---|---|---|
| **MSW - 1** | 0.53 | 0.22 | 2.92 | 1.58 |
| **MSW - 2** | 0.45 | 0.33 | 0.50 | 2.29 |
| **MSW - 3** | 0.58 | 0.14 | 1.40 | 1.60 |

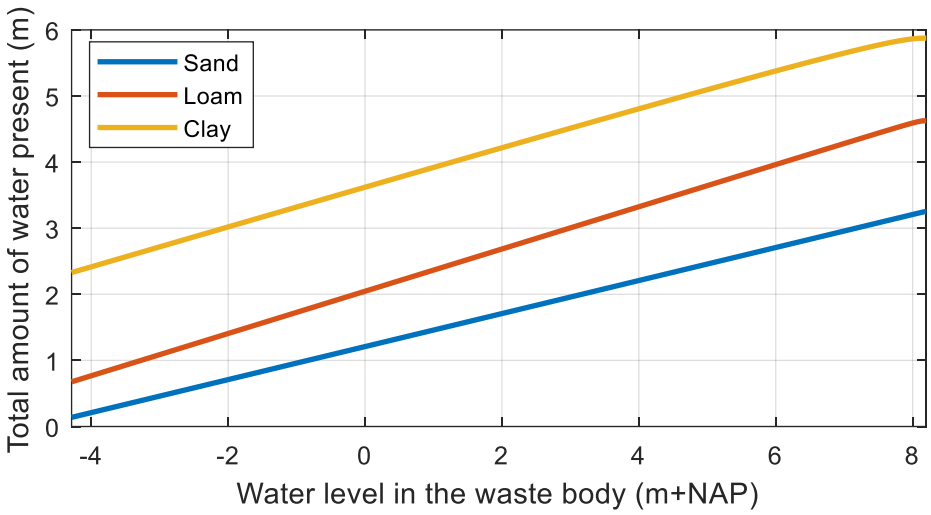


*Figure 9.6: Total water against water level*

Both the soil and waste parameters are single sets of parameters that are supposed to capture the behaviour of the entire compartment. However it can be expected that the behaviour varies temporally and spatially. Liang et al. (2008), showed that with taking into account biodegradation and settlement, the porosity increases slightly over the years for a MSW landfill, but especially in the first years after deposition. Because of this it is assumed that the van Genuchten parameters do not change over time after the first years after deposition of the waste. As the water balance model does not take into account any horizontal variability, it is also assumed that over the entire compartment the parameter, and thus also the resulting water levels, are constant. Vertically there is variability present, as it can be expected that because of the way the landfill is constructed and the weight of the waste the porosity is decreasing with depth. White et al. (2015) propose a functional relationship between the porosity and the other three van Genuchten parameters for landfill waste. According to the functional relationship the residual water content decreases with increasing porosity, which is reasonable as when the pores increase in size the amount of really small pores that permanently bind water will decrease. $\alpha$ and $n$ increase with increasing porosity, which is also in line with the expectations, as a general increase in pore size will also lead to faster drainage. The used functional relationships are given in appendix K. Similar as for the 'fixed' parameters, to implement the relationships the waste body has been discretised into vertical segments. Now it is not only the hydraulic head which is different for the segments resulting in different water contents, but also the van Genuchten parameters are different for the segments if there is a porosity gradient assumed.

Figure 9.7 shows the relationship between the total water and the water level for a few porosity gradients that have been evaluated. The maximal porosity is the porosity at the top of the landfill and the minimal porosity is the porosity at the bottom of the landfill, in between the porosity is linearly decreasing towards the bottom. In the figure can be seen that the curves are straight for the constant porosity cases and have a changing slope for the other cases. For example, if the porosity is larger at the top of the landfill, the slope of the curve will increase for higher water levels, as more and more water is needed to fill the pores towards the top of the landfill. The curve that represents a constant 0.5 porosity has the lowest total amount of water if the water level is at the drainage at -4.3 meter above NAP. This is because the highest porosity curve also has the lowest residual water content as the water drains faster trough the larger pores.

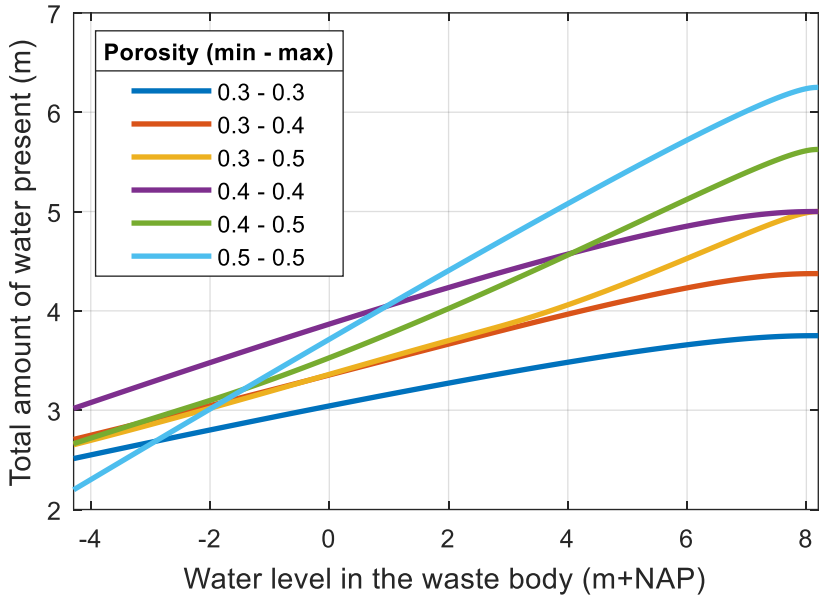


*Figure 9.7: Total water against water level with a porosity gradient*

# 10. Results and discussion

In this chapter the results of the numerical evaluation are presented and discussed. The results are obtained by using the modelled storage and applying the relationships between total water and water level obtained with the van Genuchten equation, described in section 9.3.

## 10.1 Soil parameters

Figure 10.1 shows the water levels predicted based on the soil parameters given in table 9.1, and the model inputs shown in section 9.2. The seasonal peaks in water level are clearly visible for all three soil types. The water levels are the highest for sand as the effective porosity ($\theta_s - \theta_r$) is the lowest. The predicted water levels are much higher than what was measured in the field.

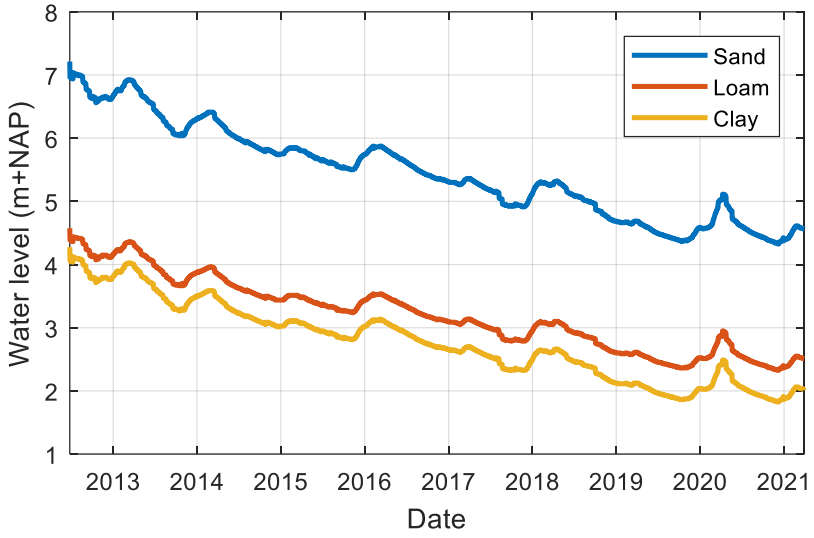


*Figure 10.1: Predicted water levels using soil van Genuchten parameters*

## 10.2 Waste parameters

Figure 10.2 shows the water levels predicted based on the three selected sets of waste parameters given in table 9.2.

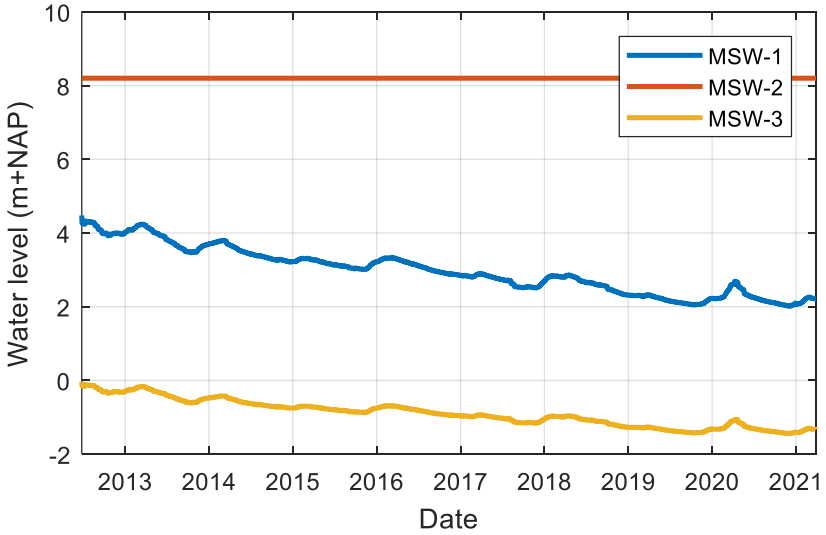


*Figure 10.2: Predicted water levels using waste van Genuchten parameters*

The differences in predicted water levels using the waste parameters are enormous and show how diverse different types of waste can be in their hydraulic behaviour. MSW-2 gives a constant water level of 8.2 meter above NAP. The reason for this is that the effective porosity for this waste is only 0.12, which is not enough to accommodate the modelled storage, and the water level is exactly the height of the waste body. The seasonal peaks are also clearly visible. The predicted water levels using MSW-3 are lower than what was measured in the field, but the effective porosity of 0.44 is probably much higher than what is the case in compartment 11Z.

## 10.3 Waste functional relationship

Figure 10.3 shows the water levels predicted based the waste parameters obtained with the functional relationships presented in appendix J. There is a large difference in water levels between the different porosity gradients. The two lines corresponding to the overall lowest porosities have during at least a part of the modelled time a water level which is above the level of the waste body, which is unrealistic. The seasonal peaks cause by the high precipitation and low evapotranspiration have a wide spread of magnitudes.

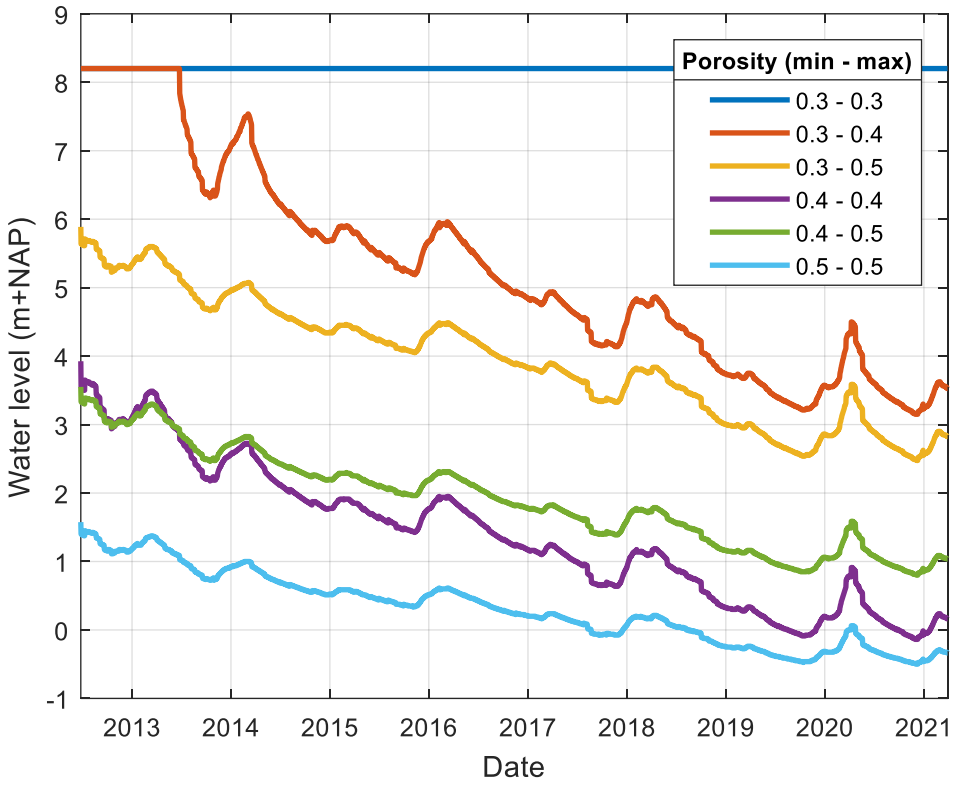


*Figure 10.3: Predicted water levels using functional relationships for waste van Genuchten parameters*

## 10.4 Comparison with the measurements

Table 10.1 shows the measured and predicted water levels. The values obtained with the functional relationships are given in the table by their minimal and maximal porosity values. Except for the probably unrealistic MSW-3 parameter set, all the predicted water levels overestimate the measured water levels. It can always be the case that the modelled storage is an overestimation, but the change in storage $\Delta S$ can be accurately determined, as how much water comes in to and goes out of the landfill is accurately measured. However considering the observed reduction of water level between March and November of 2020, the predicted values for all parameter sets underestimate the true change in

water level that was measured. If the landfill is considered to consist of separate not or poorly connected 'buckets' as described in section 6.6, the only way that the measured and predicted values are in agreement is when the buckets prefer to form around the aeration wells. The presence of these 'buckets' would on the other hand result in an overestimation of the average water level during the measurements, but still is the absolute modelled water level larger than the average measurements. The fact that the measured water level in December 2016 was lower than both March and November of 2020 does not at all reflects the fact that the base flow and also the storage in compartment 11Z is decreasing. Unless the exact van Genuchten parameters are known for the waste in compartment 11Z, which will be hard to obtain given the large heterogeneity of the waste, there is not more to obtain from the numerical evaluation except for these general observations based on all the different predicted water levels combined.

*Table 10.1: Measured (average for all the aeration wells) and predicted water levels*

| Data | Dec '16 (m+NAP) | Mar '20 (m+NAP) | Nov '20 (m+NAP) | Mar '20 – Nov '20 (m) |
|---|---|---|---|---|
| **Measured** | -0.14 | 1.41 | 0.47 | 0.92 |
| **Sand** | 5.33 | 4.87 | 4.36 | 0.51 |
| **Loam** | 3.11 | 2.75 | 2.35 | 0.39 |
| **Clay** | 2.67 | 2.28 | 1.85 | 0.43 |
| **MSW-1** | 2.87 | 2.47 | 2.03 | 0.43 |
| **MSW-2** | 8.20 | 8.20 | 8.20 | 0 |
| **MSW-3** | -0.95 | -1.17 | -1.42 | 0.25 |
| **0.3 – 0.3** | 8.20 | 8.20 | 8.20 | 0 |
| **0.3 – 0.4** | 4.88 | 4.06 | 3.20 | 0.86 |
| **0.3 – 0.5** | 3.86 | 3.27 | 2.52 | 0.75 |
| **0.4 – 0.4** | 1.20 | 0.57 | -0.09 | 0.67 |
| **0.4 – 0.5** | 1.80 | 1.35 | 0.83 | 0.51 |
| **0.5 – 0.5** | 0.22 | -0.11 | -0.47 | 0.36 |

# 11. Conclusions on the numerical evaluation

Combining the storage modelled by the water balance model for compartment 11Z with the van Genuchten equation made it possible to predict how the water level in the landfill would change over time by making the simplifying assumption of a homogenous waste body. As it was shown that with different waste types the response in terms of water level to a changing storage can be really diverse, nothing specific can be said about the water level in compartment 11Z, however based on the results some general conclusions can be made about the relation between the modelled storage and the measured water levels.

The storage of water in the compartment is decreasing over time, which can be concluded from the fact that the base flow from the waste body into the drainage is also decreasing over time as the base flow is larger if more water is stored in the landfill. A decreasing storage should translate itself to a decreasing water level. This is indeed the result of the model, but the measurements of the water levels in the aeration wells do not reflect this and show an increase of water level over time. The measurements are taken with 16 meter intervals, the distance between the aeration wells, and since there are 132 of them, it was assumed that the average of the water level in the wells reflects the average of the water level in the waste body, even while considering the bucket model because the numerous amount of wells. The only way that the change in predicted water level given a homogenous waste body over time and the change measured water level in the aeration wells over time reflect the same change in water stored in the landfill is when the water in the landfill has a preferred location just around the aeration wells.

Apart from the apparent mismatch in the change in water level over time, does the modelled storage produce for most sets of parameters also an absolute water level that is too high, especially for the first years that are modelled. The change in storage should be well defined, but in determining the absolute storage more assumptions are needed, which might cause the overestimation.

The numerical evaluation does show that the seasonal variation that was observed is indeed expected based on the water balance of the compartment, but for the other measurements the numerical evaluation is not in agreement with the obtained data.

The model should be improved to give a more accurate description of the water storage. If techniques used to estimate the total amount of water stored in the compartment, such as electrical resistivity tomography (ERT), can be optimised to get a reliable estimate of the total amount of water present this could be used to calibrate the storage term in the model. Also would it be beneficial if the output of the model could be further processed to include the horizontal variability that is also present in the bucket model, for example by making a spatial distribution of the storage instead of only determining a single value. This spatial distribution should not have to exactly represent the situation in compartment 11Z, but could show how a typical spatial distribution of water would look like.

# Part IV - Conclusions & Recommendations

# 12. Conclusions

This chapter concludes the thesis by giving the final answer to the research question and the sub questions. First the six sub questions are answered based on the results presented in the report, then the main research question is answered. At last a general conclusion is given on the entire research.

## 12.1 Research questions

**What are the water levels in the Braambergen landfill and how does this influence the magnitude of LFG fluxes in the aeration system?**

The average water level measured in the aeration wells in March 2020 is -0.6 meter above NAP for compartment 11N, 1.4 meter above NAP for compartment 11Z and -0.4 meter above NAP for compartment 12, with outliers in compartment 11Z up to 7 meters above NAP. Towards November 2020 the water level dropped due to seasonal variations and the average water level measured in compartment 11Z was 0.5 meter above NAP, showing there is no connectivity to the drainage layer. The LFG is extracted through aeration wells which have their bottom roughly at -2 meter above NAP, the perforated part extends for 1.8 meter and the magnitude of LFG flux decreases linearly with an increasing water column and becomes zero when the water column larger than this 1.8 meter.

**How does the water level in the Braambergen landfill vary spatially and temporally, and why is this variability present?**

The spatial variability of the water levels is large. In compartment 11Z there are aeration wells which are only 15 meters apart and still have a difference in water level larger than four meters, which is unthinkable in any natural aquifer. The spatial variability in water level is caused by the heterogeneity of the hydraulic behaviour of the waste, some areas receive more water due to preferential flow paths and also for some areas the drainage of leachate towards the drainage system is better. It is concluded that there is almost no horizontal flow of leachate. The temporal variation of water levels is in some of the aeration wells really large, changing meters during the year because of the seasonal variation of the weather, while for others the water level remains constant throughout the year.

**What is the spatial variability of the horizontal hydraulic conductivity in compartment 11Z of the Braambergen landfill?**

The found estimates for the horizontal hydraulic conductivities range from $1 \cdot 10^{-7}$ to $6 \cdot 10^{-4}$ meter per second, based on a recovery test analysed with the Theis solution. Only 13 of the 100 performed pumping tests gave a valid recovery curve that could be analysed. It was found that the estimates for these hydraulic conductivities only hold for small areas around the aeration wells, ranging from a few centimetres to a few meters, which is small compared to the scale of the compartment, leading to the conclusion that there must be zones of really low horizontal permeability that prevent the flow of leachate.

**What is the spatial variability of the leachate composition and properties in compartment 11Z of the Braambergen landfill?**

The spatial variability of the leachate composition of the samples taken from the aeration wells is so large that the correlation between the electrical conductivity, the ammonium concentration or the DOC between neighbouring wells is not larger then between any other wells. This is partly because the waste is heterogenous and also shows that the leachate surrounding the wells is not in equilibrium with the water surrounding neighbouring wells. A positive correlation between electrical conductivity, ammonium concentration and DOC was found for the individual samples. Also did the average values measured on the leachate samples roughly matched the values measured in the basal drain.

**What is a realistic representation of the water distribution in the Braambergen landfill?**

Based on the results of all the measurements combined can be concluded that the water that is present within the landfill is not a fully connected water body. Instead it seems that there are 'buckets' of water present, zones of relatively high permeability surrounded by zones of relatively low permeability. Once a bucket is full, it will overflow and the maximum water level in that area is capped by the height of the bucket. This explains why there is standing water present in the landfill even while the water level in the basal drain is regulated.

**Can the observed temporal variability of water levels in compartment 11Z be explained with a water balance model?**

The water balance model used for evaluation predicted the seasonal variability in water storage that was observed, but seemed to underestimate the magnitude. The long term temporal variability gave a clear mismatch between measured and modelled water level, the model and the outflow data seems to suggest a decrease in water level over time, while this was not wat was observed in the field between 2016 and 2020. Also did modelled storage resulted in an overestimation of the water level.

***How do the elevated water levels in compartment 11Z of the Braambergen landfill influence the efficiency of the waste aeration, and how can the reduced efficiency be mitigated effectively?***

The elevated water levels in compartment 11Z are caused by zones of low permeability which result in very local free standing water bodies. If there is a water column above 1.8 meter in an aeration well there is no extraction of LFG possible. Even if the water column is reduced the magnitude of LFG extracted from the aeration wells will be considerably lower in compartment 11Z compared to the other compartments due to the unfavourable flow conditions. Still can the reduced efficiency of the waste aeration due to the water present in the aeration wells can mitigated by lowering the water column in the aeration wells of the entire compartment, which can be either accomplished by lowering the water level or raising the aeration wells. The fact that the water in the landfill is present in local unconnected water bodies makes it that lowering the water level by installing gravel columns or by pumping the water out will not have an effect that extends over the entirety of the compartment. Raising the aeration wells will only have a long term effect if the water levels do not rise anymore. The water balance model predicts that the water stored in the landfill will reduce over time, but based on the measurements it is not clear whether that is really also the case for the water levels in the aeration wells. Based on the measurements it is assumed that the water level in most aeration wells are capped and will not rise above a certain level, making lifting the aeration wells a feasible option.

## 12.2 General conclusion

The general conclusion of this thesis is that the studied compartment 11Z is homogenous in its heterogeneity. With all the different measurement types performed it was in some way the objective to see whether the behaviour or the properties of the landfill and the leachate can be grouped spatially, but this was not the case. Therefore can be concluded that the only scale for which a measurement can be representative for the entire compartment is on the scale of the compartment itself. This is in line with the expectations of large heterogeneity in landfills and the unique situation of aeration system on the Braambergen made it possible to proof this.

The efficiency of the aeration system is particularly low in compartment 11Z because the conditions are unfavourable for both water and gas flow. The conditions in compartments 12 and especially 11N are more favourable because the waste, especially at the bottom of the compartments, is more permeable. Even if the amount of water in 11Z is reduced and the gas flow increases, the total amount of extracted LFG will not reach the same level as for the other compartments.

# 13. Recommendations

This chapter provides the recommendations for improvements and for further research based on the results obtained for this thesis.

For compartment 11Z there are three complete data sets of the water levels in the aeration wells, one taken in 2016 and two taken in 2020. For some wells the measurements have been taken more often, but given how heterogenous the water levels are this subset of wells provides not enough information to say anything about the general trend of all the aeration wells. To get a better insight in the change of water levels over time it would be valuable to have more complete data sets of water levels in all the aeration wells and it is therefore recommended to monitor the water levels more often.

For some of the aeration wells it is clear that these are broken. If the well is both broken and does not produce any LFG, it might be interesting to lift the well out of the landfill and then investigate the filter screen. As this well will not contribute anymore the aeration it will not be missed and this could answer the question whether or not the filter screens getting clogged is the reason of the low gas and leachate flows, or whether this is caused purely by the unfavourable waste properties.

The pumping tests gave some rough estimates of the hydraulic conductivity, based on the Theis solution for drawdown in a well. The Theis solution assumes that the well is recovering during the pumping already in which case the pumping rate is important. Another possibility to obtain the hydraulic conductivity is with a slug test, in which case is assumed that suddenly the well is dry and the leachate surrounding the well can flow in. For some of the really slowly recovering wells, this assumption is valid and if the recovery would be monitored over the hours after the pumping the recovery could be analysed as a slug test.

The leachate from the aeration wells have only been sampled once, only making it possible to assess the spatial variability, but for looking at the temporal variability the results of the leachate sampled from the basal drain by Afvalzorg were used. With the basal drain samples the information on the spatial variability is lost. Therefore it is recommended for further investigation to collect the samples from the aeration well more often such that can be investigated whether the large temporal variability of the water level also translates itself in an equally large temporal variability in the leachate properties.

The long term monitoring of the aeration wells gave interesting results. The wells have been monitored for over two months, but to really see whether over a longer time if the water level is generally decreasing or increasing it would also be interesting too to monitor the water column in some wells for an even longer duration of time. Also was the measured electrical conductivity often not stable, presumably because of the malfunction of the divers. Solving this issue would make it possible to gain more information from the measurements.

Lastly, for the numerical evaluation it is recommended to develop a method to determine from the modelled storage to a distribution of water levels, instead of only a single average water level, which was what was done in this thesis. This was enough for the scope of this thesis, but does not reflect the idea of the bucket model and can therefore not be used to say anything specific about the expected water level distribution.

# Bibliography


Afvalzorg (2021). Areal picture of the Braambergen Landfill [Online Image]. Retrieved from: https://www.afvalzorg.com/news/landfill-braambergen-back-to-life

Blight, G. E., & Fourie, A. B. (1999). Leachate generation in landfills in semi-arid climates. *Proceedings of the Institution of Civil Engineers-Geotechnical engineering*, *137*(4), 181-188.

Blume, H. P., Brümmer, G. W., Horn, R., Kandeler, E., Kögel-Knabner, I., Kretzschmar, R., ... & Welp, G. (2010). Scheffer/Schachtschabel. *Soil Science*, *16*.

Bird, R. B., Stewart, W. E., & Lightfoot, E. N. (2006). *Transport phenomena* (Vol. 1). John Wiley & Sons.

Brand, E., de Nijs, T., Claessens, J., Dijkstra, J., Comands, R. & Lieste, R. (2014). Development of emission testing values to assess sustainable landfill management on pilot landfills: Phase 2: Proposals for testing values. *RIVM Report 607710002/2014*

Brandstetter, A., Sletten, R. S., Mentler, A., & Wenzel, W. W. (1996). Estimating dissolved organic carbon in natural waters by UV absorbance (254 nm). *Zeitschrift für Pflanzenernährung und Bodenkunde*, *159*(6), 605-607.

Bröcker, C. & Kaiser, W. (2001). Feasibility Study on Sustainable Emission Reduction at the Existing Braambergen Landfill in the Netherlands. *Specific Report: Current Status of the Braambergen Landfill*.

Christensen, J. B., Jensen, D. L., Grøn, C., Filip, Z., & Christensen, T. H. (1998). Characterization of the dissolved organic carbon in landfill leachate-polluted groundwater. *Water research*, *32*(1), 125-135.

Christensen, T. H., Kjeldsen, P., Bjerg, P. L., Jensen, D. L., Christensen, J. B., Baun, A., ... & Heron, G. (2001). Biogeochemistry of landfill leachate plumes. *Applied geochemistry*, *16*(7-8), 659-718.

Directive 1999/31/EC of 26 April 1999 on the landfill of waste. Council of the European Union. *Document 31999L0031.* Retrieved from: http://data.europa.eu/eli/dir/2019/904/oj

Ehrig, H. J. (1983). Quality and quantity of sanitary landfill leachate. *Waste Management & Research*, *1*(1), 53-68.

Fellner, J., & Brunner, P. H. (2010). Modeling of leachate generation from MSW landfills by a 2-dimensional 2-domain approach. *Waste Management*, *30*(11), 2084-2095.

Fellner, J., Döberl, G., Allgaier, G., & Brunner, P. H. (2009). Comparing field investigations with laboratory models to predict landfill leachate emissions. *Waste Management*, *29*(6), 1844-1851.

Fitts, C. R. (2002). *Groundwater science.* Elsevier.

Garrod, G., & Willis, K. (1998). Estimating lost amenity due to landfill waste disposal. *Resources, conservation and recycling*, *22*(1-2), 83-95.

Hansen, A. M., Kraus, T. E., Pellerin, B. A., Fleck, J. A., Downing, B. D., & Bergamaschi, B. A. (2016). Optical properties of dissolved organic matter (DOM): Effects of biological and photolytic degradation. *Limnology and oceanography*, *61*(3), 1015-1032.

Heimovaara, H., Oonk, H., van der Sloot, H., & van Zomeren, A. (2010). Reduction of the long-term emission potential of existing landfills. *Dutch Sustainable Landfill Foundation.*

Hossain, M. S., Penmethsa, K. K., & Hoyos, L. (2009). Permeability of municipal solid waste in bioreactor landfill with degradation. *Geotechnical and Geological Engineering*, *27*(1), 43.

Hrad, M., Gamperling, O., & Huber-Humer, M. (2013). Comparison between lab- and full-scale applications of in situ aeration of an old landfill and assessment of long-term emission development after completion. *Waste Management*, *33*(10), 2061-2073.

Huber-Humer, M., Gebert, J., & Hilger, H. (2008). Biotic systems to mitigate landfill methane emissions. *Waste Management & Research*, *26*(1), 33-46.

IEA (2021). *Methane Tracker 2021*. Available from https://www.iea.org/reports/methane-tracker-2021

IPCC. (2014). *Climate change 2014: synthesis report. Contribution of Working Groups I, II and III to the fifth assessment report of the Intergovernmental Panel on Climate Change*. Available from https://www.ipcc.ch/report/ar5/syr/

Islam, J., & Singhal, N. (2004). A laboratory study of landfill-leachate transport in soils. *Water research*, *38*(8), 2035-2042.

Khanbilvardi, R. M., Ahmed, S., & Gleason, P. J. (1995). Flow investigation for landfill leachate (FILL). *Journal of environmental engineering*, *121*(1), 45-57.

Kjeldsen, P., Barlaz, M. A., Rooker, A. P., Baun, A., Ledin, A., & Christensen, T. H. (2002). Present and long-term composition of MSW landfill leachate: a review. *Critical reviews in environmental science and technology*, *32*(4), 297-336.

KNMI (2021). *Dagwaarden neerslagstations.* Available from: https://www.knmi.nl/nederland-nu/klimatologie/monv/reeksen

Kruseman, G. P., De Ridder, N. A., & Verweij, J. M. (2000). *Analysis and evaluation of pumping test data*. The Netherlands: International institute for land reclamation and improvement.

Kulikowska, D., & Klimiuk, E. (2008). The effect of landfill age on municipal leachate composition. *Bioresource technology*, *99*(13), 5981-5985.

Lee, D. T., & Schachter, B. J. (1980). Two algorithms for constructing a Delaunay triangulation. *International Journal of Computer & Information Sciences*, *9*(3), 219-242.

Leikam, K., Heyer, K. U., & Stegmann, R. (1999). Aerobic in situ stabilization of completed landfills and old sites. *Waste management & research*, *17*(6), 555-562.

Liang, B., Liu, L., Xue, Q., & Zhao, Y. (2008). Porosity prediction with settlement and biodegradation in municipal landfill. In *2008 2nd International Conference on Bioinformatics and Biomedical Engineering* (pp. 1289-1292). IEEE.

Omar, H., & Rohani, S. (2015). Treatment of landfill waste, leachate and landfill gas: A review. *Frontiers of Chemical Science and Engineering*, *9*(1), 15-32.

Oonk, H. (2020). Afvalmonstername en analyse bij de nulmeting van de iDS-pilots. *Stichting Duurzaam Storten.*

Powrie, W., & Beaven, R. P. (1999). Hydraulic properties of household waste and implications for landfills. *Proceedings of the Institution of Civil Engineers-Geotechnical Engineering*, *137*(4), 235-237.

Rees-White, T., Beaven, R., Powrie, W., & Cole, D. (2013). Investigating clogging failure mechanisms of leachate extraction wells in landfills. *Canadian geotechnical journal*, *50*(11), 1179-1187.

Renou, S., Givaudan, J. G., Poulain, S., Dirassouyan, F., & Moulin, P. (2008). Landfill leachate treatment: Review and opportunity. *Journal of hazardous materials*, *150*(3), 468-493.

Ritzkowski, M., & Stegmann, R. (2012). Landfill aeration worldwide: concepts, indications and findings. *Waste Management*, *32*(7), 1411-1419.

Scanlon, B. R., Nicot, J. P., & Massmann, J. W. (2002). Soil gas movement in unsaturated systems. *Soil physics companion*, *389*, 297-341.

Scharff, H. (2020). Landfill Geotechnics [Powerpoint slides].

Scheutz, C., Kjeldsen, P., Bogner, J. E., De Visscher, A., Gebert, J., Hilger, H. A., ... & Spokas, K. (2009). Microbial methane oxidation processes and technologies for mitigation of landfill gas emissions. *Waste management & research*, *27*(5), 409-455.

Sherene, T. (2009). Effect of dissolved organic carbon (DOC) on heavy metal mobility in soils. *Nature Environment and Pollution Technology*, *8*(4), 817-821.

Slimani, R., Oxarango, L., Sbartai, B., Tinet, A. J., Olivier, F., & Dias, D. (2017). Leachate flow around a well in MSW landfill: Analysis of field tests using Richards model. *Waste Management*, *63*, 122-130.

Van Turnhout, A. , Oonk, H., Heimovaara, T. (2020). Verbreding Toepasbaarheid Duurzaam Stortbeheer (VtDS).

Vereniging Afvalbedrijven (2014). Deelplan van Aanpak verduurzamingspilot op stortplaats Braambergen.

Wang, L. (2021). Water balance model and uncertainty [Powerpoint slides].

Wang, L., Heimovaara, T., & Gebert, J. (2021). Estimation of landfill emission potential with particle filtering. *Conference paper IWWG symposium Sardinia 2021.*

White, J., Zardava, K., Nayagum, D., & Powrie, W. (2015). Functional relationships for the estimation of van Genuchten parameter values in landfill processes models. *Waste Management*, *38*, 222-231.

Xu, X. B., Powrie, W., Zhang, W. J., Holmes, D. S., Xu, H., & Beaven, R. (2020). Experimental study of the intrinsic permeability of municipal solid waste. *Waste Management*, *102*, 304-311.

Zdeb, M., Papciak, D., & Zamorska, J. (2018). An assessment of the quality and use of rainwater as the basis for sustainable water management in suburban areas. In *E3S Web of conferences* (Vol. 45, p. 00111). EDP Sciences.

# Part V - Appendices

# A. Waste origin compartment 11

Table A.1 shows for compartment 11 (subdivided in 11N and 11Z) the percentage of waste types landfilled. Another subdivision is made based on age of the waste. Each age category, youngest, middle and oldest, includes one third of the waste present in the compartment. It is clear that for both 11N and 11Z the soil and soil decontamination residue is the primary waste origin, but there is also a clear difference between 11N and 11Z. The oldest waste, which is located at the bottom of the landfill on top of the drainage system, contains in 11N relatively high amounts of non-soil waste while in 11Z the oldest waste consist almost solely out of soil and soil decontamination residue.

*Table A.1: Percentage of waste mass per origin in compartment 11 (Oonk, 2020)*

| | | S&SR | CDW | CW | SA | CHW | S&CW | HHW |
|---|---|---|---|---|---|---|---|---|
| **11N** | youngest | 92% | 3% | 3% | 3% | | | |
| **11N** | middle | 86% | 4% | 6% | 3% | | | |
| **11N** | oldest | 42% | 18% | 27% | 1% | 1% | 1% | 8% |
| **11Z** | youngest | 95% | | 5% | | | | |
| **11Z** | middle | 94% | 3% | 2% | | 1% | | |
| **11Z** | oldest | 98% | 1% | | 1% | | | |

S&SR is soil and soil decontamination residues; CDW is construction and demolition waste; CW is commercial waste; SW is shredder waste; CHW is course household waste; S&CW is sludge and composting waste; HHW is household waste.

# B. Old gas well locations and names

Figure B.1 shows the locations of the old gas wells. Similar as for the aeration wells, the distance between adjacent wells is smaller in compartment 11Z compared to 11N and 12.


*Figure B.1: Old gas well locations and names*

# C. TIN interpolation explanation

To determine values of measured quantity between datapoints interpolation is needed. It is important to know how the interpolation has been performed, as interpolated values are not the true values but just an approximation based on the known data points and the assumption that the measured quantity is continuous in the interpolated interval. Interpolated values should therefore be interpret carefully and not be confused with actual measurements.

In this thesis 2D interpolation is used to visualize water level values in between measured locations. The method used for this is Triangulated Irregular Network (TIN) interpolation. This is a triangular interpolation method based on the Delaunay triangulation. The Delaunay triangulation algorithm finds for every set of data points in a 2D space a distinct collection of triangles connecting three data point such that for each triangle, the circumscribed circle only contains the three data points that form the triangle (Lee & Schachter, 1980), which can be seen in figure D.1, in which for simplicity only three of the six circumscribed circles have been drawn.

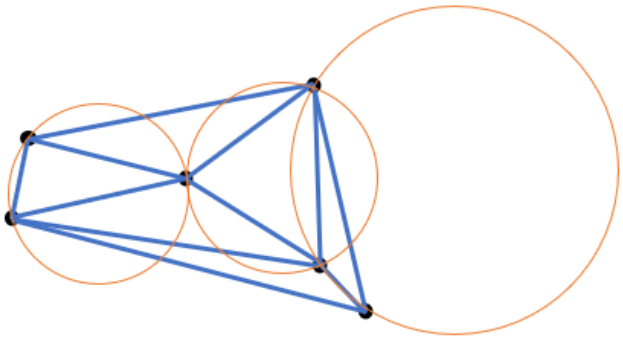

*Figure C.1: Example of a Delaunay triangulation*

With the triangles connecting the data points defined, the interpolation method can be applied. To prevent irregularities at the edges, the used method is designed such that at every edge the interpolated value is based only the two data points forming the edge. One way of doing this is shown in figure C.2 and equation C.1. The interpolation value at $x$ is a weighted combination of the known data points $P_1$, $P_2$ and $P_3$, where the weights $w_1$, $w_2$ and $w_3$ are based on the areas $A_1$, $A_2$ and $A_3$ of the triangles between the known data points and $x$.

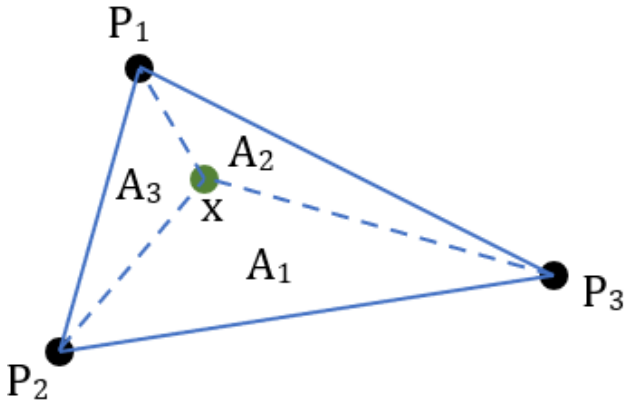


*Figure C.2: Interpolation principle*

$$x = w_1 P_1 + w_2 P_2 + w_3 P_3 = \frac{A_1}{A_{total}} P_1 + \frac{A_2}{A_{total}} P_2 + \frac{A_3}{A_{total}} P_3 \qquad \text{C.1}$$

# D. TIN interpolation water levels

Figure D.1 shows the interpolated water levels of the measurements done in December of 2016 and figure D.2 the same for the measurements from March of 2020. The contour lines shown in both figures are have a spacing of 1 meter.

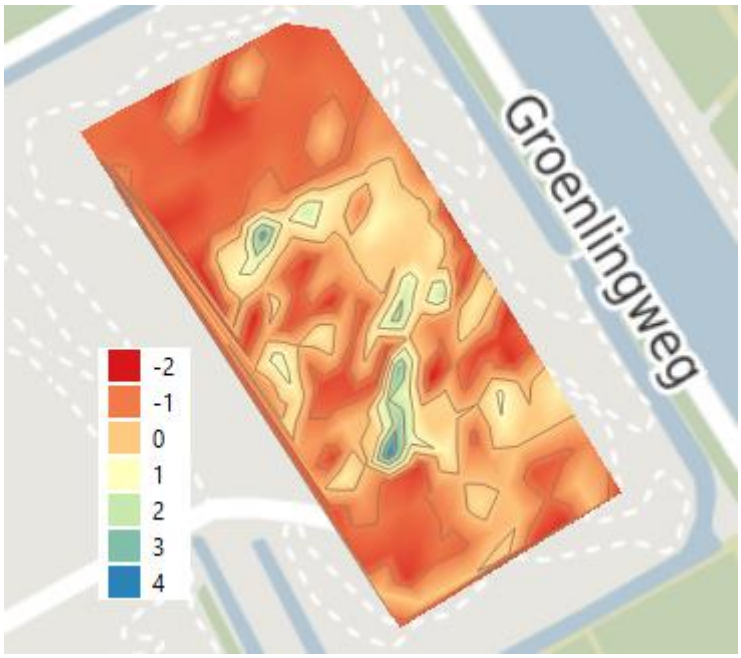


*Figure D.1: Interpolated water levels in the aeration wells measured December 2016 (in m+NAP)*

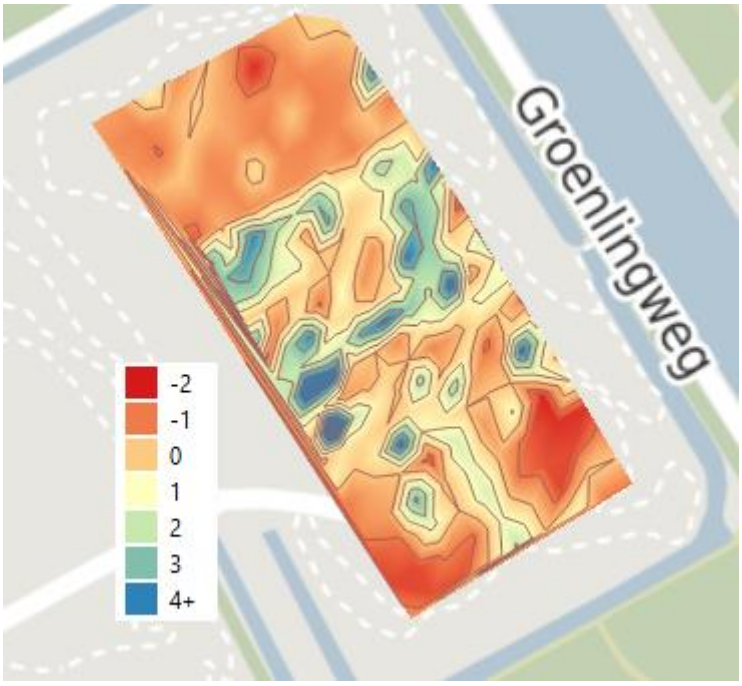


*Figure D.2: Interpolated water levels in the aeration wells measured March 2020 (in m+NAP)*

# E. Water level measurements old gas wells

Table E.1 contains a summary of the measurements of the old gas wells performed by Afvalzorg in October of 2020. Only the old gas wells located on 11Z were measured, the exact locations are shown in appendix B. The remark 'Barrier' means that the measuring device could not go deeper into the well because some barrier is present, meaning that the bottom of the well measured does not correspond to the actual bottom of the well but just the deepest point in the well that could be reached with the measuring device.

*Table E.1: Measurements old gas wells*

| Well | Water level (m+NAP) | Bottom of well (m+NAP) | Remarks |
|---|---|---|---|
| **GB40** | -3.22 | -3.32 | |
| **GB41** | - | -1.16 | Dry well, broken |
| **GB42** | -2.81 | -3.14 | |
| **GB43** | - | -2.89 | Dry well |
| **GB44** | - | -3.98 | Dry well |
| **GB45** | - | -1.72 | Dry well |
| **GB46** | - | -1.26 | Dry well |
| **GB47** | -0.79 | -1.10 | Barrier |
| **GB48** | - | -1.53 | Dry well, broken |
| **GB49** | -2.61 | -2.94 | Dry well |
| **GB50** | - | -1.32 | Dry well |
| **GB51** | -2.86 | -2.92 | |
| **GB52** | - | 5.33 | Barrier |
| **GB53** | -0.82 | -1.01 | |
| **GB54** | - | 1.97 | Dry well |
| **GB55** | - | - | Inaccessible |
| **GB56** | - | - | Well is missing |
| **GB57** | - | 1.35 | Barrier |
| **GB58** | -2.00 | -2.19 | |
| **GB59** | - | -1.59 | Dry well |

# F. Full results pumping tests

Figures F.1 to F.12 show the results for the pumping tests performed. The temperature value shown is the maximum temperature, and the specific electrical conductivity shown is the median value.

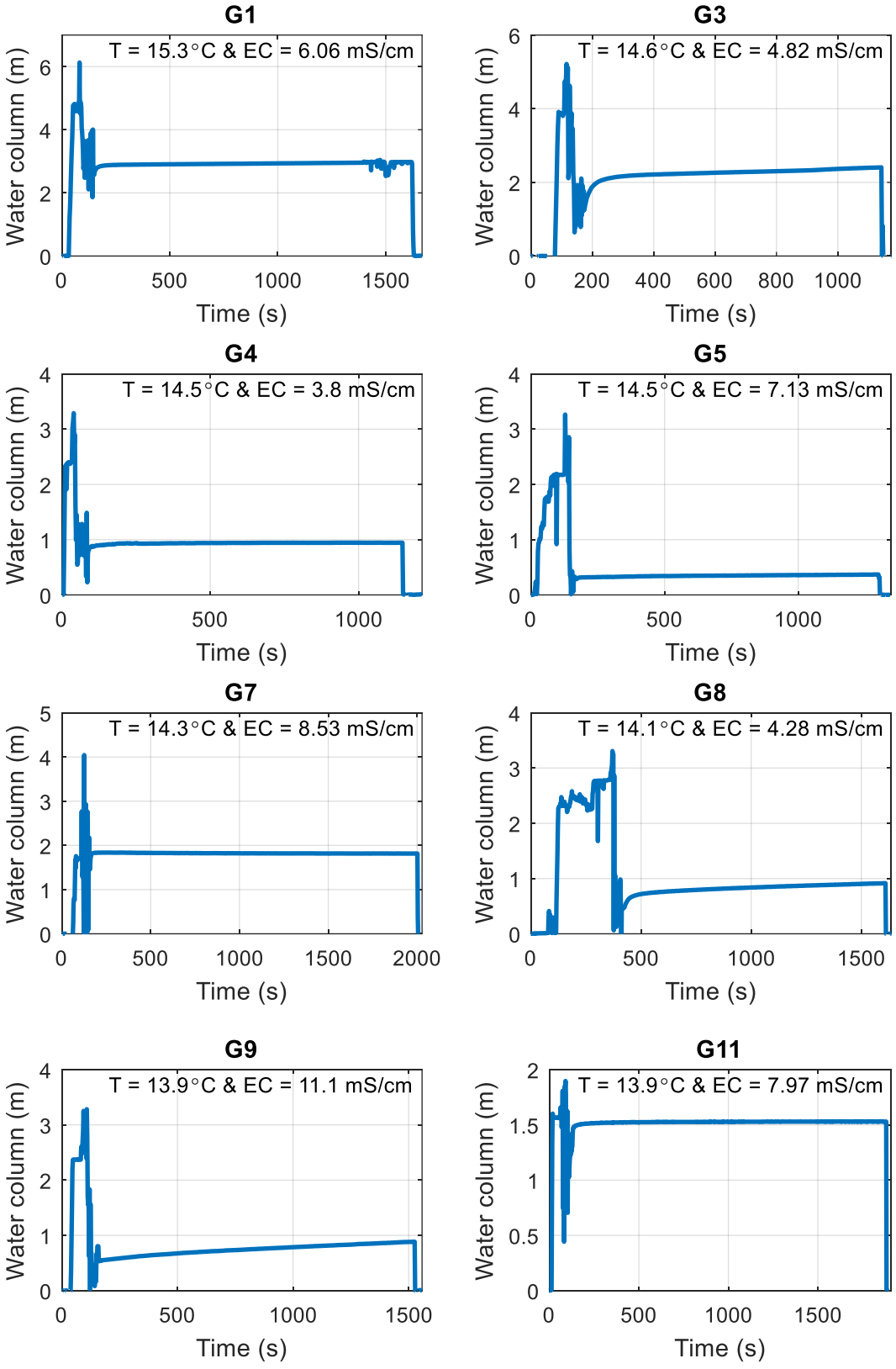


*Figure F.1: Pumping test raw data row G*

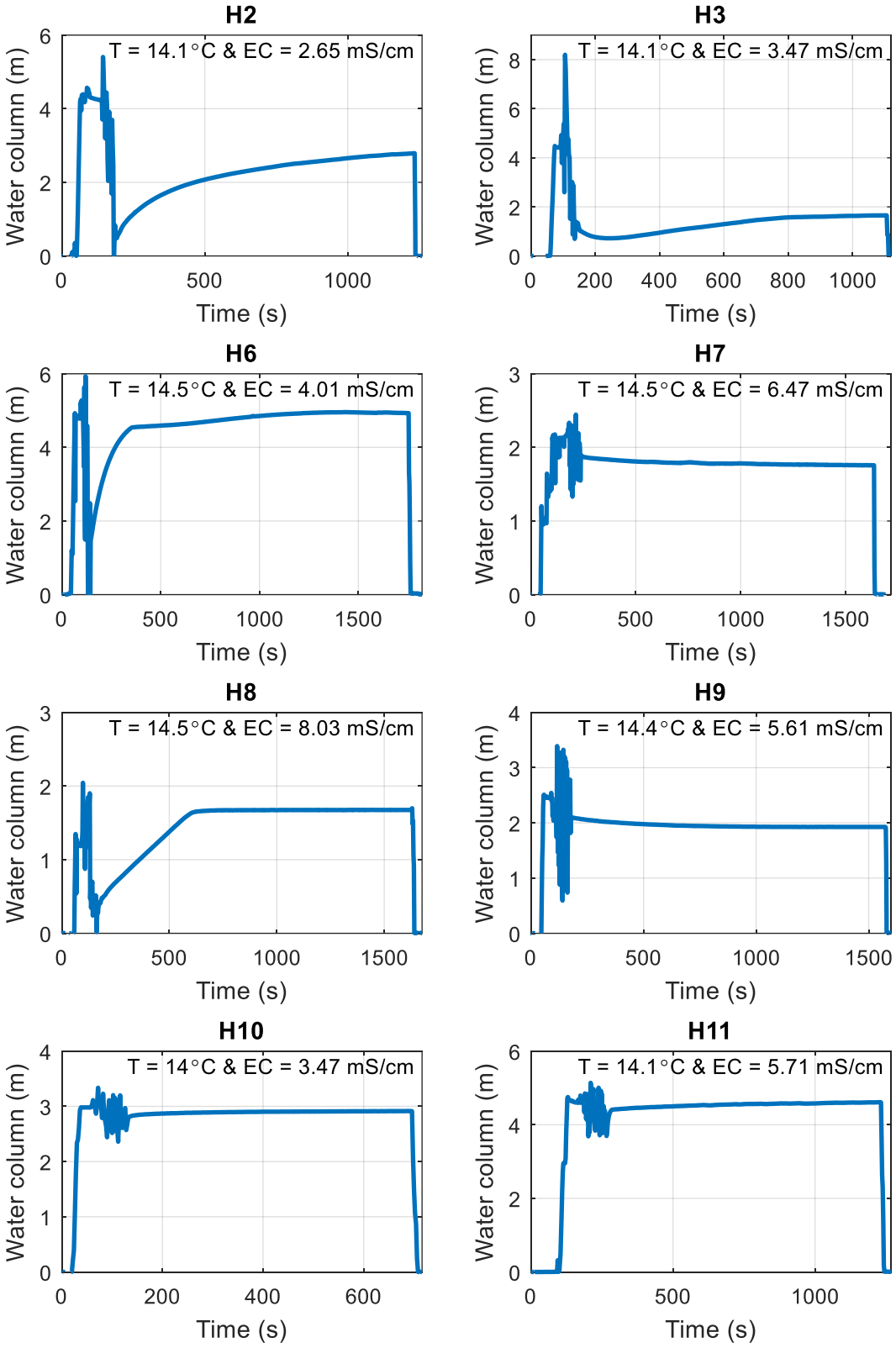


*Figure F.2: Pumping test raw data row H*

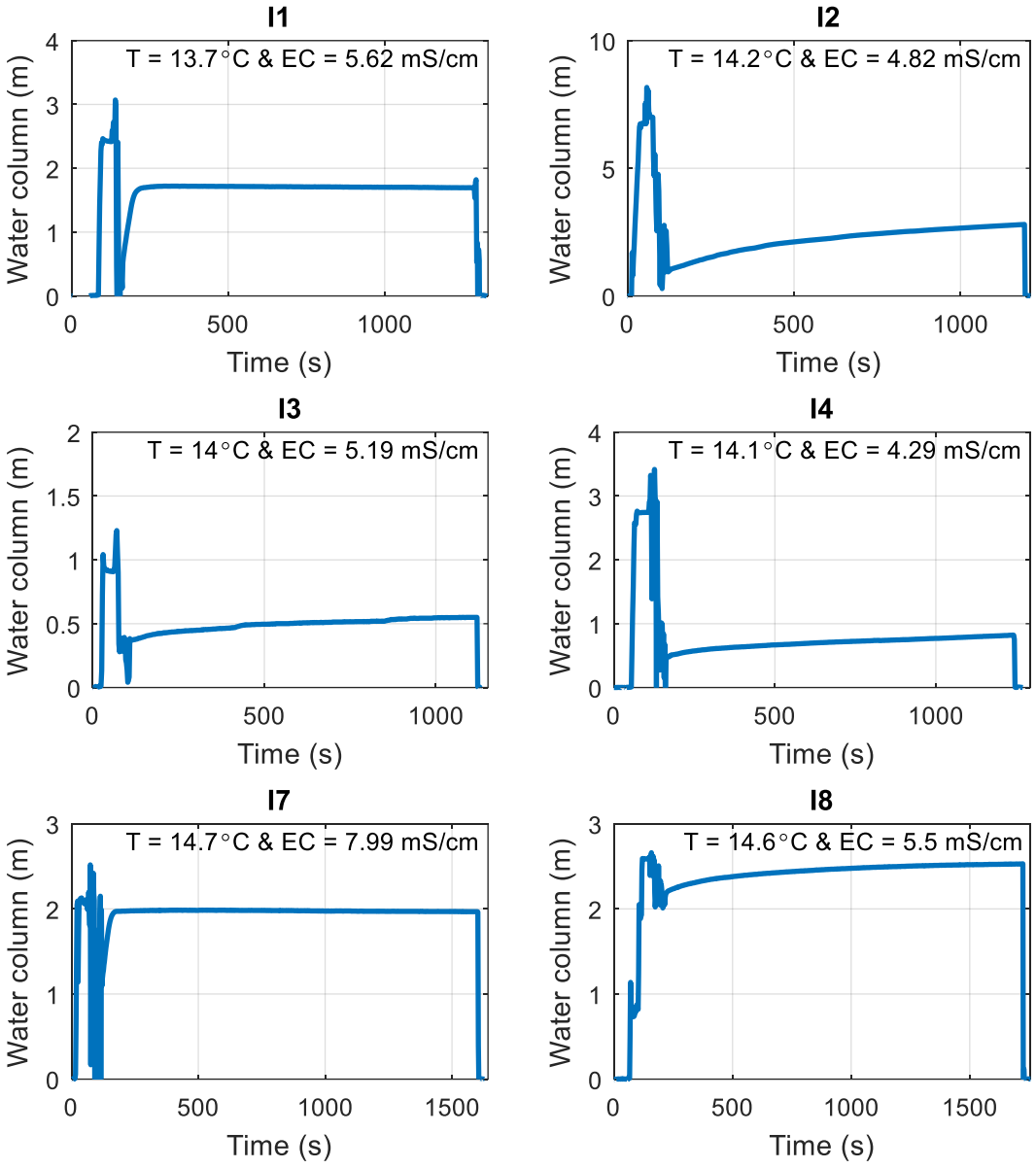


*Figure F.3: Pumping test raw data row I*

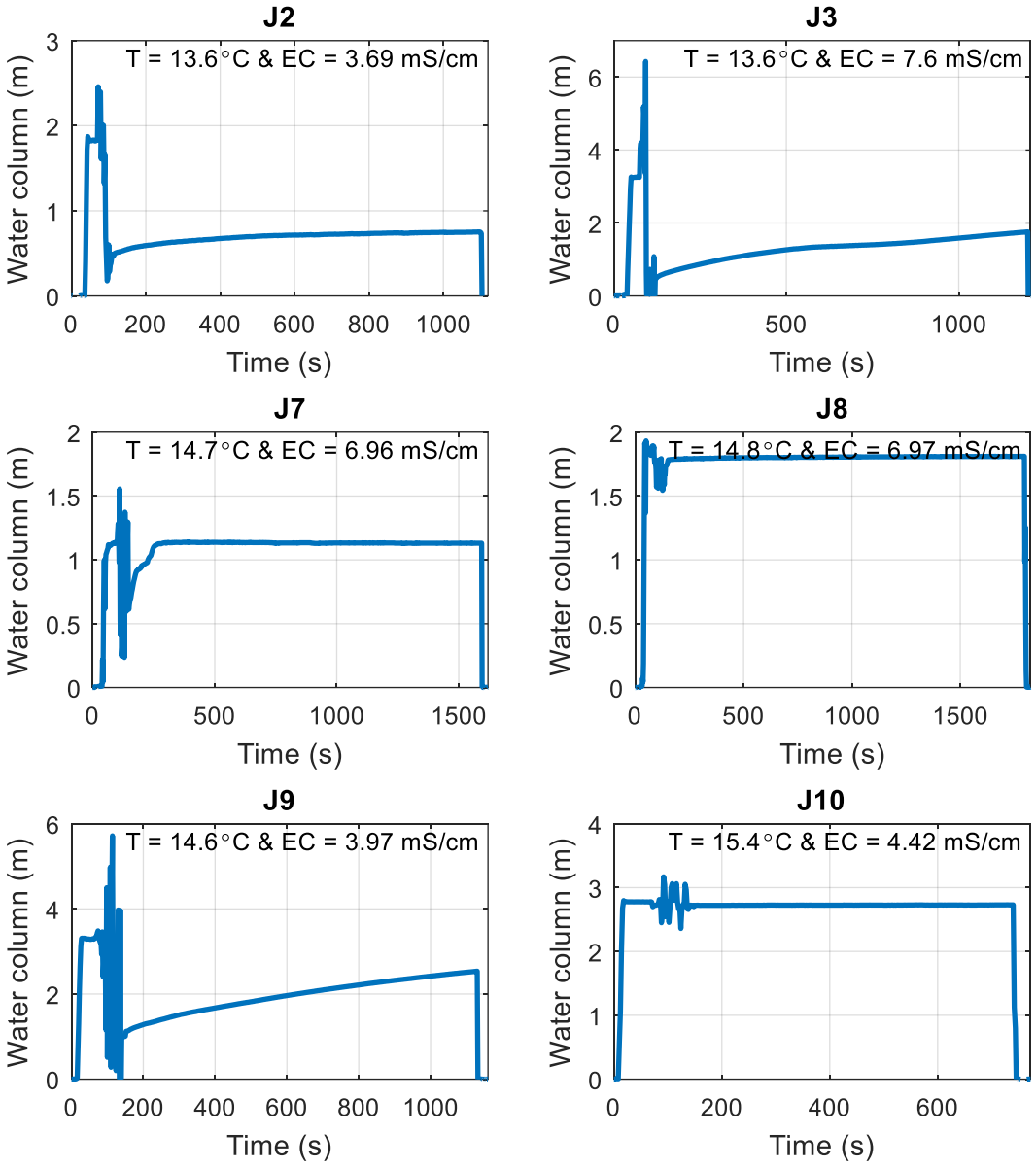


*Figure F.4: Pumping test raw data row J*

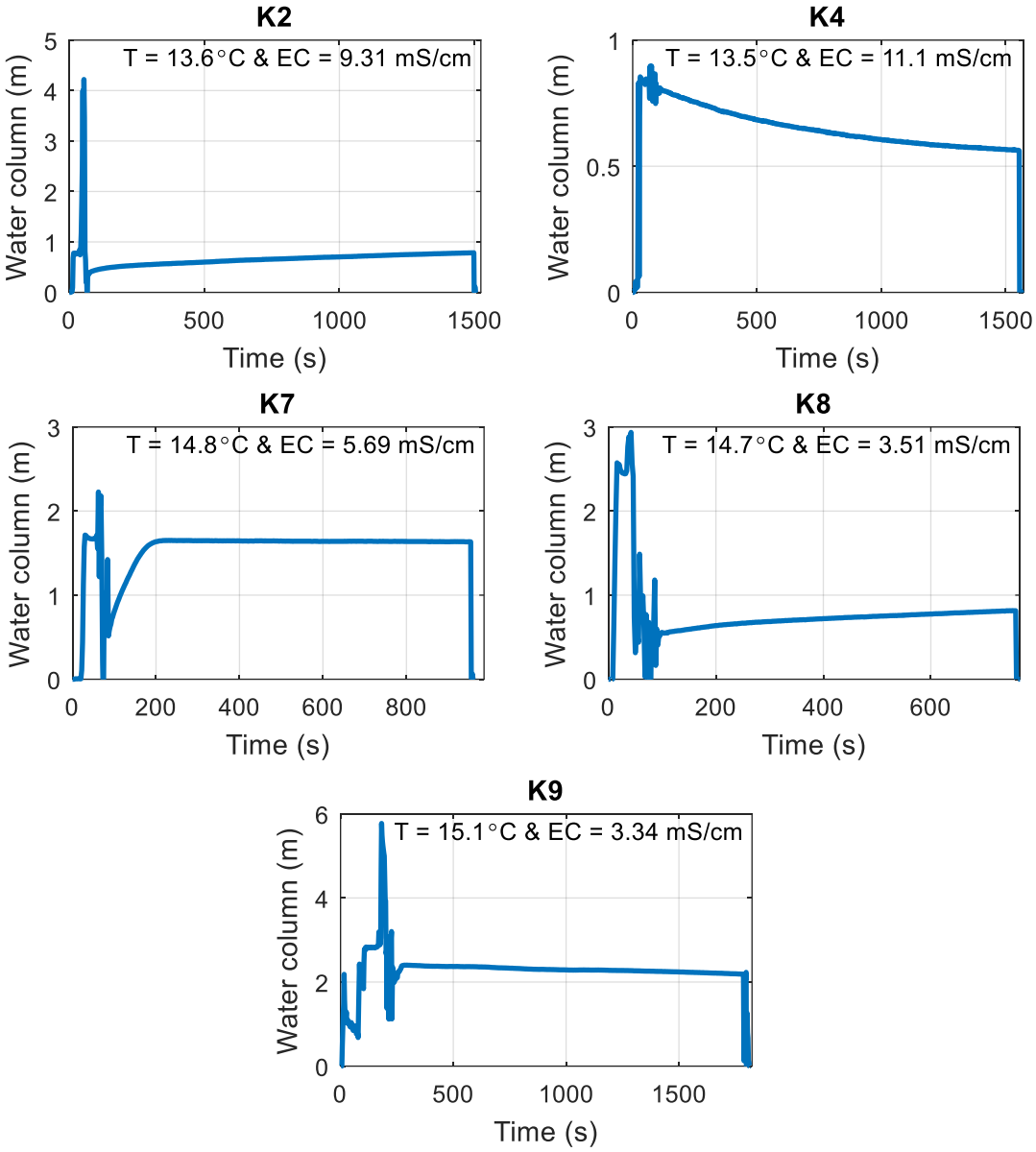


*Figure F.5: Pumping test raw data row K*

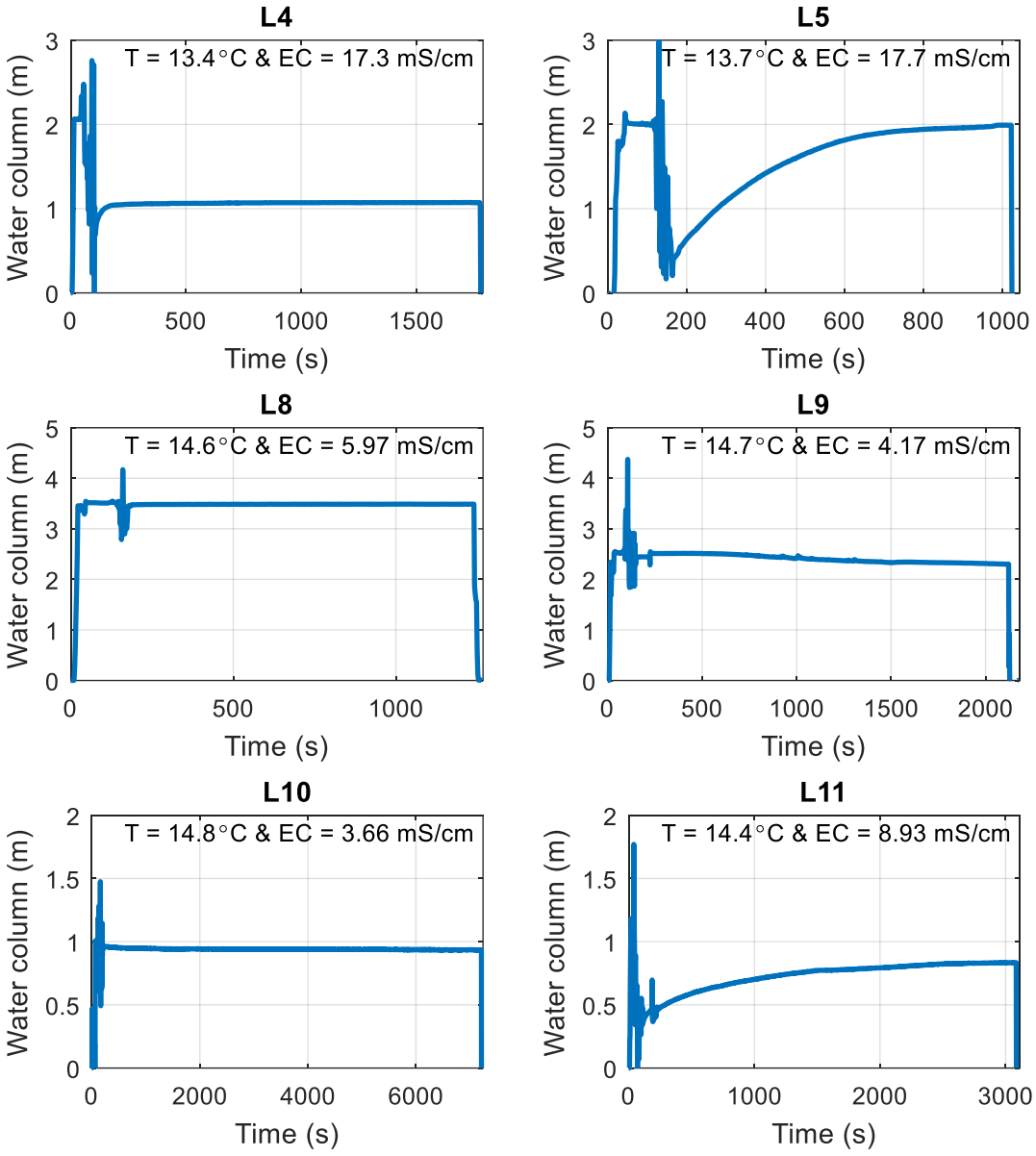


*Figure F.6: Pumping test raw data row L*

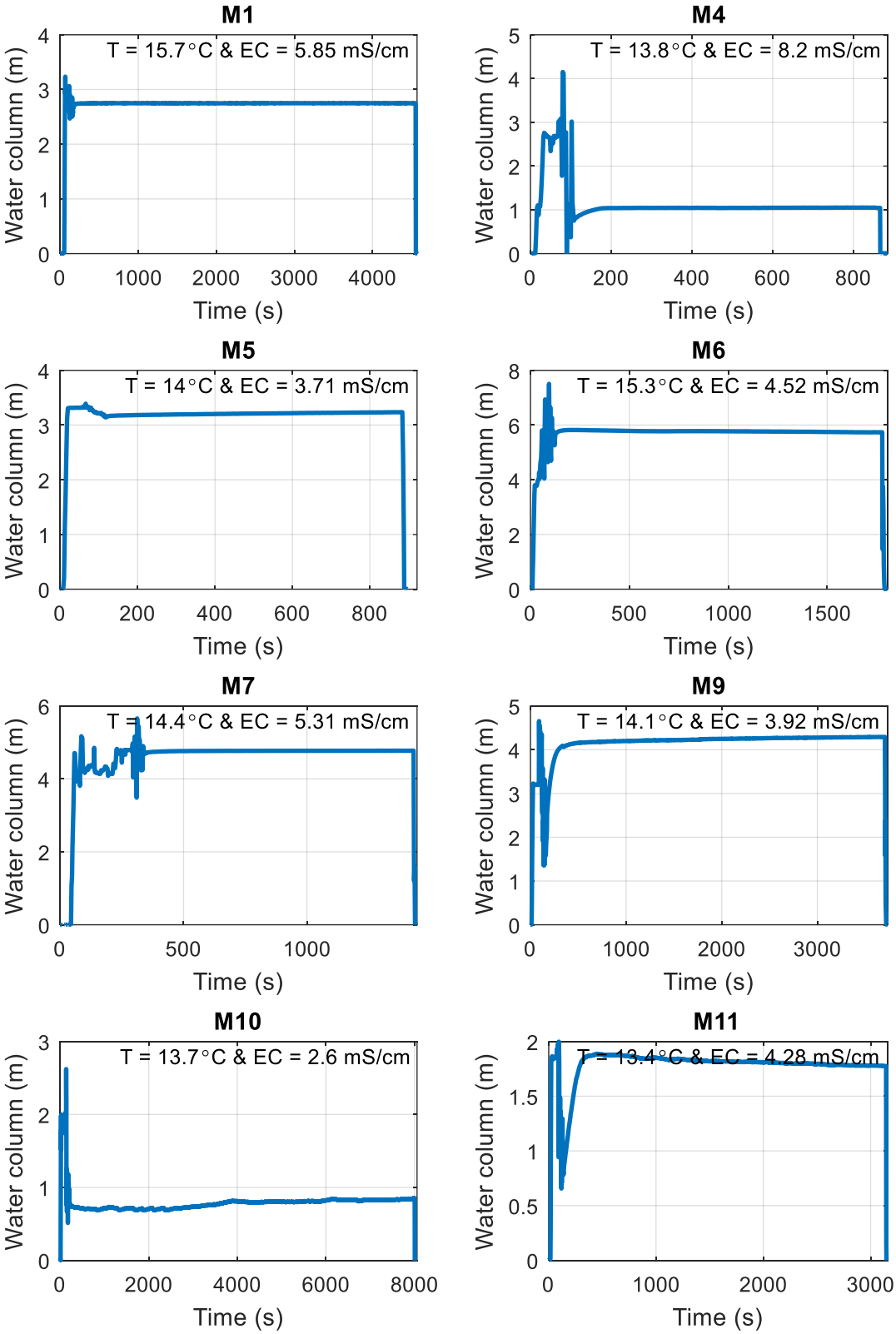


*Figure F.7: Pumping test raw data row M*

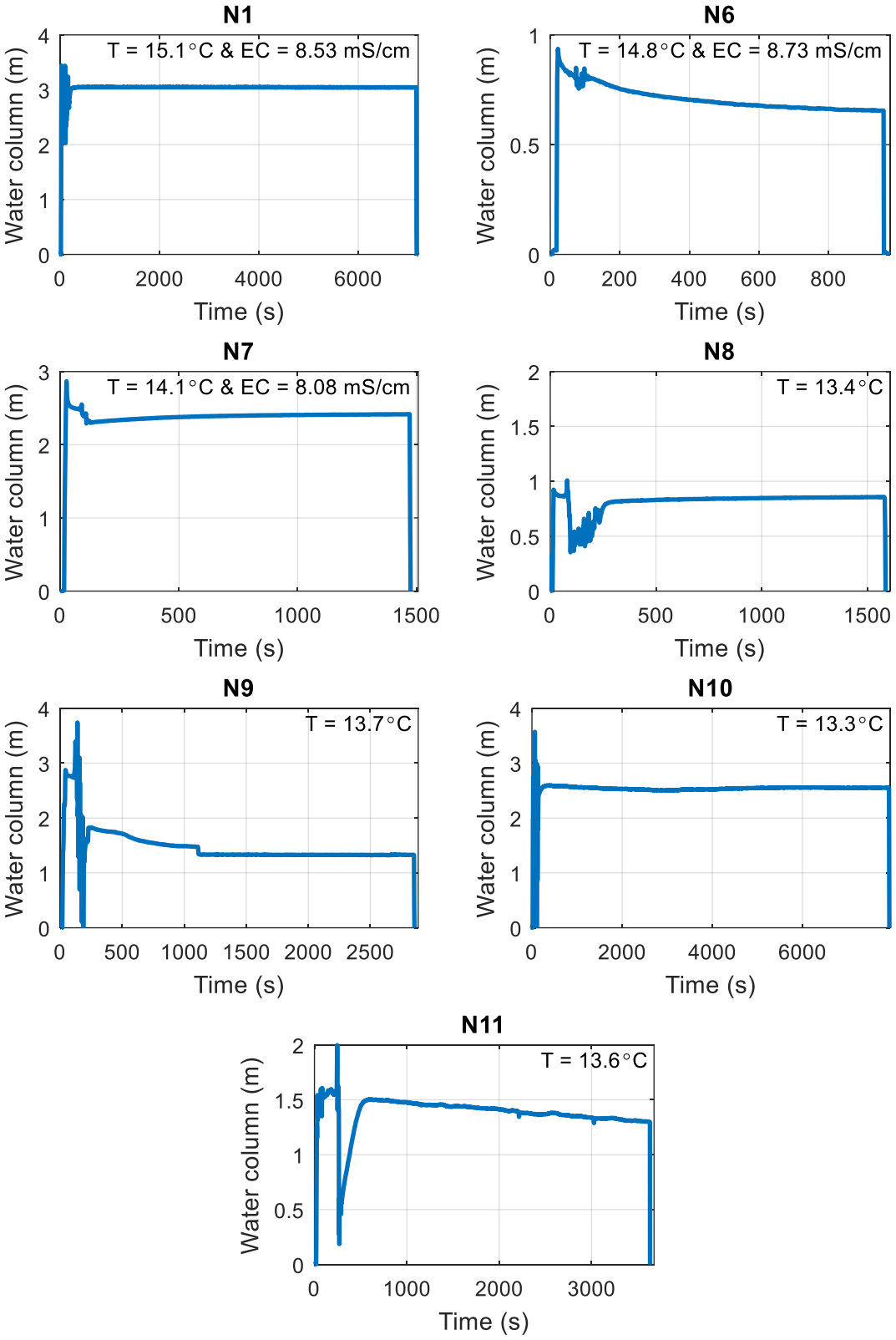


*Figure F.8: Pumping test raw data row N*

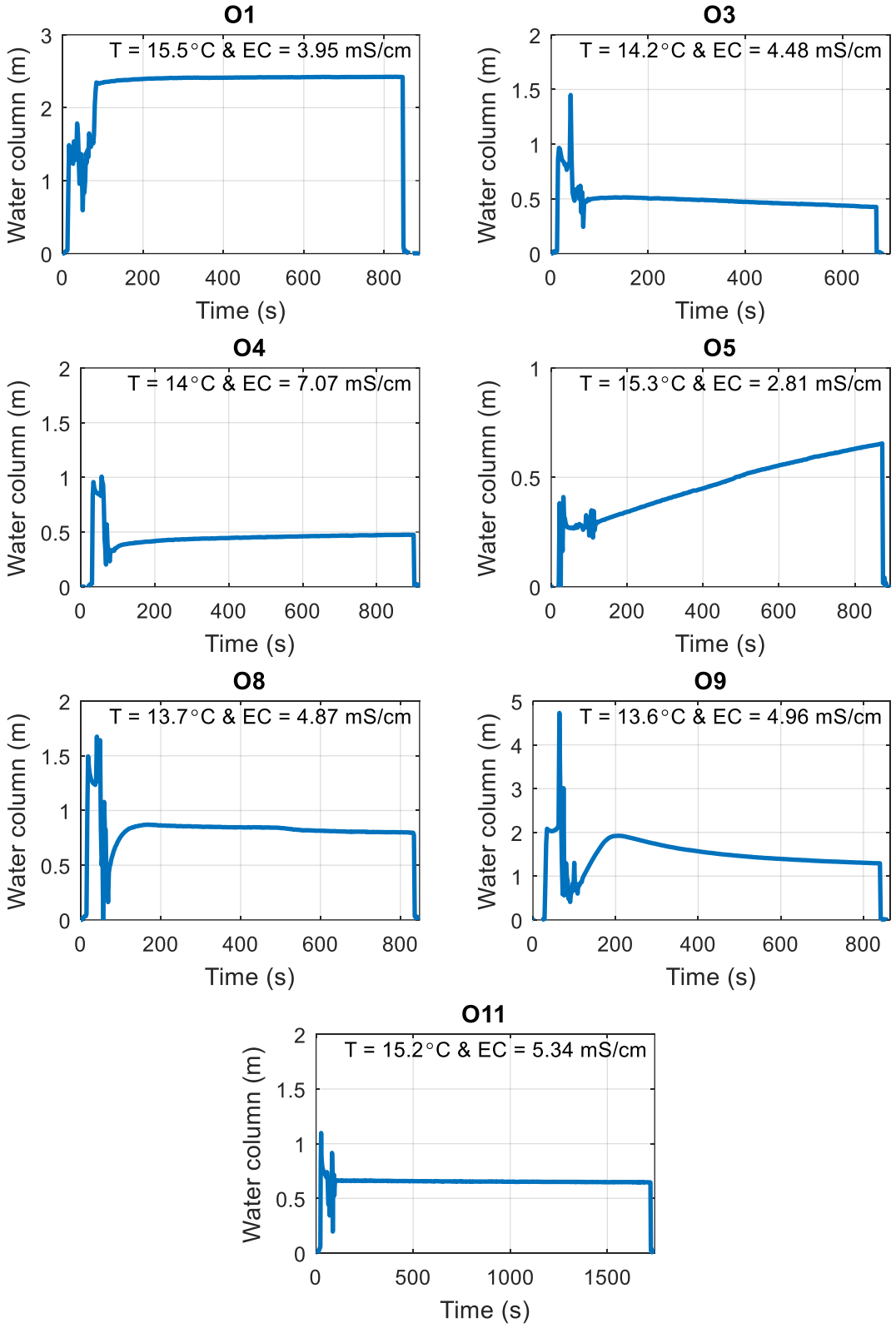


*Figure F.9: Pumping test raw data row O*

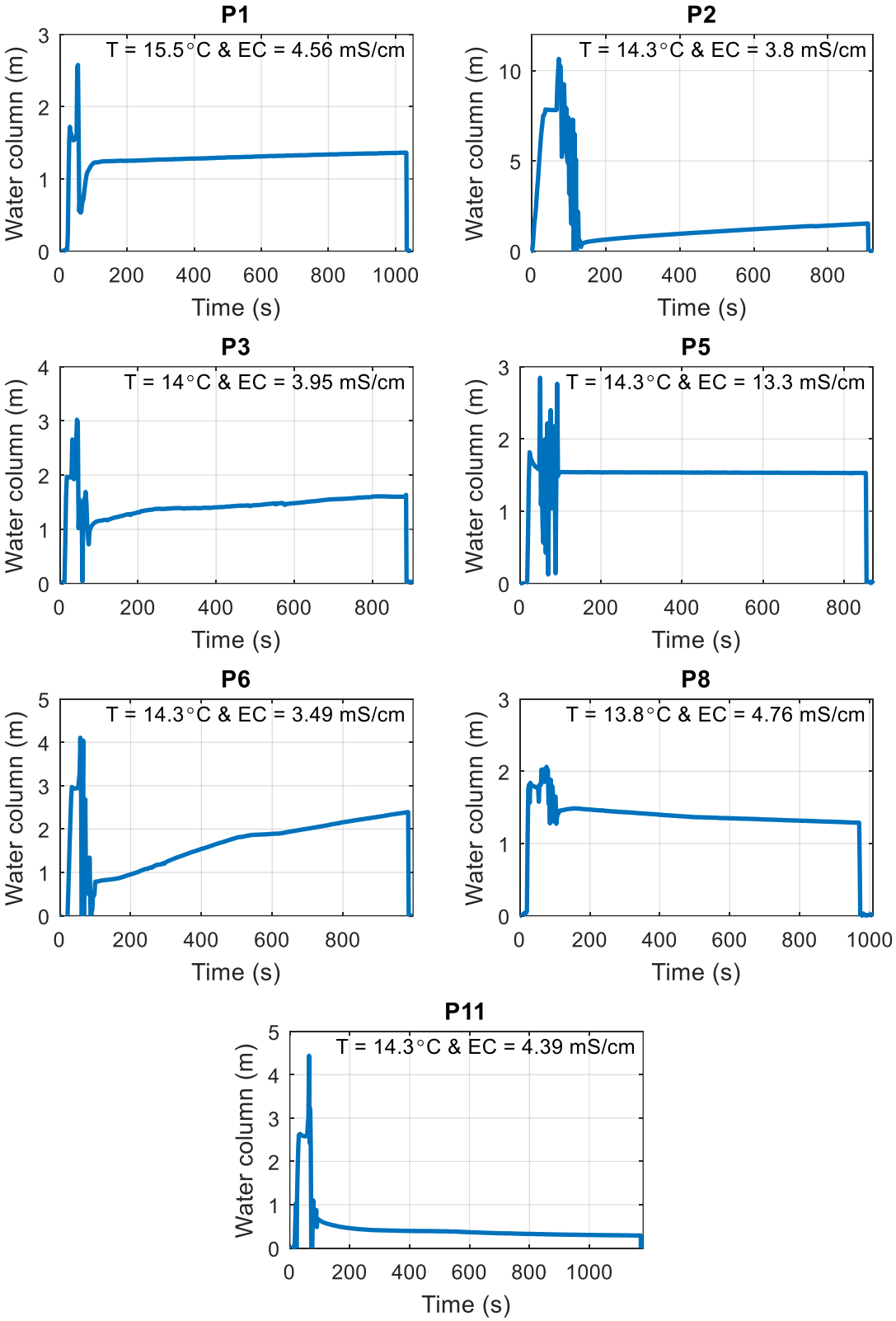


*Figure F.10: Pumping test raw data row P*

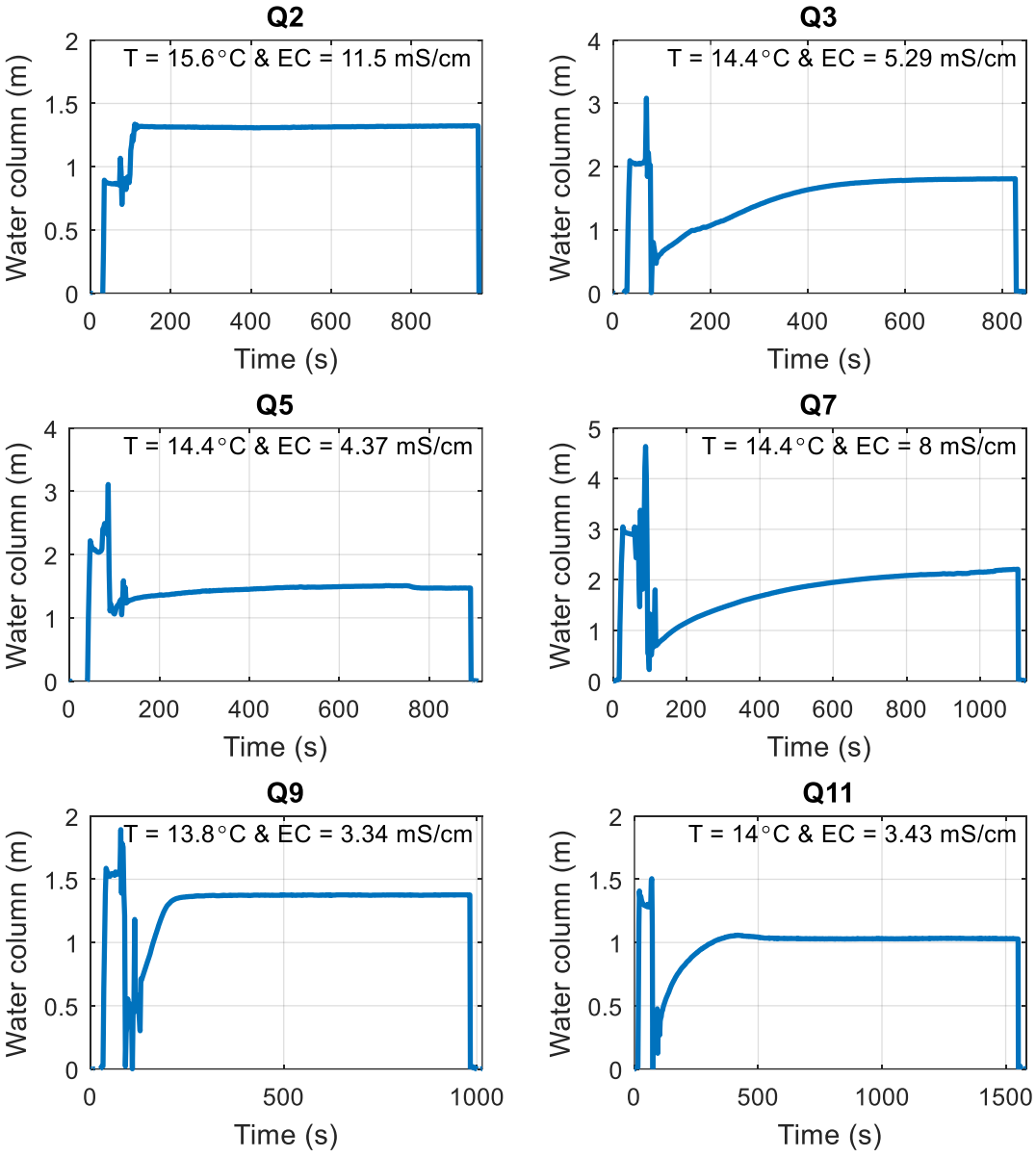


*Figure F.11: Pumping test raw data row Q*

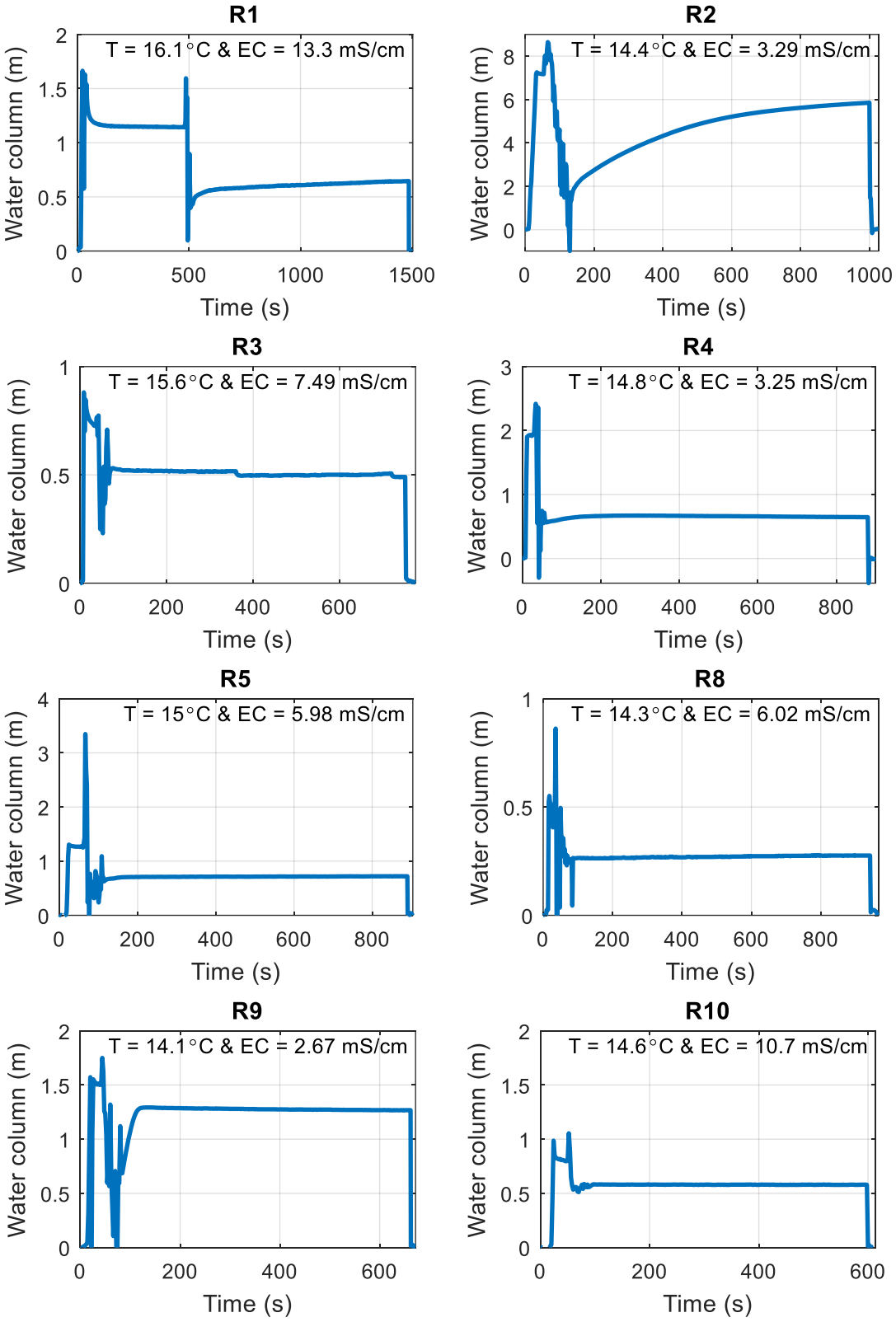


*Figure F.12: Pumping test raw data row R*

# G. Pumping tests with mechanical driver

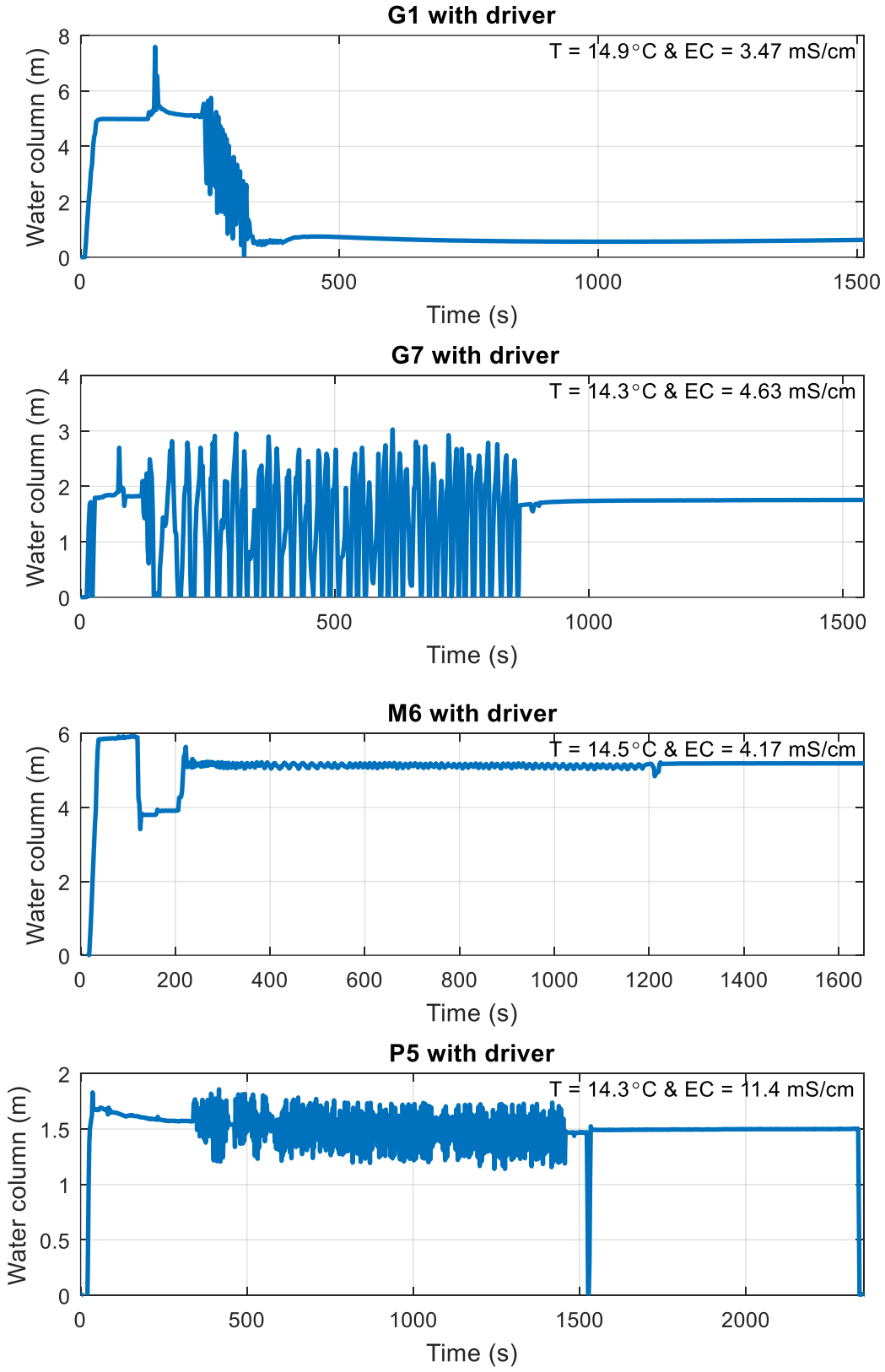


*Figure G.1: Pumping tests with mechanical driver*

# H. Selected pictures of leachate samples

Figure H.1 shows a selection of eight from the total of 87 samples taken. The figure shows that the samples are very variable, some contain a lot of sediment (R9), some almost no sediment at all (M1), while for others there seem to be suspended sediment that even after weeks has not been settled (P8). Also the colour of the leachate can very between clear, almost the colour of water (N9) to greyish (O9) to very yellowish (O10).

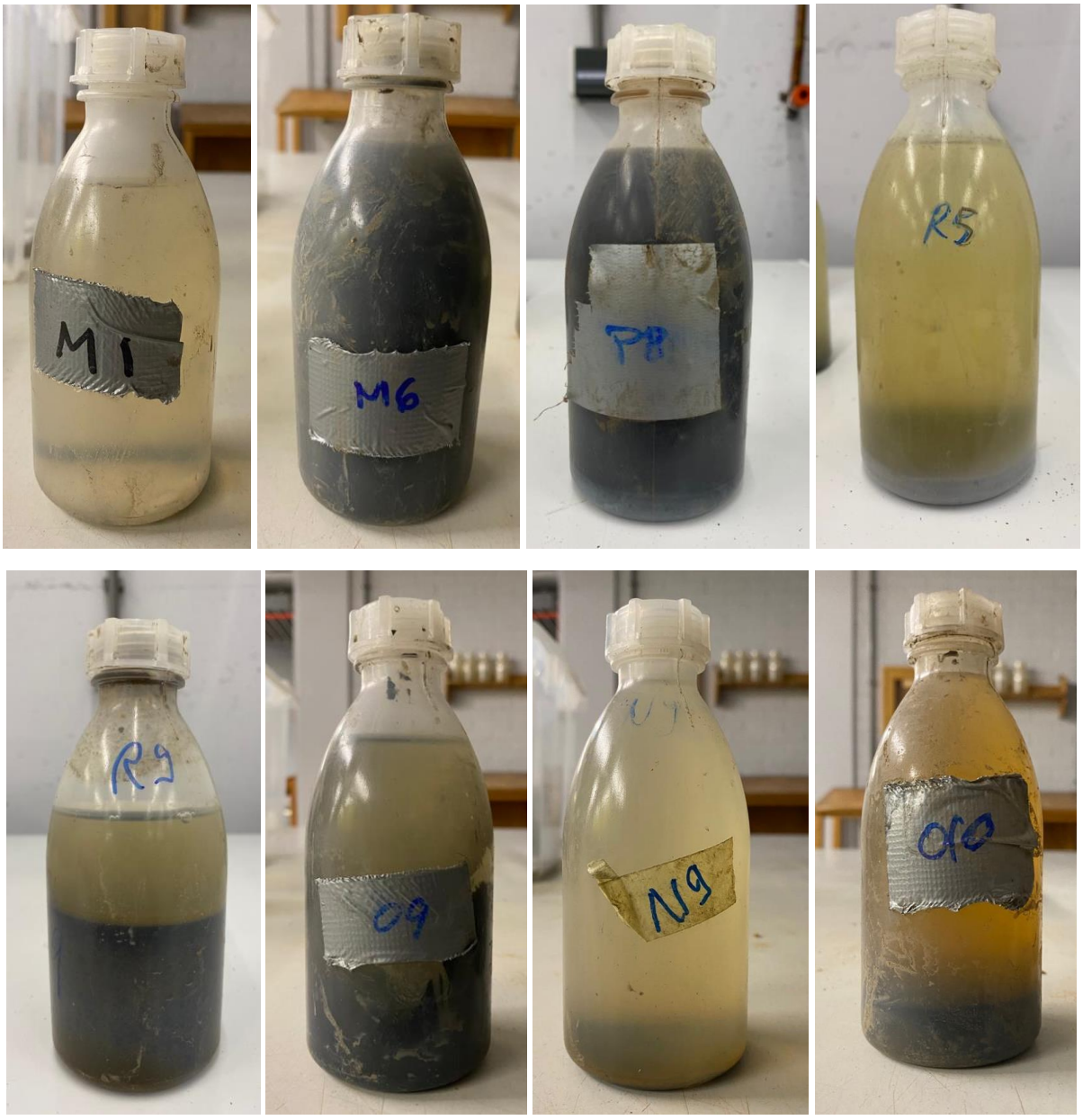


*Figure H.1: Visual variability of leachate samples*

# I. Long term monitoring results

This appendix contains all the long term aeration well monitoring results that are not presented in section 6.5. Figure I.1 shows the data obtained by the baro-diver located in the outside, and figures I.2 to I.12 show the results of the CTD-divers installed in the wells.

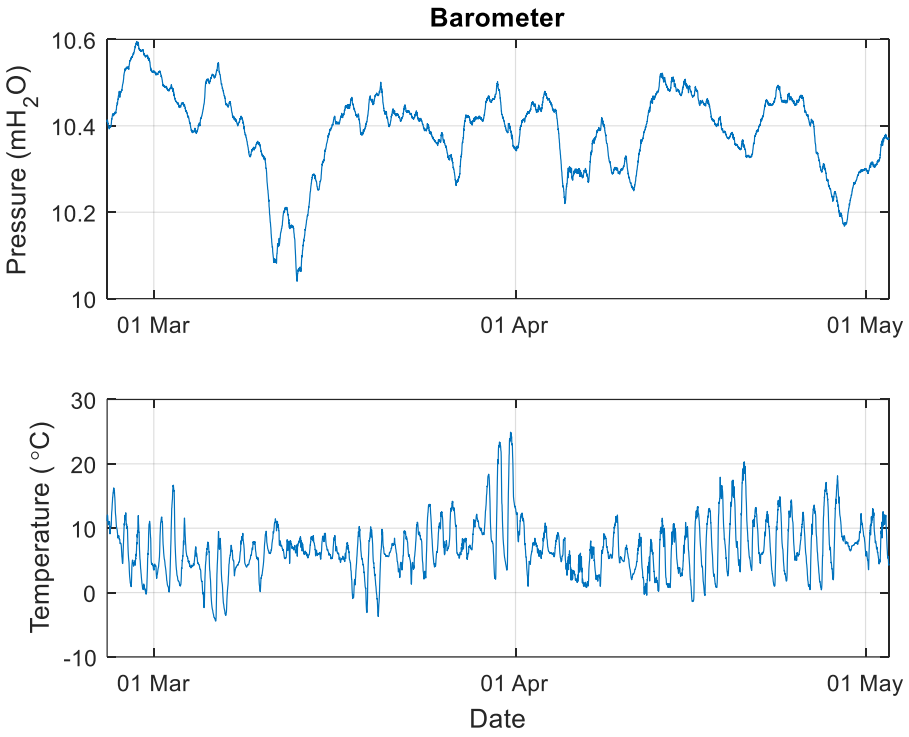


*Figure I.1: Baro-diver measured pressure and temperature*

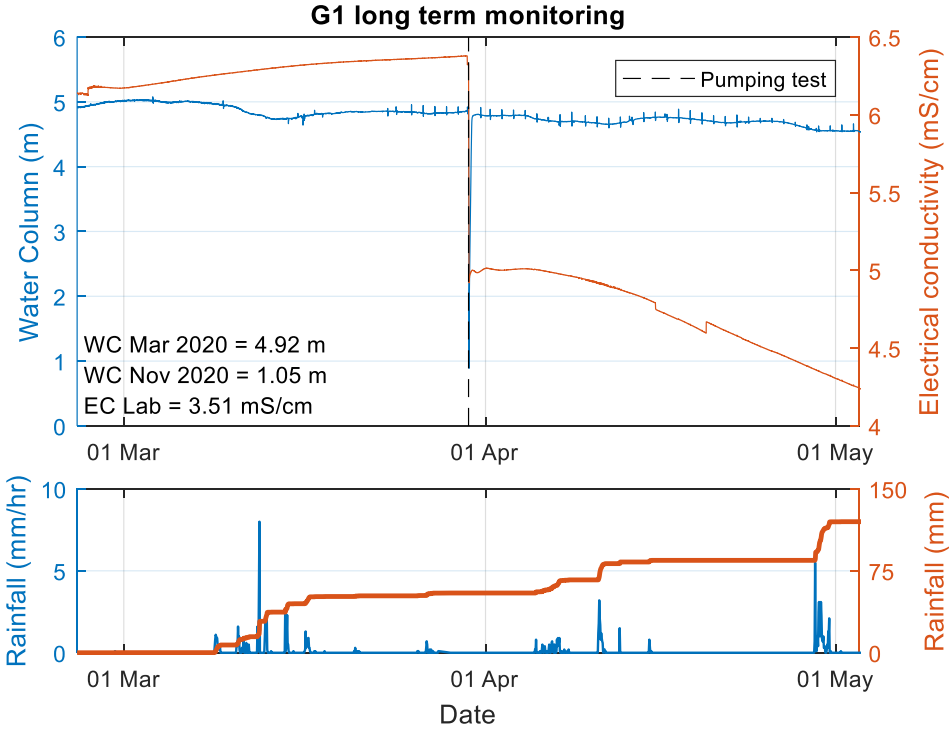


*Figure I.2: G1 long term monitoring of water levels, electrical conductivity and rainfall*

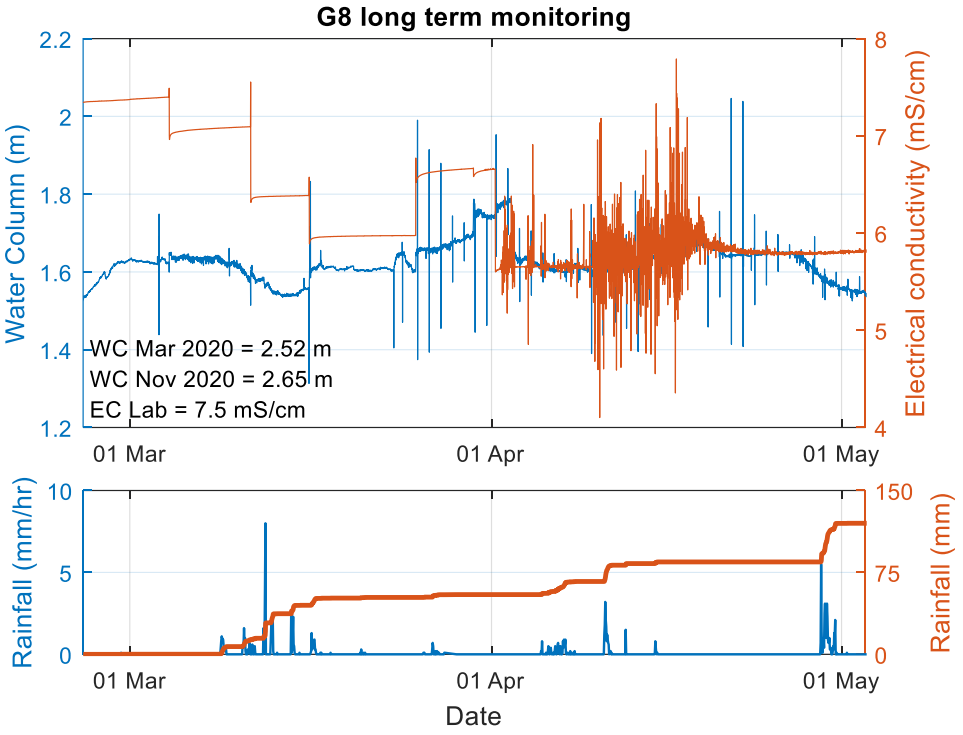


*Figure I.3: G8 long term monitoring of water levels, electrical conductivity and rainfall (lifted 3.52 meter)*

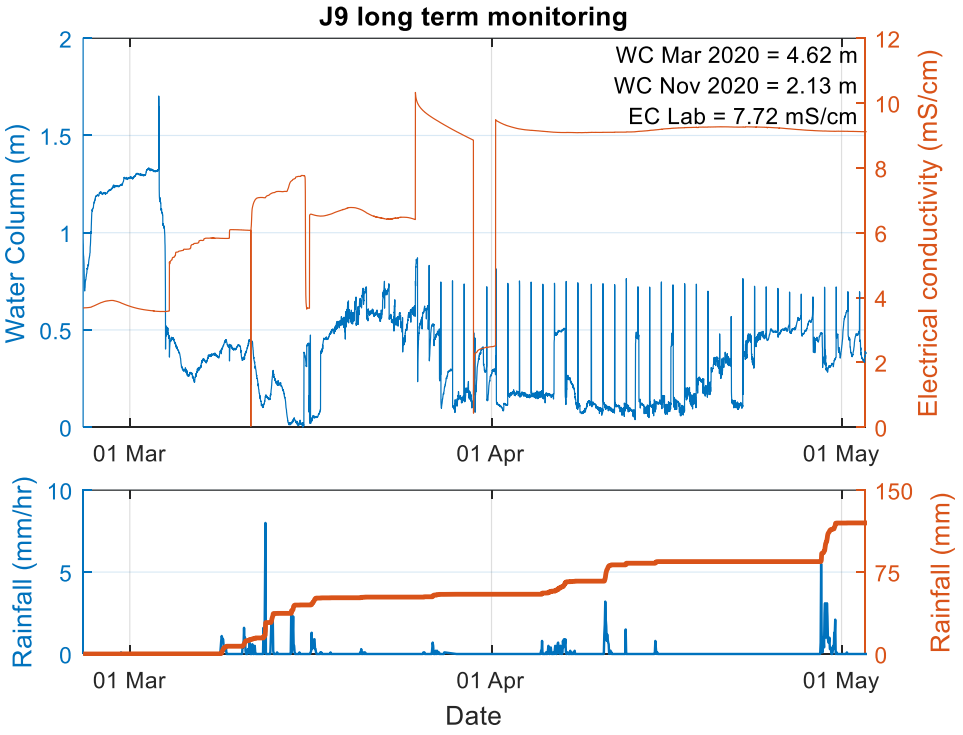


*Figure I.4: J9 long term monitoring of water levels, electrical conductivity and rainfall (lifted 3.30 meter)*

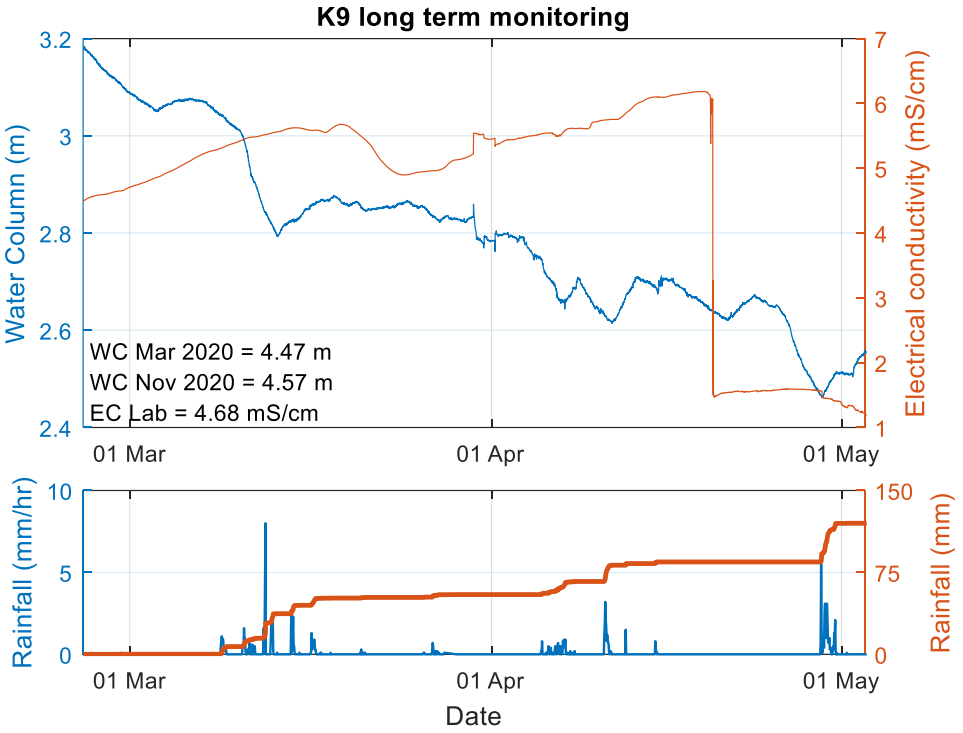


*Figure I.5: K9 long term monitoring of water levels, electrical conductivity and rainfall*

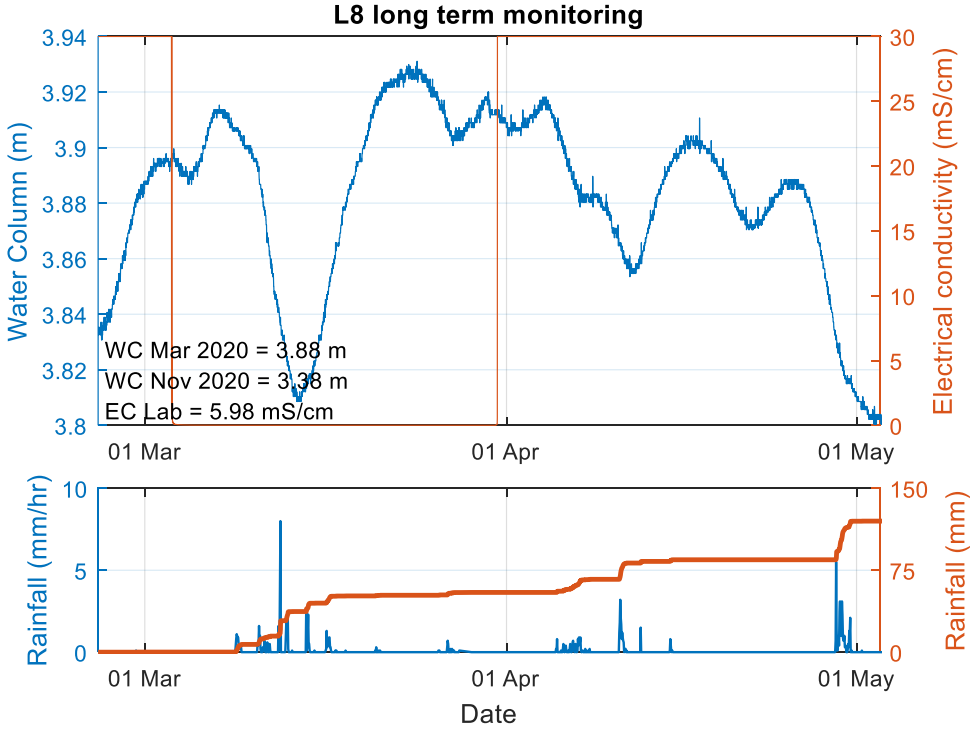


*Figure I.6: L8 long term monitoring of water levels, electrical conductivity and rainfall*

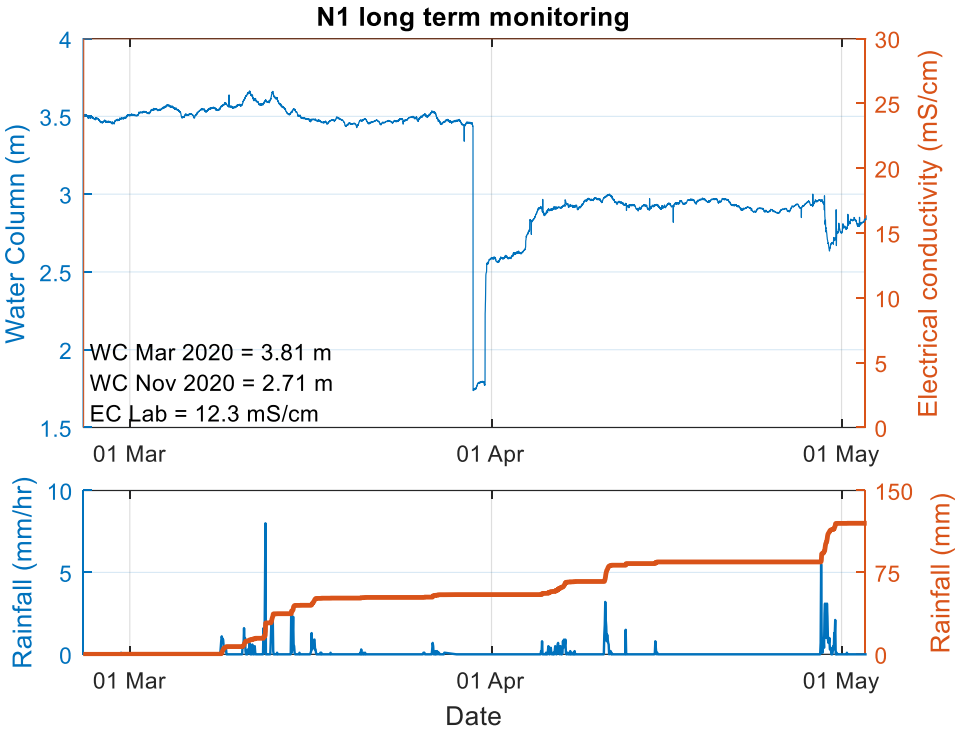


*Figure I.7: N1 long term monitoring of water levels, electrical conductivity and rainfall*

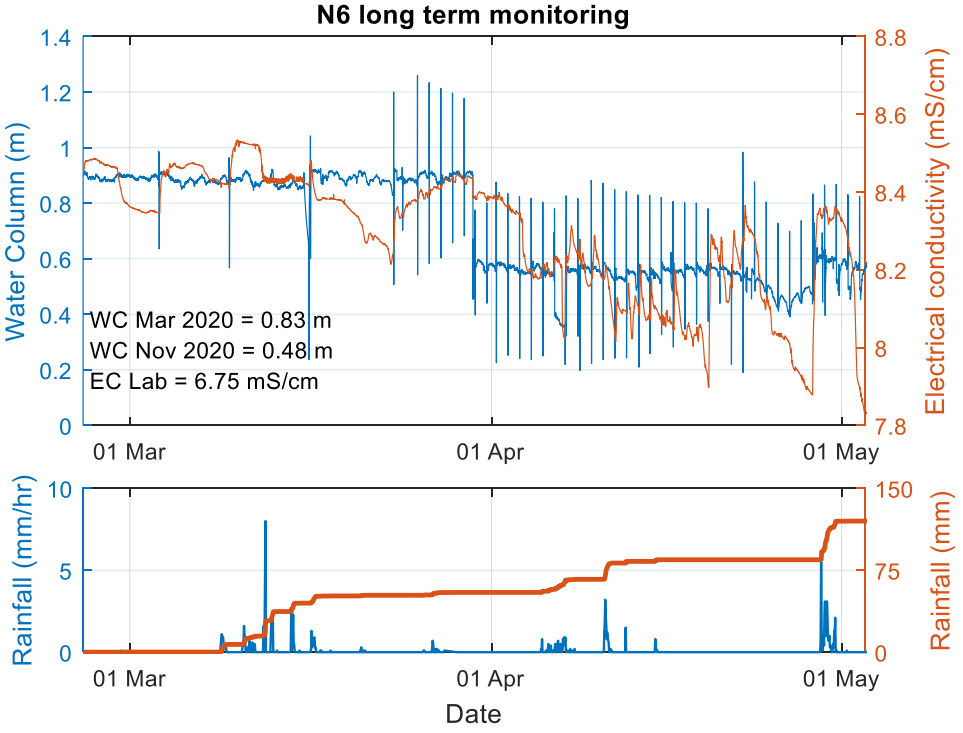


*Figure I.8: N6 long term monitoring of water levels, electrical conductivity and rainfall*

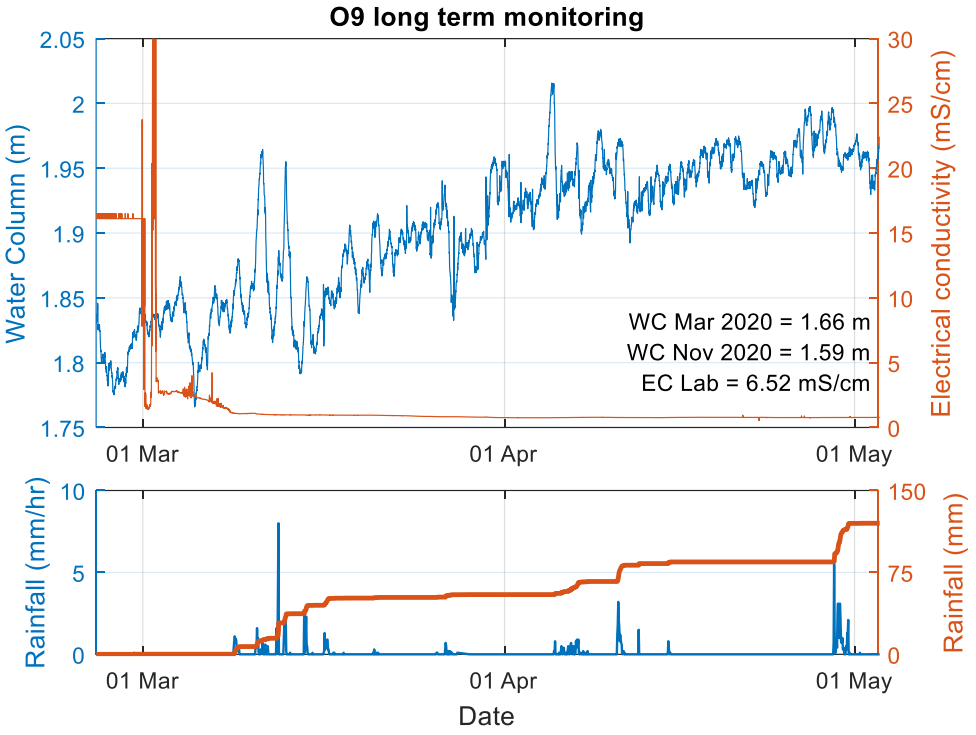


*Figure I.9: O9 long term monitoring of water levels, electrical conductivity and rainfall*

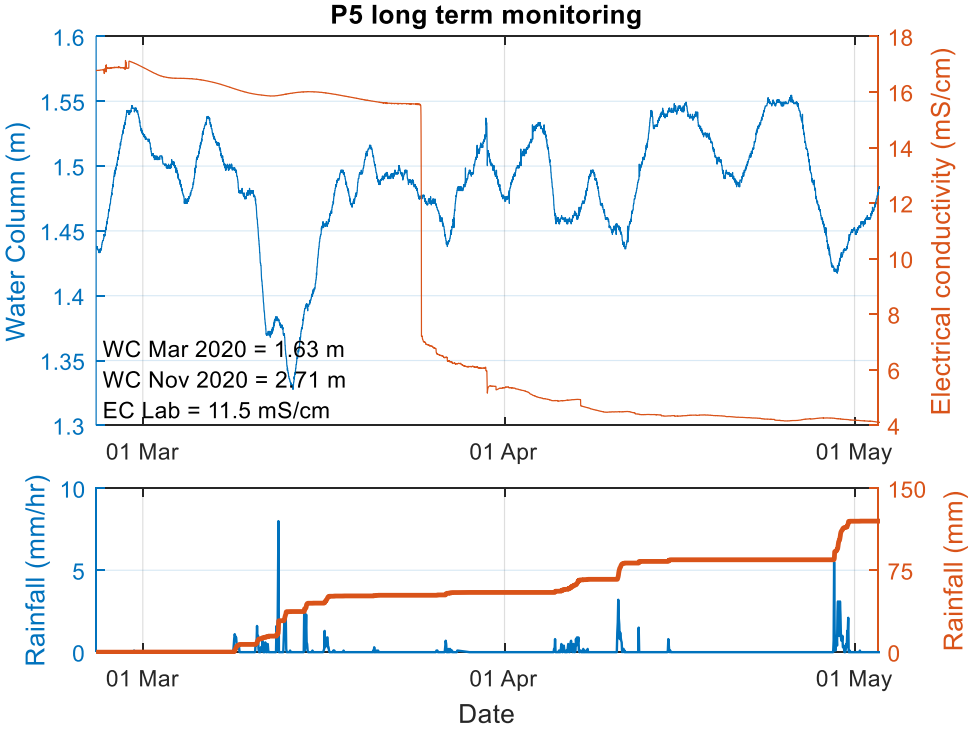


*Figure I.10: P5 long term monitoring of water levels, electrical conductivity and rainfall*

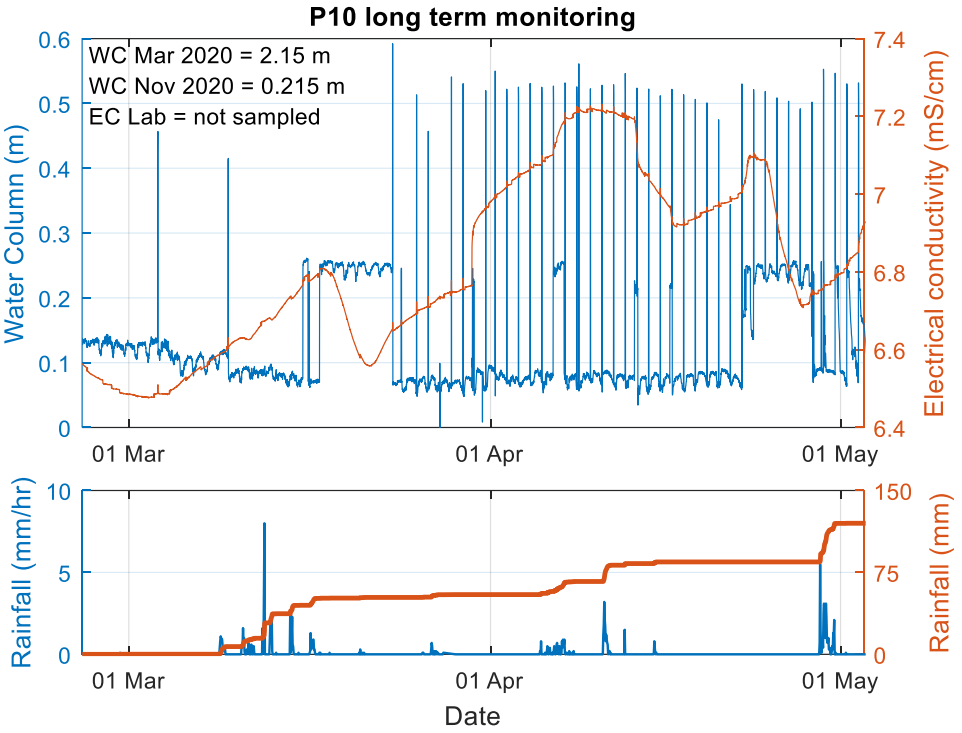


*Figure I.11: P10 long term monitoring of water levels, electrical conductivity and rainfall*

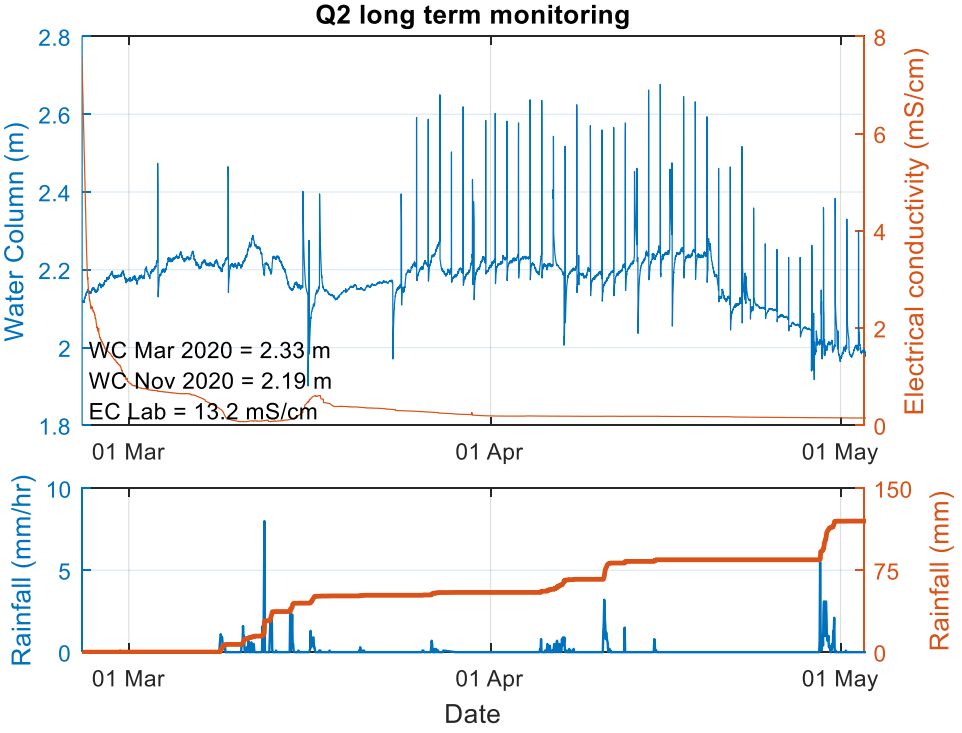


*Figure I.12: Q2 long term monitoring of water levels, electrical conductivity and rainfall*

# J. Relation between DOC and $A_{254}$

Table J.1 gives an overview of the measured values, where the absorbance values are already corrected for the fact that absorbances above two do not follow the Beer-Lambert law. To find the linear fit of equation 5.11, the datapoints of wells K1 and P8 are ignored. K1 contains much more DOC then any of the other measured wells and including that well would change the fit so much that it was concluded that K1 is not represented correctly by the fit. Well P8 has a really high absorbance while this was the only sample that was completely black even after all the solid particles had settled. Therefore it is likely that the absorbance was not only cause by the presence of DOC, but also by other components, making the sample not representable for the whole compartment. Figure J.1 shows the ten remaining data points and the linear fit.

*Table J.1: Absorbance and DOC results*

| Well | Absorbance, 254 nm (-) | DOC (mgC/l) |
|---|---|---|
| **I6** | 6.04 | 180 |
| **J2** | 0.71 | 34 |
| **J3** | 1.82 | 79.9 |
| **J7** | 3.87 | 167 |
| **K1** | 5.64 | 790 |
| **K9** | 5.63 | 178 |
| **M5** | 0.43 | 17.8 |
| **N8** | 0.91 | 32.9 |
| **N11** | 0.97 | 41.6 |
| **P8** | 11.7 | 226 |
| **Q11** | 0.81 | 37.6 |
| **R9** | 1.03 | 51.1 |

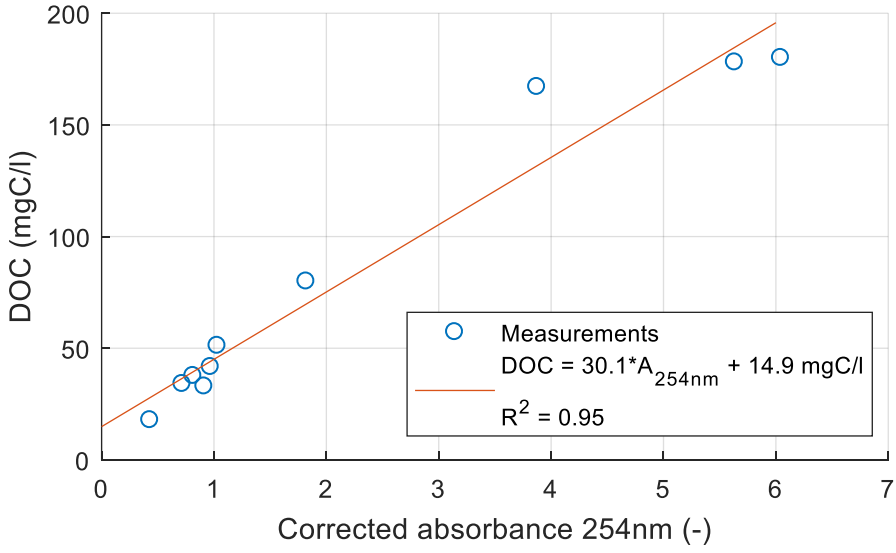


*Figure J.1: DOC and absorbance measurements and obtained relationship*

Figure J.2 shows for all the samples taken in the field in December 2020 for which the measured absorbance was above 2, the measured absorbance against the measured absorbance of the five times diluted sample and the Beer-Lambert law, which predicts that the absorbance of the five times diluted samples are five times lower than the non-diluted samples. From the figure can be concluded that diluting the samples with an absorbance above 2 was necessary, especially for samples with an

absorbance above 2.5 the Beer-Lambert law, on which equation 5.11 was based, does not hold anymore.

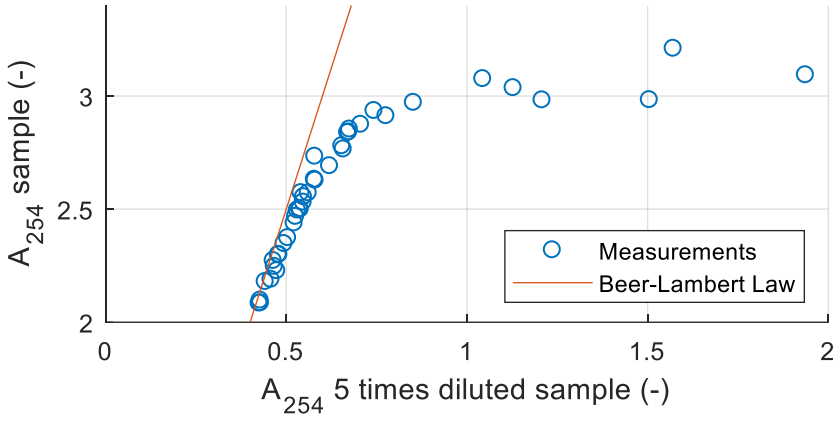


*Figure J.2: Absorbance and diluted absorbance in relation to the Beer-Lambert law*

# K. Functional relationships van Genuchten parameters

Equations K.1, K.2 and K.3 show the functional relationships used to obtain the other three van Genuchten parameters from the porosity/saturated water content $\theta_s$.

$$n = \begin{cases} 1.5 & \theta_s < 0.52 \\ 3.5 \cdot \theta_s - 0.27 & 0.52 < \theta_s < 0.62 \\ 1.9 & \theta_s > 0.62 \end{cases} \quad \text{K.1}$$

$$\alpha = \begin{cases} 0.12 & \theta_s < 0.42 \\ 7.9 \cdot \theta_s - 3.2 & 0.42 < \theta_s < 0.73 \\ 2.57 & \theta_s > 0.73 \end{cases} \quad \text{K.2}$$

$$\theta_r = \begin{cases} 0.13 & \theta_s < 0.42 \\ 0.26 - 0.3 \cdot \theta_s & 0.42 < \theta_s < 0.6 \\ 0.08 & \theta_s > 0.6 \end{cases} \quad \text{K.3}$$